The Astronomical Journal, 144:4 (36pp), 2012 July doi:10.1088/0004-6256/144/1/4

THE OBSERVED PROPERTIES OF DWARF GALAXIES IN AND AROUND THE LOCAL GROUP

Alan W. McConnachie
NRC Herzberg Institute of Astrophysics, 5071 West Saanich Road, Victoria, BC, V9E 2E7, Canada; alan.mcconnachie@nrc-cnrc.gc.ca
Received 2011 December 22; accepted 2012 April 2; published 2012 June 4

ABSTRACT

Positional, structural, and dynamical parameters for all dwarf galaxies in and around the Local Group are presented, and various aspects of our observational understanding of this volume-limited sample are discussed. Over 100 nearby galaxies that have distance estimates reliably placing them within 3 Mpc of the Sun are identified. This distance threshold samples dwarfs in a large range of environments, from the satellite systems of the MW and M31, to the quasi-isolated dwarfs in the outer regions of the Local Group, to the numerous isolated galaxies that are found in its surroundings. It extends to, but does not include, the galaxies associated with the next nearest groups, such as Maffei, Sculptor, and IC 342. Our basic knowledge of this important galactic subset and their resolved stellar populations will continue to improve dramatically over the coming years with existing and future observational capabilities, and they will continue to provide the most detailed information available on numerous aspects of dwarf galaxy formation and evolution. Basic observational parameters, such as distances, velocities, magnitudes, mean metallicities, as well as structural and dynamical characteristics, are collated, homogenized (as far as possible), and presented in tables that will be continually updated to provide a convenient and current online resource. As well as discussing the provenance of the tabulated values and possible uncertainties affecting their usage, the membership and spatial extent of the MW sub-group, M31 sub-group, and the Local Group are explored. The morphological diversity of the entire sample and notable sub-groups is discussed, and timescales are derived for the Local Group members in the context of their orbital/interaction histories. The scaling relations and mean stellar metallicity trends defined by the dwarfs are presented, and the origin of a possible "floor" in central surface brightness (and, more speculatively, stellar mean metallicity) at faint magnitudes is considered.

Key words: catalogs – galaxies: dwarf – galaxies: fundamental parameters – galaxies: general – galaxies: structure – Local Group

Online-only material: color figures

1. INTRODUCTION

There has been a veritable explosion of data, discoveries, and realizations in the past decade relating to the broad research area of the structure and content of nearby galaxies, particularly those in which it is possible to resolve the individual stars that contribute to the galaxy's luminosity, and to which this article exclusively refers. By necessity, the objects of the attention of this research are the Milky Way (MW), its satellites, and their neighbors within the so-called Local Group, but it is ever expanding to include the far richer sample of objects that fall within the loosely defined part of the universe referred to only as the Local Volume.

The rapid growth in interest in this field can be traced to two distinct developments that have occurred in tandem. The first is entirely observational: nearby galaxies subtend large areas on the sky and contain a high density of individually rather faint stellar sources. Thus, the advent of wide-field, digital, high-resolution, multiplexing capabilities on large telescopes (and the computational facilities to handle the resulting data-flow) has had a profound effect (and will continue to do so). The second is the result of an increased understanding of the nature of our immediate cosmic environment, facilitated in no small part by computational tools (hardware and software) that have allowed for a higher-resolution examination of the consequences of the prevailing cosmological paradigm. The discoveries and realizations that these advances have enabled are significant: the hierarchical nature of galaxy formation and the realization that some of the relics of that process may still be identifiable at $z = 0$; the quest for a better understanding of dark matter and the realization that the smallest galaxies nearest to us may be the darkest laboratories in the universe; the chemical evolution of the universe and the realization that the nucleosynthetic imprints of the earliest generations of star formation may still be found in the Galaxy and its satellites. These are but a few examples. A new phrase has developed to collectively describe the aforementioned research and its motivations, and which contrasts it with its higher-redshift cousins: "near-field cosmology."

The phrase "near-field cosmology" is relatively recent and dates from the Annual Review article of Freeman & Bland-Hawthorn (2002). As such, it is sometimes considered a new field within astrophysics as a whole, although this is grossly unfair to its early exponents. Indeed, what could be argued as two of the most important papers in astrophysics—those of Eggen et al. (1962) and Searle & Zinn (1978)—are quintessential examples of observational near-field cosmology. The former took a well-defined sample of stars for which high-quality spectroscopic and photometric data existed and from that motivated a collapse model for the formation of the Galaxy. The latter used complexities within the stellar populations of the Galactic globular cluster system to motivate a scenario where the Galaxy (or part of it) is built through the accretion of smaller stellar systems. The principle ideas from both papers continue to form critical aspects of modern galaxy formation theory.

Many more galaxies are now able to have their resolved stellar content examined than was possible at the time of these early studies. The content and structure of the Andromeda Galaxy (M31) provide an excellent comparison (and, increasingly, contrast) to our own Galaxy (e.g., Courteau et al. 2011; Huxor et al. 2011; Watkins et al. 2010; McConnachie et al. 2009; Yin et al. 2009; Ibata et al. 2007; Chapman et al. 2007; Kalirai

et al. 2006; Koch et al. 2008, and references therein). Even excluding this prominent astronomical target, however, there are still nearly a hundred or so galaxies for which their individual stars can be brought into focus by astronomers wanting to unearth fossil signatures of galactic formation.

The overwhelming majority of nearby galaxies—indeed, the overwhelming majority of galaxies in the entire universe—are dwarf galaxies. Exactly how low a luminosity or how small a mass is required before a galaxy is deemed meager enough to warrant this popular designation is generally not well defined or accepted. Kormendy (1985) famously showed that when surface brightness is plotted against luminosity for elliptical galaxies, two relations are apparently formed, one for "giant" galaxies and one for "dwarf" galaxies. This has usually been interpreted as evidence that these systems should be separated into two distinct groups (in terms of different formation mechanisms). Some more recent studies, on the other hand, suggest that there is actually a continuous sequence connecting the dwarf and giant regimes, and that the change in the form of the scaling relations with luminosity does not necessitate fundamental differences between low- and high-luminosity systems (e.g., Graham & Guzmán 2003, and references therein). With these considerations in mind, and for the purpose of this article, I consider dwarfs to have absolute visual magnitudes fainter than $M_V \sim -18$ (also adopted by Grebel et al. 2003). In what follows, this places all nearby galaxies but the MW, the Large Magellanic Cloud, M31, M33, NGC 55, and NGC 300 in the dwarf category.

The closest galaxies to the MW are its own satellites, the most prominent of which are the Large and Small Magellanic Clouds (LMC/SMC), both of which are naked-eye objects. The earliest reference to the Magellanic Clouds that survives is by the Persian astronomer Abd al-Rahman al-Sufi in his 964 work, *Book of Fixed Stars* (which also includes the earliest recorded reference to the Andromeda Galaxy). A millennium or so later, Shapley (1938a) discovered "a large rich cluster with remarkable characteristics" in the constellation of Sculptor. He speculated that it was

> ...a super-cluster of the globular type and of galactic dimensions; or a symmetrical Magellanic Cloud devoid of its characteristic bright stars, clusters, and luminous diffuse nebulosity; or a nearby spheroidal galaxy, highly resolved, and of abnormally low surface brightness. These phrases are merely different ways of describing the same thing and of pointing out the uniqueness of the object.

Over seventy years later, a large body of research still devotes itself to understanding the detailed properties and structural, chemical, and dynamical characteristics of this class of stellar system. The prototype described above is referred to as the Sculptor dwarf spheroidal (dSph) galaxy.

Excellent discussions of the observational properties of—and our astrophysical understanding of—the nearest (Local Group) dwarf galaxies can be found in a large number of dedicated review articles (e.g., Gallagher & Wyse 1994; Grebel 1997; Mateo 1998; van den Bergh 2000; Geisler et al. 2007; Tolstoy et al. 2009). The compilations of observational data presented in numerous works by S. van den Bergh, in particular van den Bergh (2000), and the Annual Review article by Mateo (1998) are particularly valuable resources for the astronomical community. Since their original publication, however, there have been notable advances (in part a product of the observational and theoretical factors described earlier). Not least of these is the *more than doubling* of the number of known galaxies in the Local Group. In the surroundings of the Local Group too, there have been significant new discoveries, and techniques and observations that used to be applicable only to the MW satellites or nearby Local Group galaxies can now be applied to these more distant relatives.

The ability to reach the resolved populations of ever more distant galaxies is important not just for the improvement in statistics that it offers, but also in terms of the increasing range of environments that it allows us to study. The overwhelming amount of detailed information regarding the stellar population properties of dwarf galaxies comes from studies of the MW satellite systems. Given the sensitivity of low-mass systems to both internal (e.g., feedback through star formation) and external (e.g., ram and tidal stripping) environmental mechanisms, this might be expected to bias our understanding toward conditions that hold only for the MW environment. Within the very nearby universe, however, there are a large number of environments able to be probed, from the surroundings of the MW and M31, to the more isolated, outlying members of the Local Group, to the very isolated dwarf galaxies that surround the Local Group, to the numerous nearby groups that populate and form our immediate neighborhood. A large number of dedicated surveys in the past few years are systematically examining galaxies in the Local Volume at a range of wavelengths, and which include among their targets some of the more distant galaxies in this sample. These surveys are obtaining precision insights into local galaxies that naturally compliment lower-resolution studies of their more numerous, but more distant, cousins (e.g., SINGS, Kennicutt et al. 2003; the Spitzer LVL, Dale et al. 2009; THINGS, Walter et al. 2008; FIGGS, Begum et al. 2008b; HST ANGRRR/ANGST, Dalcanton et al. 2009; the GALEX survey of galaxies in the Local Volume, Lee et al. 2011; the Hα survey of Kennicutt et al. 2008; and many others).

I have alluded to several motivations for pursuing studies of nearby galaxies, be they related to cosmic chemical processing, dynamical evolution, galactic formation mechanisms, environment, near-field cosmology, or a wealth of other research areas on which much can be written. It is not the purpose of this article to contribute to those discussions here; the recent Annual Review article by Tolstoy et al. (2009) provides an excellent, current overview of the status of research into many of these topics using Local Group galaxies. Rather, this article attempts to collate, homogenize, and critically review our observational understanding of aspects of the nearby populations of dwarf galaxies, with particular emphasis on the origins and uncertainties of some key observable parameters. I will discuss science topics only when such discussions relate directly to observational measurements, and those measurements, in my opinion, provide grounds for caution, or when such discussion provides a context for highlighting observational relationships between parameters. This article primarily focuses on the stellar properties of the galaxies (and derived properties, such as the implied dark matter content) and cites observations conducted mostly at ultraviolet–optical–near-infrared wavelengths, with less discussion on their gaseous and dust content. With the intense efforts currently underway to provide a more full characterization of these systems, I expect that some numbers provided in this article will be out of date by the time it is published. As such, tables presented herein will be continually updated to provide a convenient, online library of

dwarf galaxy parameters for general reference and use by the community.

The layout of the article is as follows. Section 2 describes the selection of the sample and gives a general summary of my methodology and reasoning in the construction of the data set. Section 3 reviews the discovery space of the galaxies and discusses general issues relating to distances, velocities, and the membership (or otherwise) of larger-scale groups/sub-groups. Section 4 reviews the observed photometric and structural characteristics of the sample and discusses aspects of the scaling relations that they define. Section 5 reviews their masses (stellar, H I, and dynamical) and internal kinematics and discusses issues related to morphological classifications and our dynamical understanding of the sample. Section 6 presents a compilation of available mean stellar metallicities and discusses associated observational trends. Section 7 concludes and summarizes.

2. CONSTRUCTING THE DATA SET

The sample of galaxies discussed in this article consists of all known galaxies with distances determined from measurements of resolved stellar populations (usually Cepheids, RR Lyrae, tip of the red giant branch, TRGB, but also including horizontal branch level and main-sequence fitting; see Tammann et al. 2008 for a thorough discussion of the former three methods and references) that place them within 3 Mpc of the Sun. Consequently, this sample contains the satellite systems of two major galaxies (the MW and M31), the quasi-isolated, outlying members of the Local Group, and the nearby isolated dwarf galaxies that do not clearly belong to any major galaxy grouping. It is therefore expected that this sample may be valuable (as, indeed, various individual members and sub-sets have already proven valuable) for examining the role played by environment in dwarf galaxy evolution, as discussed in Section 1. There is also a practical motivation for the choice of distance limit, namely, that a much larger threshold will start to select members of nearby groups (the closest of which is the Maffei group at ∼3 Mpc, although its awkward location at low Galactic latitudes prevents accurate distances from being determined for its members; see Fingerhut et al. 2007) and would expand the scope of this article considerably.

Of course, there are no solid boundaries between galaxy groups, filaments, and the field, and some of the galaxies discussed herein are likely dynamically associated with neighboring structures like the Sculptor (e.g., Karachentsev et al. 2003a) or IC 342 (e.g., Karachentsev et al. 2003b) groups, for example. Nevertheless, at the time of writing, the adoption of these selection criteria identifies exactly 100 galaxies (not including the MW and M31), of which 73 are definite or very likely members of the Local Group. It is likely that our basic knowledge of all of these galaxies and their resolved stellar content can be improved dramatically over the coming years with existing observational capabilities, and the more distant galaxies provide stepping stones into the Local Volume for future resolved stellar population studies enabled by next-generation facilities like the 30 m class telescopes. It is with an eye to the latter considerations that the distance is not limited to the zero-velocity surface of the Local Group ($R_{\rm LG}$).

The ensuing discussion will focus on dwarf galaxies. Of the 102 galaxies that are listed in the subsequent tables, virtually no discussion will be given to the MW and M31, and numbers relating to M33, NGC 55, and NGC 300 are included for completeness only. The same caveat applies to the Magellanic Clouds, since here the research body and available data are so extensive and far exceed those that exists for most other dwarf-like systems that the reader is referred to the many review articles, books, and conferences that deal specifically with these bodies (e.g., Westerlund 1997; van Loon & Oliveira 2009, and references therein).

In compiling this catalog of galaxies, and in addition to the papers cited in each table, I have made extensive use of the NASA Extragalactic Database, the HyperLeda database (Paturel et al. 2003), Mateo (1998), van den Bergh (2000), and Karachentsev et al. (2004). The requirement that all galaxies have distances based on resolved stellar populations leads to the exclusion of a few galaxies that have low velocities that could potentially place them within 3 Mpc, but which lack any direct distance measurement (e.g., see Table 1 of Karachentsev et al. 2004). The low-latitude galaxy Dwingeloo 1 is also excluded by this criterion, since its distance of ∼2.8 Mpc is based on a Tully–Fisher estimate (Karachentsev et al. 2003b; this galaxy is very likely a member of the Maffei group). The (uncertain) TRGB measurement of MCG9-20-1 by Dalcanton et al. (2009) places it at a distance of ∼1.6 Mpc, although its radial velocity of $v_{\odot} \sim 954$ km s^{-1} is very high if it is really this close, and the photometric data now seem to favor a larger distance (K. Gilbert & J. Dalcanton 2011, private communication), so it too has been excluded from the list. Finally, there are a few galaxies for which it is unclear if they lie closer or farther than 3 Mpc (e.g., UGCA 92, $D = 3.01 \pm 0.24$ Mpc; Karachentsev et al. 2006). I exclude such galaxies, even if the quoted uncertainties would bring them within range of the distance cut. Of course, if future estimates should clearly indicate a closer distance, then the online version of the tables will be updated as appropriate.

In compiling these references, I have favored, where possible, papers that are based on analysis of the resolved stellar populations. In the interest of homogeneity and in an (ill-fated) attempt to minimize the inevitable systematic differences between measurements for different galaxies, I also generally try to limit the number of distinct publications, studies, and/or methodologies that contribute to the overall data set, favoring large surveys of multiple galaxies in preference to studies of individual galaxies. However, if there appear to be significant discrepancies in the literature over observed values, then these differences are indicated either in the footnotes and/or in the text. Infrequently, I have estimated uncertainties where none were given in the original publications.

My primary intent in compiling this data set is to provide useful information on the population of (dwarf) galaxies in the nearby universe. I have tried to ensure that the references collected herein—while not complete in any way—are generally recent enough and relevant enough that I hope they will be able to provide the reader with a starting point from which most of the germane literature can be traced.

3. BASIC PROPERTIES, POSITIONS, AND VELOCITIES

Table 1 lists basic information for all nearby galaxies that satisfy the selection criteria discussed in the previous section.

Column 1. Galaxy name.
Column 2. Common alternative names.
Column 3. Indicator whether they are associated with MW [G], M31 [A], the Local Group [L], or are nearby neighbors [N].
Column 4. Morphological (Hubble) type. The distinction between dwarf elliptical (dE) and dwarf spheroidal (dSph) is based

Table 1
Basic Information

(1) Galaxy	(2) Other Names	(3)	(4)	(5) R.A. J2000	(6) Decl. J2000	(7) Original Publication	(8) Comments
The MW sub-group (in order of distance from the MW)							
The Galaxy	The MW	G	S(B)bc	$17^h45^m40\overset{s}{.}0$	$-29^d00^m28^s$	...	Position refers to Sgr A*
Canis Major		G	????	$07^h12^m35\overset{s}{.}0$	$-27^d40^m00^s$	Martin et al. (2004a)	MW disk substructure?
Sagittarius dSph		G	dSph	$18^h55^m19\overset{s}{.}5$	$-30^d32^m43^s$	Ibata et al. (1994)	Tidally disrupting
Segue (I)		G	dSph	$10^h07^m04\overset{s}{.}0$	$+16^d04^m55^s$	Belokurov et al. (2007)	
Ursa Major II		G	dSph	$08^h51^m30\overset{s}{.}0$	$+63^d07^m48^s$	Zucker et al. (2006a)	
Bootes II		G	dSph	$13^h58^m00\overset{s}{.}0$	$+12^d51^m00^s$	Walsh et al. (2007)	
Segue II		G	dSph	$02^h19^m16\overset{s}{.}0$	$+20^d10^m31^s$	Belokurov et al. (2009)	
Willman 1	SDSS J1049+5103	G	dSph	$10^h49^m21\overset{s}{.}0$	$+51^d03^m00^s$	Willman et al. (2005a)	Cluster?
Coma Berenices		G	dSph	$12^h26^m59\overset{s}{.}0$	$+23^d54^m15^s$	Belokurov et al. (2007)	
Bootes III		G	dSph?	$13^h57^m12\overset{s}{.}0$	$+26^d48^m00^s$	Grillmair (2009)	Very diffuse. Tidal remnant?
LMC	Nubecula Major	G	Irr	$05^h23^m34\overset{s}{.}5$	$-69^d45^m22^s$	...	
SMC	Nubecula Minor NGC 292	G	dIrr	$00^h52^m44\overset{s}{.}8$	$-72^d49^m43^s$	...	
Bootes (I)		G	dSph	$14^h00^m06\overset{s}{.}0$	$+14^d30^m00^s$	Belokurov et al. (2006)	
Draco	UGC 10822 DDO 208	G	dSph	$17^h20^m12\overset{s}{.}4$	$+57^d54^m55^s$	Wilson (1955)	
Ursa Minor	UGC 9749 DDO 199	G	dSph	$15^h09^m08\overset{s}{.}5$	$+67^d13^m21^s$	Wilson (1955)	
Sculptor		G	dSph	$01^h00^m09\overset{s}{.}4$	$-33^d42^m33^s$	Shapley (1938a)	The prototypical dSph
Sextans (I)		G	dSph	$10^h13^m03\overset{s}{.}0$	$-01^d36^m53^s$	Irwin et al. (1990)	
Ursa Major (I)		G	dSph	$10^h34^m52\overset{s}{.}8$	$+51^d55^m12^s$	Willman et al. (2005b)	
Carina		G	dSph	$06^h41^m36\overset{s}{.}7$	$-50^d57^m58^s$	Cannon et al. (1977)	
Hercules		G	dSph	$16^h31^m02\overset{s}{.}0$	$+12^d47^m30^s$	Belokurov et al. (2007)	Tidally disrupting? Remnant? Cluster?
Fornax		G	dSph	$02^h39^m59\overset{s}{.}3$	$-34^d26^m57^s$	Shapley (1938b)	
Leo IV		G	dSph	$11^h32^m57\overset{s}{.}0$	$-00^d32^m00^s$	Belokurov et al. (2007)	Binary w/ Leo V?
Canes Venatici II	SDSS J1257+3419	G	dSph	$12^h57^m10\overset{s}{.}0$	$+34^d19^m15^s$	Sakamoto & Hasegawa (2006) Belokurov et al. (2007)	
Leo V		G	dSph	$11^h31^m09\overset{s}{.}6$	$+02^d13^m12^s$	Belokurov et al. (2008)	Cluster? Binary w/ Leo IV?
Pisces II		G	dSph	$22^h58^m31\overset{s}{.}0$	$+05^d57^m09^s$	Belokurov et al. (2010)	Awaiting spectr. confirmation
Canes Venatici (I)		G	dSph	$13^h28^m03\overset{s}{.}5$	$+33^d33^m21^s$	Zucker et al. (2006b)	
Leo II	Leo B UGC 6253 DDO 93	G	dSph	$11^h13^m28\overset{s}{.}8$	$+22^d09^m06^s$	Harrington & Wilson (1950)	
Leo I	UGC 5470 DDO 74 Regulus Dwarf	G/L	dSph	$10^h08^m28\overset{s}{.}1$	$+12^d18^m23^s$	Harrington & Wilson (1950)	
The M31 sub-group (in order of distance from M31)							
Andromeda	M31 NGC 224 UGC 454	A	Sb	$00^h42^m44\overset{s}{.}3$	$+41^d16^m09^s$	...	
M32	NGC 221 UGC 452	A	cE	$00^h42^m41\overset{s}{.}8$	$+40^d51^m55^s$	Legentil (1755)	
Andromeda IX		A	dSph	$00^h52^m53\overset{s}{.}0$	$+43^d11^m45^s$	Zucker et al. (2004)	

Table 1
(Continued)

(1) Galaxy	(2) Other Names	(3)	(4)	(5) R.A. J2000	(6) Decl. J2000	(7) Original Publication	(8) Comments
NGC 205	M110 UGC 426	A	dE/dSph	$00^h40^m22^s.1$	$+41^d41^m07^s$	Messier (1798)	
Andromeda XVII		A	dSph	$00^h37^m07^s.0$	$+44^d19^m20^s$	Irwin et al. (2008)	
Andromeda I		A	dSph	$00^h45^m39^s.8$	$+38^d02^m28^s$	van den Bergh (1972)	
Andromeda XXVII		A	dSph	$00^h37^m27^s.1$	$+45^d23^m13^s$	Richardson et al. (2011)	Tidally disrupting? Remnant?
Andromeda III		A	dSph	$00^h35^m33^s.8$	$+36^d29^m52^s$	van den Bergh (1972)	
Andromeda XXV		A	dSph	$00^h30^m08^s.9$	$+46^d51^m07^s$	Richardson et al. (2011)	
Andromeda XXVI		A	dSph	$00^h23^m45^s.6$	$+47^d54^m58^s$	Richardson et al. (2011)	
Andromeda XI		A	dSph	$00^h46^m20^s.0$	$+33^d48^m05^s$	Martin et al. (2006)	
Andromeda V		A	dSph	$01^h10^m17^s.1$	$+47^d37^m41^s$	Armandroff et al. (1998)	
Andromeda X		A	dSph	$01^h06^m33^s.7$	$+44^d48^m16^s$	Zucker et al. (2007)	
Andromeda XXIII		A	dSph	$01^h29^m21^s.8$	$+38^d43^m08^s$	Richardson et al. (2011)	
Andromeda XX		A	dSph	$00^h07^m30^s.7$	$+35^d07^m56^s$	McConnachie et al. (2008)	
Andromeda XII		A/L	dSph	$00^h47^m27^s.0$	$+34^d22^m29^s$	Martin et al. (2006)	Unbound to M31?
NGC 147	UGC 326 DDO 3	A	dE/dSph	$00^h33^m12^s.1$	$+48^d30^m32^s$	Herschel (1833)	Binary w/ NGC 185? Tidal stream
Andromeda XXI		A	dSph	$23^h54^m47^s.7$	$+42^d28^m15^s$	Martin et al. (2009)	
Andromeda XIV		A/L	dSph	$00^h51^m35^s.0$	$+29^d41^m49^s$	Majewski et al. (2007)	Unbound to M31? In Pisces
Andromeda XV		A	dSph	$01^h14^m18^s.7$	$+38^d07^m03^s$	Ibata et al. (2007)	
Andromeda XIII		A	dSph	$00^h51^m51^s.0$	$+33^d00^m16^s$	Martin et al. (2006)	In Pisces
Andromeda II		A	dSph	$01^h16^m29^s.8$	$+33^d25^m09^s$	van den Bergh (1972)	In Pisces
NGC 185	UGC 396	A	dE/dSph	$00^h38^m58^s.0$	$+48^d20^m15^s$	Herschel (1789)	Binary w/ NGC 147?
Andromeda XXIX		A	dSph	$23^h58^m55^s.6$	$+30^d45^m20^s$	Bell et al. (2011)	In Pegasus
Andromeda XIX		A	dSph	$00^h19^m32^s.1$	$+35^d02^m37^s$	McConnachie et al. (2008)	
Triangulum	M33 NGC 598 UGC 1117	A	Sc	$01^h33^m50^s.9$	$+30^d39^m37^s$	[a]	
Andromeda XXIV		A	dSph	$01^h18^m30^s.0$	$+46^d21^m58^s$	Richardson et al. (2011)	
Andromeda VII	Casseopia dSph	A	dSph	$23^h26^m31^s.7$	$+50^d40^m33^s$	Karachentsev & Karachentseva (1999)	
Andromeda XXII		A	dSph	$01^h27^m40^s.0$	$+28^d05^m25^s$	Martin et al. (2009)	M33 satellite? In Pisces
IC 10	UGC 192	A	dIrr	$00^h20^m17^s.3$	$+59^d18^m14^s$	Swift (1888)	
LGS 3 (Local Group Suspect 3)	Pisces (I)	A	dIrr/dSph	$01^h03^m55^s.0$	$+21^d53^m06^s$	Karachentseva (1976) Kowal et al. (1978)	
Andromeda VI	Pegasus dSph	A	dSph	$23^h51^m46^s.3$	$+24^d34^m57^s$	Karachentsev & Karachentseva (1999) Armandroff et al. (1999)	
Andromeda XVI		A/L	dSph	$00^h59^m29^s.8$	$+32^d22^m36^s$	Ibata et al. (2007)	In Pisces
The rest of the Local Group and its neighbors (in order of distance from the barycenter of the Local Group)							
Andromeda XXVIII		A/L	dSph?	$22^h32^m41^s.2$	$+31^d12^m58^s$	Slater et al. (2011)	In Pegasus
IC 1613	DDO 8 UGC 668	L	dIrr	$01^h04^m47^s.8$	$+02^d07^m04^s$	Wolf (1906)	
Phoenix		L/G	dIrr/dSph	$01^h51^m06^s.3$	$-44^d26^m41^s$	Schuster & West (1976)[b]	
NGC 6822	IC 4895 DDO 209 Barnard's Galaxy	L/G	dIrr	$19^h44^m56^s.6$	$-14^d47^m21^s$	Barnard (1884)	Polar ring morph.

Table 1
(Continued)

(1) Galaxy	(2) Other Names	(3)	(4)	(5) R.A. J2000	(6) Decl. J2000	(7) Original Publication	(8) Comments
Cetus		L	dSph	$00^h26^m11\overset{s}{.}0$	$-11^d02^m40^s$	Whiting et al. (1999)	Isolated dSph
Pegasus dIrr	UGC 12613 DDO 216	L/A	dIrr/dSph	$23^h28^m36\overset{s}{.}3$	$+14^d44^m35^s$	A. G. Wilson. Reported in Holmberg (1958)	
Leo T		L/G	dIrr/dSph	$09^h34^m53\overset{s}{.}4$	$+17^d03^m05^s$	Irwin et al. (2007)	
WLM (Wolf-Lundmark--Melotte)	UGCA 444 DDO 221	L	dIrr	$00^h01^m58\overset{s}{.}2$	$-15^d27^m39^s$	Wolf (1910) Melotte (1926), including K. E. Lundmark	Defines R_{LG}
Leo A	Leo III UGC 5364 DDO 69	L	dIrr	$09^h59^m26\overset{s}{.}5$	$+30^d44^m47^s$	Zwicky (1942)	Defines R_{LG}
Andromeda XVIII		L	dSph	$00^h02^m14\overset{s}{.}5$	$+45^d05^m20^s$	McConnachie et al. (2008)	Isolated dSph
Aquarius	DDO 210	L	dIrr/dSph	$20^h46^m51\overset{s}{.}8$	$-12^d50^m53^s$	van den Bergh (1959)	Defines R_{LG}
Tucana		L	dSph	$22^h41^m49\overset{s}{.}6$	$-64^d25^m10^s$	Lavery (1990)[c]	Isolated dSph; defines R_{LG}
Sagittarius dIrr	UKS 1927-177	L	dIrr	$19^h29^m59\overset{s}{.}0$	$-17^d40^m41^s$	Cesarsky et al. (1977) Longmore et al. (1978)	Defines R_{LG}
UGC 4879	VV 124	L	dIrr/dSph	$09^h16^m02\overset{s}{.}2$	$+52^d50^m24^s$	Kopylov et al. (2008)[d]	Defines R_{LG}
NGC 3109	DDO 236 UGCA 194	N	dIrr	$10^h03^m06\overset{s}{.}9$	$-26^d09^m35^s$	Herschel (1847)	Loose NGC 3109 subgroup. Interacting with Antlia?
Sextans B	UGC 5373 DDO 70	N	dIrr	$10^h00^m00\overset{s}{.}1$	$+05^d19^m56^s$	A. G. Wilson? See Holmberg (1958)[e]	Loose NGC 3109 subgroup
Antlia		N	dIrr	$10^h04^m04\overset{s}{.}1$	$-27^d19^m52^s$	Whiting et al. (1997)[f]	Loose NGC 3109 subgroup. Interacting with NGC 3109?
Sextans A	UGCA 205 DDO 75	N	dIrr	$10^h11^m00\overset{s}{.}8$	$-04^d41^m34^s$	Zwicky (1942)	Loose NGC 3109 sub-group
HIZSS 3(A)		N	(d)Irr?	$07^h00^m29\overset{s}{.}3$	$-04^d12^m30^s$	Henning et al. (2000)[g]	Zone of obscuration. Binary with B?
HIZSS 3B		N	(d)Irr?	$07^h00^m29\overset{s}{.}3$	$-04^d12^m30^s$	Henning et al. (2000)[h]	Zone of obscuration. Binary with A?
KKR 25		N	dIrr/dSph	$16^h13^m48\overset{s}{.}0$	$+54^d22^m16^s$	Karachentsev et al. (2001b)	
ESO 410- G 005	UKS 0013-324	N	dIrr/dSph	$00^h15^m31\overset{s}{.}6$	$-32^d10^m48^s$	Lauberts (1982) Longmore et al. (1982)	NGC 55 sub-group, forming "bridge" to Sculptor?
NGC 55		N	Irr	$00^h14^m53\overset{s}{.}6$	$-39^d11^m48^s$	Dunlop (1828)	NGC 55 sub-group, forming "bridge" to Sculptor?
ESO 294- G 010		N	dIrr/dSph	$00^h26^m33\overset{s}{.}4$	$-41^d51^m19^s$	Lauberts (1982)	NGC 55 sub-group, forming "bridge" to Sculptor?
NGC 300		N	Sc	$00^h54^m53\overset{s}{.}5$	$-37^d41^m04^s$	Dunlop (1828)	NGC 55 sub-group, forming "bridge" to Sculptor?
IC 5152		N	dIrr	$22^h02^m41\overset{s}{.}5$	$-51^d17^m47^s$	D. Stewart. Reported in Pickering (1899)	
KKH 98		N	dIrr	$23^h45^m34\overset{s}{.}0$	$+38^d43^m04^s$	Karachentsev et al. (2001a)	
UKS 2323-326	UGCA 438	N	dIrr	$23^h26^m27\overset{s}{.}5$	$-32^d23^m20^s$	Longmore et al. (1978)	NGC 55 sub-group, forming "bridge" to Sculptor?
KKR 3	KK 230	N	dIrr	$14^h07^m10\overset{s}{.}5$	$+35^d03^m37^s$	Karachentseva & Karachentsev (1998)[i]	Member of the Canes Venatici I cloud
GR 8	UGC 8091 VV 558 DDO 155	N	dIrr	$12^h58^m40\overset{s}{.}4$	$+14^d13^m03^s$	Reaves (1956)[j]	Gibson Reaves gave this galaxy his initials
UGC 9128	DDO 187	N	dIrr	$14^h15^m56\overset{s}{.}5$	$+23^d03^m19^s$	van den Bergh (1959)	
UGC 8508		N	dIrr	$13^h30^m44\overset{s}{.}4$	$+54^d54^m36^s$	Vorontsov-Vel'Yaminov & Krasnogorskaya (1962)	
IC 3104	ESO 020- G 004 UKS 1215-794	N	dIrr	$12^h18^m46\overset{s}{.}0$	$-79^d43^m34^s$	D. Stewart. Reported in Pickering (1908)	
DDO 125	UGC 7577	N	dIrr	$12^h27^m40\overset{s}{.}9$	$+43^d29^m44^s$	van den Bergh (1959)	
UGCA 86		N	dIrr	$03^h59^m48\overset{s}{.}3$	$+67^d08^m19^s$	Nilson (1974)	Companion of IC 342
DDO 99	UGC 6817	N	dIrr	$11^h50^m53\overset{s}{.}0$	$+38^d52^m49^s$	van den Bergh (1959)	
IC 4662	ESO 102- G 014	N	dIrr	$17^h47^m08\overset{s}{.}8$	$-64^d38^m30^s$	R. Innes. Reported in Lunt (1902)	

Table 1
(Continued)

(1) Galaxy	(2) Other Names	(3)	(4)	(5) R.A. J2000	(6) Decl. J2000	(7) Original Publication	(8) Comments
DDO 190	UGC 9240	N	dIrr	$14^h24^m43\overset{s}{.}4$	$+44^d31^m33^s$	van den Bergh (1959)	
KKH 86		N	dIrr	$13^h54^m33\overset{s}{.}5$	$+04^d14^m35^s$	Karachentsev et al. (2001a)	
NGC 4163	UGC 7199 NGC 4167[k]	N	dIrr	$12^h12^m09\overset{s}{.}1$	$+36^d10^m09^s$	Herschel (1789)	
DDO 113	UGCA 276 KDG 90	N	dIrr	$12^h14^m57\overset{s}{.}9$	$+36^d13^m08^s$	van den Bergh (1959)	

Notes.

[a] Discovery credited to G. B. Hodierna (see Steinicke 2010).

[b] Originally thought to be a globular cluster. Canterna & Flower (1977) subsequently identified its galactic nature.

[c] This author first suggested that this object is a member of the Local Group, but it had previously been cataloged by Corwin et al. (1985).

[d] These authors calculate a new distance to UGC 4879 and show that it is on the periphery of the Local Group. While included in the "Atlas and Catalog of Interacting Galaxies" by Vorontsov-Velyaminov (1959), earlier references to this object have not been found.

[e] Holmberg (1958) credits Wilson (1955) with discovery, but this object is not listed in this manuscript.

[f] These authors rediscovered this galaxy and showed that it was in the periphery of the Local Group, but it had earlier been cataloged by Corwin et al. (1985), Feitzinger & Galinski (1985), and Arp & Madore (1987).

[g] HIZSS 3 resolved into two sources by Begum et al. (2005). Position corresponds to the "HIZSS3 system."

[h] HIZSS 3 resolved into two sources by Begum et al. (2005). Position corresponds to the "HIZSS3 system."

[i] See also Karachentseva et al. (1999).

[j] Discovered on inspection of photographic plates from a survey discussed in Shane (1947). C. D. Shane speculated that some of the nebulae that were visible could be Local Group dwarf galaxies.

[k] The original coordinates of NGC 4167 are coincident with the coordinates of NGC 4163, but Sulentic & Tifft (1973) note that NGC 4167 is "non-existent."

solely on luminosity and is therefore somewhat arbitrary. Objects fainter than $M_V \sim -18$ are given a "d" (dwarf) prefix and are again somewhat arbitrary.
Columns 5 and 6. Celestial coordinates (J2000).
Column 7. Original publication. For more details relating to the discoveries of the NGC/IC galaxies, the reader is referred to Steinicke (2010).[1]
Column 8. Comments.

Table 2 lists position and velocity information for the galaxy sample.

Column 1. Galaxy name.
Columns 2 and 3. Galactic coordinates (l, b).
Column 4. Foreground extinction, $E(B-V)$: these correspond to values derived by Schlegel et al. (1998) from an all-sky COBE/DIRBE and IRAS/ISSA 100 μm map, at the coordinates of the centroid of each galaxy. While Schlegel et al. (1998) estimate that values for $E(B-V)$ are generally accurate to 16%, a major (and sometimes overlooked, including by this author!) caveat for their use in the direction of nearby (large) galaxies is that the brightest galaxies at *IRAS* 60 μm[2] were excised from these maps and replaced by the "most likely value" of the underlying 100 μm emission (see Section 4.2 of Schlegel et al. 1998). The resulting values are not, therefore, directly observed, and any variation across the area occupied by the galaxy is not traced by these maps. For this compilation, the affected galaxies are NGC 6822, IC 1613, M33, NGC 205, NGC 3109, NGC 55, and NGC 300. The LMC, SMC, and M31 (and by necessity also M32) were not excised.
Columns 5 and 6. Distance modulus, heliocentric distance: all distance moduli are based on resolved stellar population analysis (generally Cepheid, RR Lyrae, or TRGB measurements, but also horizontal branch level and main-sequence fitting). Note that many TRGB estimates do not include the formal uncertainty in the absolute magnitude of the TRGB (Bellazzini et al. 2001, 2004a; Rizzi et al. 2007).
Column 7. Heliocentric velocity: for most Local Group galaxies, the velocity corresponds to the optical velocity of the galaxy. For some of the more distant galaxies, velocities are measured from H I.
Columns 8–10. Distance–velocity pairs for the Galactocentric (MW), M31, and Local Group frames of reference: these are calculated by first assuming that the barycenter of the Local Group is located at the mid point of the vector connecting the MW and M31 (for an adopted M31 distance modulus of $(m-M)_0 = 24.47$; McConnachie et al. 2005). The latter galaxy is more luminous (e.g., Hammer et al. 2007, and references therein), but dynamical mass estimates for both of these galaxies have produced conflicting results regarding which is more massive (e.g., Little & Tremaine 1987; Kochanek 1996; Wilkinson & Evans 1999; Evans & Wilkinson 2000; Evans et al. 2000; Klypin et al. 2002; Ibata et al. 2004; Geehan et al. 2006; Watkins et al. 2010; McMillan 2011), a result nearly exclusively due to the lack of a sufficient number of dynamical tracers at large radii. Given this uncertainty, I conclude that assuming their masses to be roughly the same is reasonable, simple, and convenient. Velocities are converted to the Local Group frame using the solar apex derived by Karachentsev & Makarov (1996) and subtracting the component of the MW's velocity in the direction of each dwarf. M31-centric velocities are obtained by subtracting the component of the Local Group centric velocity of M31 in the direction of each dwarf. Galactocentric distances and velocities are calculated in the usual way, for an adopted Galactic rotation velocity at the Sun of 220 km s^{-1} at a radius of 8.5 kpc from the Galactic center.
Column 11. References.

Figure 1 shows Aitoff projections of the Galactic coordinates of all galaxies in the sample. The top panel shows only those objects identified as definite or likely MW satellites, the middle panel shows definite or likely M31 sub-group members (blue points) and quasi-isolated Local Group galaxies (green points), and the bottom panel shows galaxies surrounding the Local Group within a distance of 3 Mpc. Some confirmed members of all galaxy groups within 5 Mpc are also shown in the bottom panel (gray points) to highlight the location of the Local Group and its neighbors with respect to these nearby structures (Karachentsev 2005). In this respect, it is important to highlight the work of I. Karachentsev, B. Tully, and their colleagues in both the identification of nearby galaxies and groups and the determination of accurate distances to many of our neighbors in order to understand the structure of the Local Volume (e.g., see Karachentsev & Tikhonov 1994; Karachentsev et al. 2003a, 2004; Tully 1987; Tully et al. 2006, 2009).

3.1. Membership of the MW Sub-group

Figure 2 shows Galactocentric velocity versus distance for all galaxies within 600 kpc for which necessary data exist. Here, the Galactocentric velocity listed in Table 2 has been multiplied by a factor of $\sqrt{3}$ to provide a crude estimate of the unknown tangential velocities of these galaxies. Dashed curves show the escape velocity from a $10^{12}\,M_\odot$ point mass (a reasonable approximation to the escape velocity curve of the MW for the purposes of this discussion). The vertical dashed line indicates the approximate cosmological virial radius of the MW, $R_{\rm vir} \sim 300$ kpc (Klypin et al. 2002; these authors define $R_{\rm vir}$ as the radius within which the mean density of the model dark matter halo is a factor $\Delta \simeq 340$ larger than the critical density of the universe).

With the obvious caveat regarding the generally unknown tangential components of the velocities of the galaxies, Figure 2 can be used to define membership of the MW subgroup. In particular, all galaxies within 300 kpc of the MW are likely bound satellites. This is with the exception of Leo I, which may be unbound unless its tangential components are significantly overestimated (also see Mateo et al. 2008; Sohn et al. 2007; Zaritsky et al. 1989, and references therein). Leo T, NGC 6822, and Phoenix may all be bound in this simple model, but their large distance from the MW makes their membership of the MW subgroup ambiguous. I note that no potential satellite of the MW or M31 (Section 3.2) is clearly unbound as a result of the magnitude of its radial velocity alone; all the potential satellites with large radial velocities relative to their host may be bound if their tangential velocities are sufficiently small. For the purpose of the classification in Column 3 of Table 1, and in the forthcoming discussion, I only include as definite MW satellites those objects that are bound by the dashed curves in Figure 2 and which have $D_G \leqslant R_{\rm vir}$. It is interesting to note that the radial distribution of satellites is such that they are found at all radii out to ~280 kpc from the MW, at which point there is a notable gap in the distribution until the next set of objects

[1] See also http://www.klima-luft.de/steinicke/index_e.htm
[2] Specifically, the 70 galaxies listed in Table 2 of Rice et al. (1988) with fluxes greater than or equal to 0.6 Jy.

Table 2
Positions and Velocities

(1) Galaxy	(2) l	(3) b	(4) $E(B-V)$	(5) $(m-M)_o$		(6) $D_\odot$ (kpc)		(7) $v_\odot$ (km s^{-1})		(8) $[D_{MW},v_M W]$ (kpc, km s^{-1})	(9) $[D_{M31},v_{M31}]$ (kpc, km s^{-1})	(10) $[D_{\rm LG},v_{\rm LG}]$ (kpc, km s^{-1})	(11) References[a]
The Galaxy													
Canis Major[b]	240.0	−8.0	0.264	14.29	0.30	7	1	87.0[c]	4.0	[13, −117]	[786, −185]	[394, −172]	(1) (2)
Sagittarius dSph	5.6	−14.2	0.153	17.10	0.15	26	2	140.0	2.0	[18, 169]	[791, 149]	[400, 159]	(3) (4)
Segue (I)	220.5	+50.4	0.031	16.80	0.20	23	2	208.5	0.9	[28, 113]	[792, 56]	[401, 69]	(5) (6)
Ursa Major II	152.5	+37.4	0.094	17.50	0.30	32	4	−116.5	1.9	[38, −33]	[771, 11]	[380, −3]	(7) (8)
Bootes II	353.7	+68.9	0.031	18.10	0.06	42	1	−117.0	5.2	[40, −116]	[807, −174]	[416, −156]	(9) (10)
Segue II	149.4	−38.1	0.185	17.70	0.10	35	2	−39.2	2.5	[41, 43]	[753, 141]	[361, 112]	(11)
Willman 1	158.6	+56.8	0.014	17.90	0.40	38	7	−12.3	2.5	[43, 35]	[780, 44]	[390, 41]	(12) (13)
Coma Berenices	241.9	+83.6	0.017	18.20	0.20	44	4	98.1	0.9	[45, 82]	[802, 32]	[412, 46]	(5) (8)
Bootes III	35.4	+75.4	0.021	18.35	0.1	47	2	197.5	3.8	[46, 240]	[800, 207]	[410, 219]	(14) (15)
LMC	280.5	−32.9	0.926	18.52	0.09	51	2	262.2[d]	3.4	[50, 68]	[811, −6]	[421, 12]	(16)[e] (17)
SMC	302.8	−44.3	0.419	19.03	0.12	64	4	145.6[f]	0.6	[61, 5]	[811, −48]	[422, −35]	(18)[g] (19)
Bootes (I)	358.1	+69.6	0.017	19.11	0.08	66	2	99.0	2.1	[64, 106]	[819, 51]	[430, 69]	(20) (13)
Draco	86.4	+34.7	0.027	19.40	0.17	76	6	−291.0	0.1	[76, −96]	[754, −32]	[366, −46]	(21) (22)
Ursa Minor	105.0	+44.8	0.032	19.40	0.10	76	3	−246.9	0.1	[78, −85]	[758, −31]	[370, −44]	(23)[h] (24)
Sculptor	287.5	−83.2	0.018	19.67	0.14	86	6	111.4	0.1	[86, 79]	[765, 106]	[379, 97]	(25) (26)
Sextans (I)	243.5	+42.3	0.047	19.67	0.10	86	4	224.2	0.1	[89, 72]	[839, −14]	[450, 6]	(27)[i] (26)
Ursa Major (I)	159.4	+54.4	0.020	19.93	0.10	97	4	−55.3	1.4	[102, −7]	[777, 4]	[391, 0]	(28) (8)
Carina	260.1	−22.2	0.061	20.11	0.13	105	6	222.9	0.1	[107, 7]	[841, −70]	[454, −53]	(29) (26)
Hercules	28.7	+36.9	0.063	20.60	0.20	132	12	45.2	1.1	[126, 145]	[826, 133]	[444, 141]	(30) (31)
Fornax	237.1	−65.7	0.021	20.84	0.18	147	12	55.3	0.1	[149, −33]	[772, −24]	[394, −30]	(29) (26)
Leo IV	264.4	+57.4	0.026	20.94	0.09	154	6	132.3	1.4	[155, 13]	[899, −78]	[513, −54]	(32) (8)
Canes Venatici II	113.6	+82.7	0.010	21.02	0.06	160	4	−128.9	1.2	[161, −95]	[837, −122]	[458, −113]	(33) (8)
Leo V	261.9	+58.5	0.027	21.25	0.12	178	10	173.3	3.1	[179, 59]	[915, −30]	[530, −7]	(34)
Pisces II	79.2	−47.1	0.065	21.30:		182:		...	...	[181, —]	[660, —]	[285, —]	(35)
Canes Venatici (I)	74.3	+79.8	0.014	21.69	0.10	218	10	30.9	0.6	[218, 78]	[864, 54]	[493, 62]	(36) (8)
Leo II	220.2	+67.2	0.017	21.84	0.13	233	14	78.0	0.1	[236, 24]	[901, −29]	[529, −16]	(37)[j] (22)
Leo I	226.0	+49.1	0.036	22.02	0.13	254	15	282.5	0.1	[258, 174]	[922, 111]	[551, 125]	(38) (39)
Andromeda	121.2	−21.6	0.684	24.47	0.07	783	25	−300.0	4.0	[787, −122]	[0, 0]	[392, −34]	(40) (41)
M32	121.2	−22.0	0.154	24.53	0.21	805	78	−199.0	6.0	[809, −22]	[23, 100]	[414, 67]	(42) (43)
Andromeda IX	123.2	−19.7	0.075	24.42	0.07	766	25	−207.7	2.7	[770, −32]	[40, 90]	[375, 56]	(40) (44)
NGC 205	120.7	−21.1	0.085	24.58	0.07	824	27	−246.0	1.0	[828, −67]	[42, 56]	[433, 22]	(40) (45)
Andromeda XVII	120.2	−18.5	0.074	24.50	0.10	794	37	...	...	[798, —]	[45, —]	[404, —]	(46)
Andromeda I	121.7	−24.8	0.053	24.36	0.07	745	24	−375.8	1.4	[749, −204]	[58, −82]	[355, −116]	(40) (47)
Andromeda XXVII	120.4	−17.4	0.080	24.59	0.12	828	46	...	...	[832, —]	[75, —]	[439, —]	(48)
Andromeda III	119.4	−26.3	0.056	24.37	0.07	748	24	−345.6	1.8	[752, −171]	[75, −49]	[360, −83]	(40) (47)
Andromeda XXV	119.2	−15.9	0.101	24.55	0.12	813	45	...	...	[817, —]	[88, —]	[426, —]	(48)
Andromeda XXVI	118.1	−14.7	0.110	24.41	0.12	762	42	...	...	[766, —]	[103, —]	[377, —]	(48)
Andromeda XI	121.7	−29.1	0.080	24.40	$^{+0.2}_{-0.5}$	759	$^{+70}_{-175}$	−419.6	4.4	[763, −255]	[104, −134]	[374, −167]	(44)
Andromeda V	126.2	−15.1	0.125	24.44	0.08	773	28	−403.0	4.0	[778, −229]	[110, −109]	[389, −143]	(40) (49)
Andromeda X	125.8	−18.0	0.129	24.23	0.21	701	68	−163.8	1.2	[706, 8]	[110, 128]	[314, 95]	(50) (47)
Andromeda XXIII	131.0	−23.6	0.066	24.43	0.13	769	46	...	...	[774, —]	[127, —]	[388, —]	(48)
Andromeda XX	112.9	−26.9	0.059	24.52	$^{+0.74}_{-0.24}$	802	$^{+273}_{-89}$	...	...	[805, —]	[129, —]	[420, —]	(51)
Andromeda XII	122.0	−28.5	0.110	24.70	0.30	871	120	−558.4	3.2	[875, −393]	[133, −272]	[485, −306]	(44)
NGC 147	119.8	−14.3	0.172	24.15	0.09	676	28	−193.1	0.8	[680, −4]	[142, 118]	[292, 85]	(40) (52)
Andromeda XXI	111.9	−19.2	0.093	24.67	0.13	859	51	...	...	[862, —]	[150, —]	[476, —]	(53)
Andromeda XIV	123.0	−33.2	0.060	24.33	0.33	735	112	−481.0	2.0	[739, −326]	[162, −208]	[361, −240]	(54) (47)
Andromeda XV	127.9	−24.5	0.047	24.00	0.20	631	58	−339.0	7.0	[636, −180]	[174, −61]	[247, −95]	(55) (56)
Andromeda XIII	123.0	−29.9	0.082	24.80	$^{+0.1}_{-0.4}$	912	$^{+42}_{-168}$	−195.0	8.4	[916, −34]	[180, 86]	[528, 53]	(44)
Andromeda II	128.9	−29.2	0.061	24.07	0.06	652	18	−193.6	1.0	[657, −44]	[184, 73]	[276, 40]	(40) (47)
NGC 185	120.8	−14.5	0.184	23.95	0.09	617	26	−203.8	1.1	[621, −17]	[187, 105]	[234, 72]	(40) (52)
Andromeda XXIX	109.8	−30.8	0.046	24.32	0.22	731	74	...	...	[734, —]	[188, —]	[363, —]	(57)
Andromeda XIX	115.6	−27.4	0.062	24.85	0.13	933	56	...	...	[936, —]	[189, —]	[548, —]	(51)
Triangulum[k]	133.6	−31.3	0.041	24.54	0.06	809	22	−179.2	1.7	[814, −45]	[206, 69]	[442, 37]	(40) (58)
Andromeda XXIV	127.8	−16.3	0.083	23.89	0.12	600	33	...	...	[605, —]	[208, —]	[220, —]	(48)
Andromeda VII	109.5	−10.0	0.194	24.41	0.10	762	35	−309.4	2.3	[765, −98]	[218, 24]	[401, −8]	(40) (47)
Andromeda XXII	132.6	−34.1	0.079	24.50:[l]		794:		...	...	[799, —]	[221, —]	[432, —]	(53)
IC 10	119.0	−3.3	1.568	24.50	0.12	794	44	−348.0	1.0	[798, −150]	[252, −32]	[440, −64]	(59) (43)
LGS 3	126.8	−40.9	0.040	24.43	0.07	769	25	−286.5	0.3	[773, −155]	[269, −43]	[422, −74]	(40) (60)
Andromeda VI	106.0	−36.3	0.063	24.47	0.07	783	25	−354.0	3.0	[785, −180]	[269, −62]	[435, −93]	(40) (49)
Andromeda XVI	124.9	−30.5	0.067	23.60	0.20	525	48	−385.0	5.0	[529, −229]	[279, −110]	[153, −143]	(55) (56)
Andromeda XXVIII	91.0	−22.9	0.096	24.10	$^{+0.5}_{-0.2}$	661	$^{+152}_{-61}$	...	...	[661, —]	[368, —]	[364, —]	(61)
IC 1613	129.7	−60.6	0.025	24.39	0.12	755	42	−233.0	1.0	[758, −154]	[520, −64]	[517, −90]	(62) (63)
Phoenix	272.2	−68.9	0.016	23.09	0.10	415	19	−13.0[m]	9.0	[415, −103]	[868, −104]	[556, −106]	(64) (65)

Table 2
(Continued)

(1) Galaxy	(2) l	(3) b	(4) $E(B-V)$	(5) $(m-M)_o$		(6) $D_\odot$ (kpc)		(7) $v_\odot$ (km s^{-1})		(8) $[D_{MW}, v_M W]$ (kpc, km s^{-1})	(9) $[D_{M31}, v_{M31}]$ (kpc, km s^{-1})	(10) $[D_{LG}, v_{LG}]$ (kpc, km s^{-1})	(11) References[a]
NGC 6822	25.4	−18.4	0.231	23.31	0.08	459	17	−57.0	2.0	[452, 43]	[897, 65]	[595, 64]	(66) (67)[n]
Cetus	101.5	−72.9	0.029	24.39	0.07	755	24	−87.0	2.0	[756, −27]	[681, 46]	[603, 26]	(40) (68)
Pegasus dIrr	94.8	−43.6	0.068	24.82	0.07	920	30	−183.3	5.0	[921, −21]	[474, 89]	[618, 60]	(40) (69)[o]
Leo T	214.9	+43.7	0.031	23.10	0.10	417	19	38.1	2.0	[422, −58]	[991, −108]	[651, −98]	(70) (8)
WLM	75.9	−73.6	0.038	24.85	0.08	933	34	−130.0	1.0	[932, −73]	[836, −6]	[794, −24]	(40) (71)
Leo A	196.9	+52.4	0.021	24.51	0.12	798	44	22.3	2.9	[803, −19]	[1200, −46]	[941, −41]	(72) (73)
Andromeda XVIII	113.9	−16.9	0.106	25.66	0.13	1355	81	...	...	[1358, —]	[591, —]	[969, —]	(51)
Aquarius	34.0	−31.3	0.051	25.15	0.08	1072	39	−140.7	2.5	[1066, −27]	[1173, 17]	[1053, 9]	(40) (69)[o]
Tucana	322.9	−47.4	0.031	24.74	0.12	887	49	194.0[p]	4.3	[882, 99]	[1355, 62]	[1076, 73]	(74) (75)
Sagittarius dIrr	21.1	−16.3	0.124	25.14	0.18	1067	88	−78.5	1.0	[1059, 8]	[1356, 20]	[1156, 22]	(76) (60)[q]
UGC 4879	164.7	+42.9	0.016	25.67	0.04	1361	25	−70.0[r]	15.0	[1367, −27]	[1395, −4]	[1321, −12]	(77) (78)
NGC 3109	262.1	+23.1	0.067	25.57	0.08	1300	48	403.0	2.0	[1301, 193]	[1987, 83]	[1633, 110]	(79) (67)
Sextans B	233.2	+43.8	0.031	25.77	0.03	1426	20	304.0	1.0	[1430, 171]	[1943, 97]	[1659, 114]	(59) (63)
Antlia	263.1	+22.3	0.079	25.65	0.10	1349	62	362.0	2.0	[1350, 151]	[2039, 39]	[1684, 66]	(59) (80)
Sextans A	246.1	+39.9	0.045	25.78	0.08	1432	53	324.0	2.0	[1435, 163]	[2027, 73]	[1711, 94]	(59) (67)
HIZSS 3(A)	217.7	+0.1	1.013	26.12	0.14	1675	108	288.0	2.5	[1682, 139]	[1923, 105]	[1760, 109]	(81)[s] (82)
HIZSS 3B	217.7	+0.1	1.013	26.12	0.14	1675	108	322.6	1.4	[1682, 174]	[1923, 140]	[1760, 143]	(81)[s] (82)
KKR 25	83.9	+44.4	0.009	26.40	0.07	1905	61	−139.5	1.0	[1904, 31]	[1853, 77]	[1838, 67]	(59) (83)
ESO 410- G 005	357.8	−80.7	0.014	26.42	0.04	1923	35	...	...	[1922, —]	[1862, —]	[1852, —]	(59)
NGC 55	332.9	−75.7	0.013	26.43	0.12	1932	107	129.0	2.0	[1930, 98]	[1964, 117]	[1909, 111]	(84) (67)
ESO 294- G 010	320.4	−74.4	0.006	26.54	0.04	2032	37	117.0	5.0	[2030, 72]	[2090, 85]	[2023, 81]	(59) (85)
NGC 300	299.2	−79.4	0.013	26.59	0.06	2080	57	146.0	2.0	[2079, 103]	[2078, 122]	[2042, 116]	(59) (67)
IC 5152	343.9	−50.2	0.025	26.45	0.05	1950	45	122.0	2.0	[1945, 81]	[2211, 68]	[2047, 73]	(59) (67)
KKH 98	109.1	−22.4	0.123	27.01	0.09	2523	105	−136.9	1.0	[2526, 60]	[1762, 184]	[2140, 152]	(59) (83)
UKS 2323-326	11.9	−70.9	0.015	26.72	0.09	2208	92	62.0	5.0	[2205, 74]	[2153, 107]	[2145, 99]	(59) (86)
KKR 3	63.7	+72.0	0.014	26.70	0.12	2188	121	63.3	1.8	[2187, 135]	[2464, 121]	[2297, 127]	(59) (87)
GR 8	310.7	+77.0	0.026	26.69	0.12	2178	120	213.9	2.5	[2177, 182]	[2699, 117]	[2421, 136]	(59) (69)[o]
UGC 9128	25.6	+70.5	0.023	26.80	0.04	2291	42	152.0	1.0	[2288, 195]	[2686, 159]	[2465, 172]	(59) (63)
UGC 8508	111.1	+61.3	0.015	27.06	0.03	2582	36	56.0	5.0	[2583, 165]	[2609, 184]	[2566, 181]	(88) (89)
IC 3104	301.4	−17.0	0.410	26.78	0.18	2270	188	429.0	4.0	[2266, 242]	[2923, 144]	[2588, 170]	(90) (67)
DDO 125	137.8	+72.9	0.020	27.06	0.05	2582	59	194.9	0.2	[2584, 245]	[2764, 237]	[2646, 240]	(88) (83)
UGCA 86	139.8	+10.6	0.938	27.36	0.17	2965	232	67.0	4.0	[2971, 209]	[2387, 302]	[2663, 275]	(91) (41)
DDO 99	166.2	+72.7	0.026	27.07	0.14	2594	167	251.0	4.0	[2596, 272]	[2824, 252]	[2683, 257]	(88) (89)
IC 4662	328.5	−17.8	0.070	26.94	0.17	2443	191	302.0	3.0	[2436, 192]	[3027, 116]	[2722, 139]	(91) (67)
DDO 190	82.0	+64.5	0.012	27.23	0.03	2793	39	150.0	4.0	[2793, 256]	[2917, 263]	[2829, 263]	(88) (92)
KKH 86	339.0	+62.6	0.027	27.06	0.16	2582	190	287.2	0.7	[2578, 259]	[3157, 186]	[2856, 209]	(88) (83)
NGC 4163	163.2	+77.7	0.020	27.28	0.03	2858	39	165.0	5.0	[2860, 184]	[3119, 159]	[2966, 166]	(88) (93)
DDO 113	161.1	+78.1	0.020	27.35	0.06	2951	82	284.0	6.0	[2953, 305]	[3210, 280]	[3058, 287]	(88) (41)

[a] **References:** (1) Bellazzini et al. 2006; (2) Martin et al. 2005; (3) Monaco et al. 2004; (4) Ibata et al. 1994; (5) Belokurov et al. 2007; (6) Simon et al. 2011; (7) Zucker et al. 2006a; (8) Simon & Geha 2007; (9) Walsh et al. 2008; (10) Koch et al. 2009; (11) Belokurov et al. 2009; (12) Willman et al. 2006; (13) Martin et al. 2007; (14) Grillmair 2009; (15) Carlin et al. 2009; (16) Clementini et al. 2003; (17) van der Marel et al. 2002; (18) Udalski et al. 1999; (19) Harris & Zaritsky 2006; (20) Dall'Ora et al. 2006; (21) Bonanos et al. 2004; (22) Walker et al. 2007; (23) Carrera et al. 2002; (24) Walker et al. 2009c; (25) Pietrzyński et al. 2008; (26) Walker et al. 2009b; (27) Lee et al. 2009; (28) Okamoto et al. 2008; (29) Pietrzyński et al. 2009; (30) Coleman et al. 2007; (31) Adén et al. 2009a; (32) Moretti et al. 2009; (33) Greco et al. 2008; (34) Belokurov et al. 2008; (35) Belokurov et al. 2010; (36) Martin et al. 2008a; (37) Bellazzini et al. 2005; (38) Bellazzini et al. 2004b; (39) Mateo et al. 2008; (40) McConnachie et al. 2005; (41) de Vaucouleurs et al. 1991; (42) Fiorentino et al. 2010; (43) Huchra et al. 1999; (44) Collins et al. 2010; (45) Geha et al. 2006b; (46) Irwin et al. 2008; (47) Kalirai et al. 2010; (48) Richardson et al. 2011; (49) Evans et al. 2000; (50) Zucker et al. 2007; (51) McConnachie et al. 2008; (52) Geha et al. 2010; (53) Martin et al. 2009; (54) Majewski et al. 2007; (55) Ibata et al. 2007; (56) Letarte et al. 2009; (57) Bell et al. 2011; (58) Corbelli & Schneider 1997; (59) Tully et al. 2006; (60) Young & Lo 1997b; (61) Slater et al. 2011; (62) Bernard et al. 2010; (63) Hoffman et al. 1996; (64) Hidalgo et al. 2009; (65) Irwin & Tolstoy 2002; (66) Gieren et al. 2006; (67) Koribalski et al. 2004; (68) Lewis et al. 2007; (69) Young et al. 2003; (70) Irwin et al. 2007; (71) Leaman et al. 2009; (72) Dolphin et al. 2002; (73) Brown et al. 2007; (74) Bernard et al. 2009; (75) Fraternali et al. 2009; (76) Momany et al. 2002; (77) Jacobs et al. 2011; (78) Kopylov et al. 2008; (79) Soszyński et al. 2006; (80) Barnes & de Blok 2001; (81) Silva et al. 2005; (82) Begum et al. 2005; (83) Huchtmeier et al. 2003; (84) Gieren et al. 2008; (85) Jerjen et al. 1998; (86) da Costa et al. 1998; (87) Begum et al. 2006; (88) Dalcanton et al. 2009; (89) Begum et al. 2008b; (90) Karachentsev et al. 2002b; (91) Karachentsev et al. 2006; (92) Haynes et al. 1998; (93) Huchra et al. 1995.

[b] Significant distance/velocity gradients.

[c] Corresponding to RC stars at $6 < D < 7$ kpc.

[d] Carbon stars.

[e] See their Figure 8 for an excellent summary.

[f] Red giant branch stars.

[g] Distance calculated using their LMC–SMC offset of 0.51 ± 0.03 for the adopted LMC distance modulus.

[h] Also Bellazzini et al. (2002), but note that these estimates are ∼0.2 mag larger than some previous values.

[i] cf. Dolphin (2002), which also estimates distances by comparing real and model CMDs.

[j] Note this estimate is ∼0.2 mag larger than some previous values.

Table 2
(Continued)

[k] Range in distance estimates from $750 \lesssim D \lesssim 950$.
[l] Assumed to be at M31–M33 distance.
[m] Alternative value in Gallart et al. (2001).
[n] See Demers et al. (2006) for velocities of 110 C-stars.
[o] Uncertainty due to intrinsic asymmetries is gas distribution, L. Young (2010, private communication).
[p] Optical velocity suggests that Tucana is not associated with nearby H I cloud.
[q] See also Begum et al. (2006).
[r] Optical spectroscopy suggests that $v_h \sim -70$ km s^{-1}; however, H I analysis by Bellazzini et al. (2011) gives $v_h \sim -25$ km s^{-1}. No clear reason for the discrepancy currently exists.
[s] Distance calculated prior to realization that HIZSS 3 was two systems, and will most likely correspond more closely to the more massive A system.

at >400 kpc. A similar gap is present at a similar radius for satellites around M31 (Section 3.2; but see the recent discovery of Andromeda XXVIII by Slater et al. 2011). This tentatively suggests that this gap could be used to observationally define the limiting radius of the sub-groups (or equivalently, the extent of the two host galaxies) and appears consistent with previous work and other galaxy groups (e.g., Cen A, Sculptor, IC 342: Karachentsev et al. 2002a, 2003a, 2003b; see also Grebel et al. 2003).

Pisces II is the most recently discovered satellite to the MW (Belokurov et al. 2010) and does not appear in Figure 2 since it currently lacks a velocity measurement. At the time of writing, 15 new satellites have been discovered since 2005, all of them using the Sloan Digital Sky Survey (SDSS) and hence confined to its footprint. Irwin (1994) originally argued that the MW sub-group was essentially complete at Galactic latitudes away from the disk for objects of comparable luminosity as (or brighter than) Sextans. The fact that only one of the new satellites (Canes Venatici) is comparable in luminosity to any of the previously known MW satellites backs up this claim. Indeed, Koposov et al. (2008) demonstrate that most of the newly discovered galaxies are at the limits of detection of SDSS, implying that—even within the SDSS footprint—a large number of galaxies still await discovery. This was explored further by Tollerud et al. (2008), who conclude that there may by many hundreds of unseen faint satellites.

It is worth emphasizing the problems caused by the Galactic disk in searching for satellites. Figure 3 shows the distribution of MW satellites with (absolute) latitude. The histogram shows the observed distribution of all 27 satellites, whereas the dashed line indicates a uniform distribution, normalized to match observations at $|b| > 30^\circ$. There are three satellites at $|b| < 30^\circ$ (one of which is Canis Major, on which there is still considerable debate as to whether it is a dwarf galaxy or an unrelated disk substructure; e.g., Martin et al. 2004a, 2004b; Momany et al. 2004; Martínez-Delgado et al. 2005; Moitinho et al. 2006; Butler et al. 2007; López-Corredoira et al. 2007), a number that is very low considering this accounts for half of the sky. Obscuration by the Galactic disk, however, does not become a serious problem until $|b| \lesssim 20^\circ$. While some of the area probed by SDSS reaches to very low Galactic latitudes, the majority of the Legacy area is located at $b > 30^\circ$, likely explaining the dearth of satellites at intermediate latitudes.

Two photometric surveys currently underway—the Pan-STARRS (Kaiser et al. 2002) PS1 survey in the north and SkyMapper (Keller et al. 2007) in the south—together will map the entire sky to equivalent or deeper magnitude limits to SDSS and consequently should reveal the presence of many more satellites. These should remove the spatial bias introduced by SDSS. In addition, other wide-field (but not all-hemisphere) surveys such as that made possible with the soon-to-be-commissioned Subaru/HyperSuprimeCam will allow for even fainter satellites to be detected (if they exist). In the more distant future, the Large Synoptic Survey Telescope will re-examine the southern hemisphere sky to even greater depth. Judging by recent discoveries, there is every reason to expect that large numbers of very faint satellites will be discovered by all these projects. However, objects behind the Galactic plane will likely remain hidden, and it is unlikely that (m)any bright ($M_V < -8$) Galactic dwarf galaxies at higher Galactic latitudes remain to be discovered.

3.2. Membership of the M31 Sub-group

Figure 4 shows M31-centric velocity versus distance for all galaxies within 600 kpc of Andromeda for which these measurements exist. Again, the M31-centric velocity listed in Table 2 has been multiplied by a factor of $\sqrt{3}$ to account for the unknown tangential velocities of these galaxies. Following Figure 2, dashed curves show the escape velocity from a $10^{12}\,M_\odot$ point mass, and the vertical dashed line indicates the approximate cosmological virial radius of M31, $R_{\rm vir} \sim 300$ kpc (e.g., Klypin et al. 2002).

Whereas only Leo I around the MW stands out as a possible unbound satellite from its radial velocity (Mateo et al. 2008), M31 has at least two close-in dwarf galaxies that are likely unbound, Andromeda XII (Chapman et al. 2007) and XIV (Majewski et al. 2007). The Pegasus dwarf irregular galaxy (DIG) and IC 1613 are both extremely distant from Andromeda but could arguably be dynamically associated. In this respect they are similar to NGC 6822, LeoT, and Phoenix around the MW. It is often overlooked that IC 10 and LGS 3 are clear M31 satellites (as close to M31 as the Andromeda VI and XVI dSphs). However, these two galaxies differ from the majority of satellites insofar as they both have non-negligible gas fractions and younger stellar populations. LGS 3 is generally classified as being morphologically akin to LeoT (a "transition-type" dwarf; see Section 5 for discussion), whereas IC 10 is generally classified as a low-mass dwarf irregular. Indeed, as a whole, the M31 satellite system contrasts with the MW satellites in the variety of morphological types present. Around the MW, only the LMC and SMC are not classified as dSphs. However, in addition to the dSph satellites, M31 also has a transition dwarf (LGS 3), a dwarf irregular (IC 10, although it is much lower luminosity than either of the Magellanic Clouds), three dwarf elliptical galaxies (NGC 205, 147, and 185), a compact elliptical (M32), and a low-mass spiral galaxy (M33).

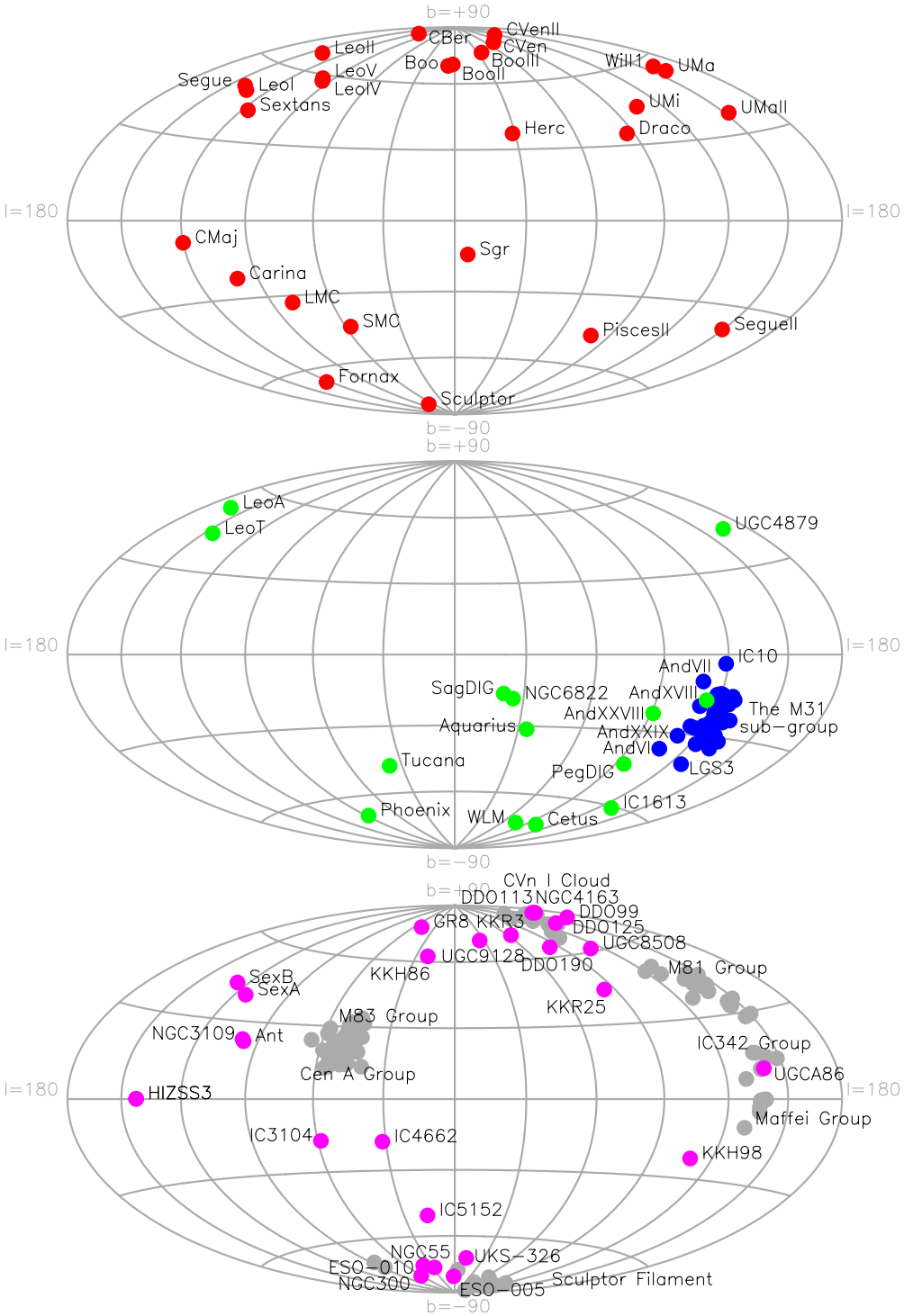

Figure 1. Aitoff projections of the Galactic coordinates of MW galactic satellites (top panel); the M31 sub-group (blue) and isolated Local Group galaxies (green; middle panel); the nearest galaxies to the Local Group that have distances based on resolved stellar populations that place them within 3 Mpc (magenta; bottom panel). The positions of nearby galaxy groups are indicated in gray in the bottom panel.

(A color version of this figure is available in the online journal.)

In the past seven years we have seen a rapid growth in the number of known M31 satellites through focused wide-field studies of the environment around Andromeda. All the new dwarfs have been discovered as overdensities of red giant branch (RGB) stars. This, therefore, imposes a basic magnitude limit on the galaxies that can be found, since it requires galaxies to have enough stars that a reasonable number are passing through the RGB phase. An exact study of the selection effects for dwarf galaxy searches around M31 has yet to be published, but the practical limit of these searches appears to be around $M_V \sim -6$. The most extensive survey of M31's environs, by the Pan-Andromeda Archaeological Survey (PAndAS; McConnachie et al. 2009), provides complete spatial coverage out to a maximum projected radius from M31 of 150 kpc. As shown in McConnachie et al. (2009) and Richardson et al. (2011), the projected radial distribution of satellites shows no sign of

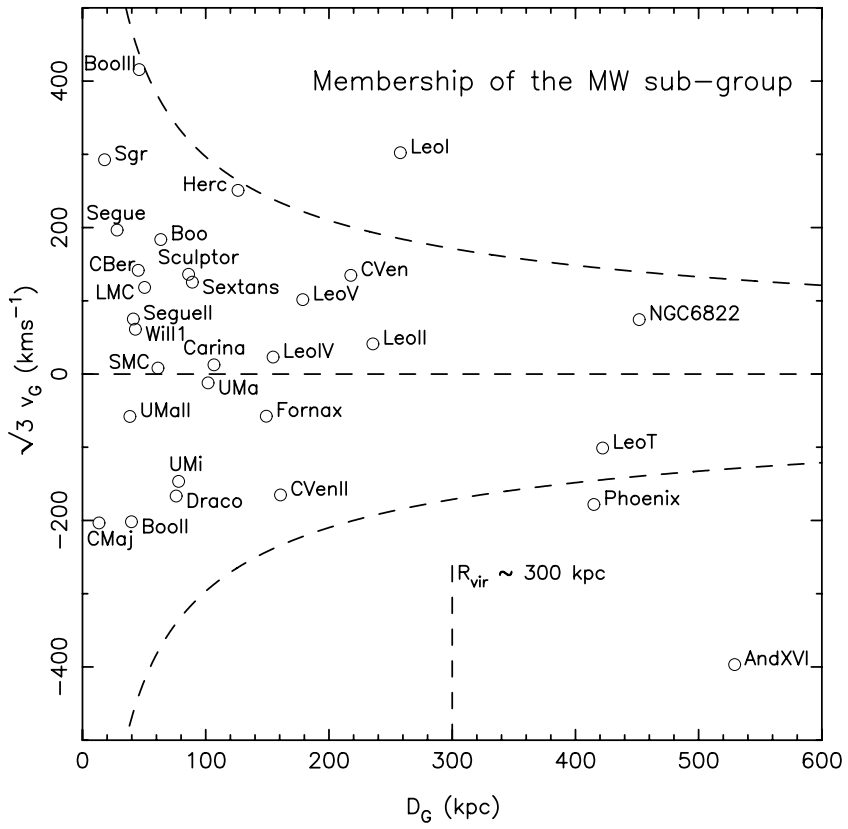

Figure 2. Galactocentric velocity vs. distance for all galaxies in the proximity of the MW. The y-ordinate has been multiplied by a factor of $\sqrt{3}$ to account for the unknown tangential motions of the galaxies. Dashed curves show the escape velocity from a $10^{12}\,M_{\odot}$ point mass. The vertical dashed line indicates the approximate location of the expected cosmological virial radius of the MW ($R_{\rm vir} \sim 300$ kpc).

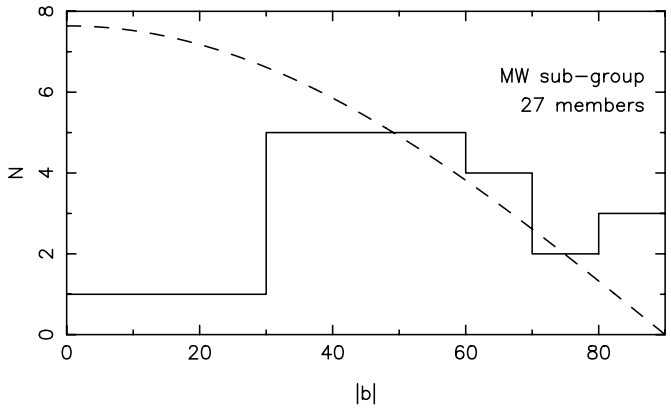

Figure 3. Galactic latitude distribution of MW dwarf galaxies. The dashed curve shows an isotropic distribution normalized to match the current number of dwarfs known at $|b| > 30^{\circ}$ (24) and highlights the dearth of objects at low Galactic latitude.

declining within this radius. It is highly probable, therefore, that a large number of satellites remain to be discovered at large radius (recently verified by the discoveries of Andromeda XXVIII (Slater et al. 2011) and Andromeda XXIX (Bell et al. 2011) in the SDSS DR8). At small radius ($\lesssim$60 kpc), there is also a deficit of galaxies due to the dominance of M31 stellar populations in this region, making it difficult to identify any low-luminosity satellites that may be superimposed in front of (or behind) the main body of M31.

Within both the MW and the M31 sub-group there are at least three potential dynamical associations of satellites ("sub-sub-groups"). Around the MW, Leo IV and V are in close proximity to each other (positions and velocities) and may well constitute a binary system (Belokurov et al. 2008; de Jong et al. 2010). Within the M31 sub-group, Andromeda XXII is only about 40 kpc in projection from M33, whereas it is over 200 kpc in projection from M31 (Martin et al. 2009). Thus, Andromeda XXII may actually be the only known satellite of M33 (the bright dSph Andromeda II is also considerably closer to M33 than M31, but in a region where the gravitational potential of M31 clearly dominates). A second possible pairing is found to the north of M31 and includes NGC 185 and 147. Van den Bergh (1998) postulated that NGC 185 and 147 were a binary system; they are separated by only 1° in projection and their distances imply a three-dimensional separation of ∼60 kpc. Their velocities differ by only ∼10 km s^{-1}, and such a small separation in phase-space seems unlikely (but not impossible) if these galaxies are not, or never have been, a binary system.

3.3. Membership of the Local Group, and Identification of Nearby Neighbors

Figure 5 shows Local-Group-centric velocity versus distance from the barycenter of the Local Group for all galaxies in the sample for which these data exist. The Local-Group-centric velocity listed in Table 2 has been multiplied by a factor of $\sqrt{3}$ to account for the unknown tangential components. Dashed curves indicate the escape velocity from a point mass of $2 \times 10^{12}\,M_{\odot}$. Dotted curves indicate the escape velocity from a point mass of $5 \times 10^{12}\,M_{\odot}$, the approximate total dynamical mass of the Local Group as implied from the timing argument (e.g., Lynden-Bell 1981). Many of the points at $D_{\rm LG} \lesssim 500$ kpc represent galaxies

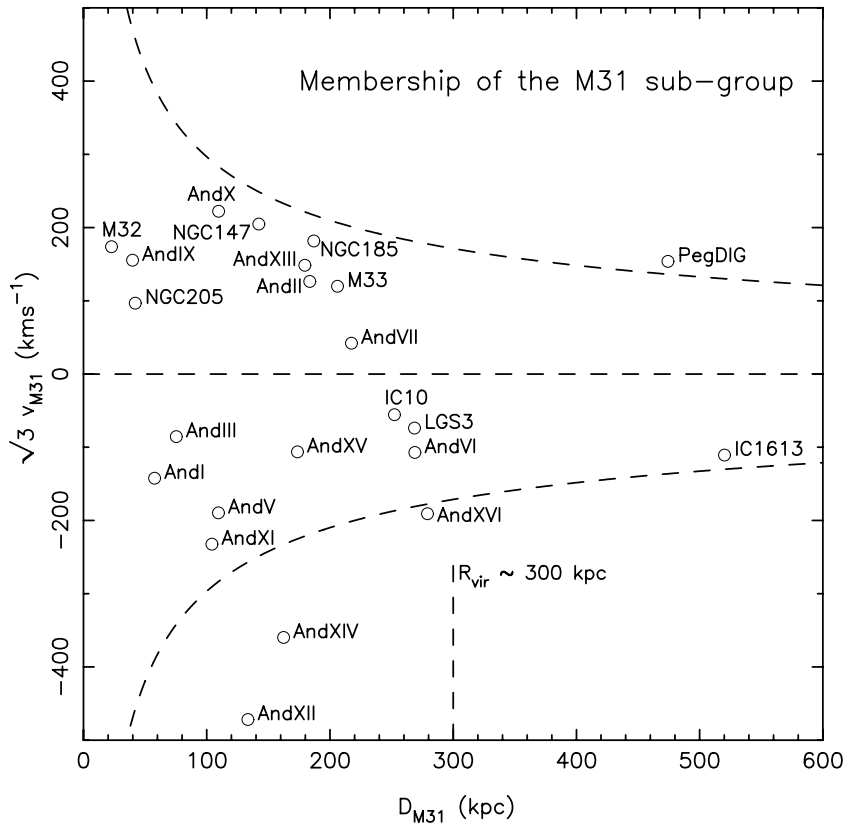

Figure 4. M31-centric velocity vs. distance for all galaxies in the proximity of M31. The *y*-ordinate has been multiplied by a factor of $\sqrt{3}$ to account for the unknown tangential motions of the galaxies. Dashed curves show the escape velocity from a $10^{12}\ M_{\odot}$ point mass. The vertical dashed line indicates the approximate location of the expected cosmological virial radius of M31 ($R_{\rm vir} \sim 300$ kpc).

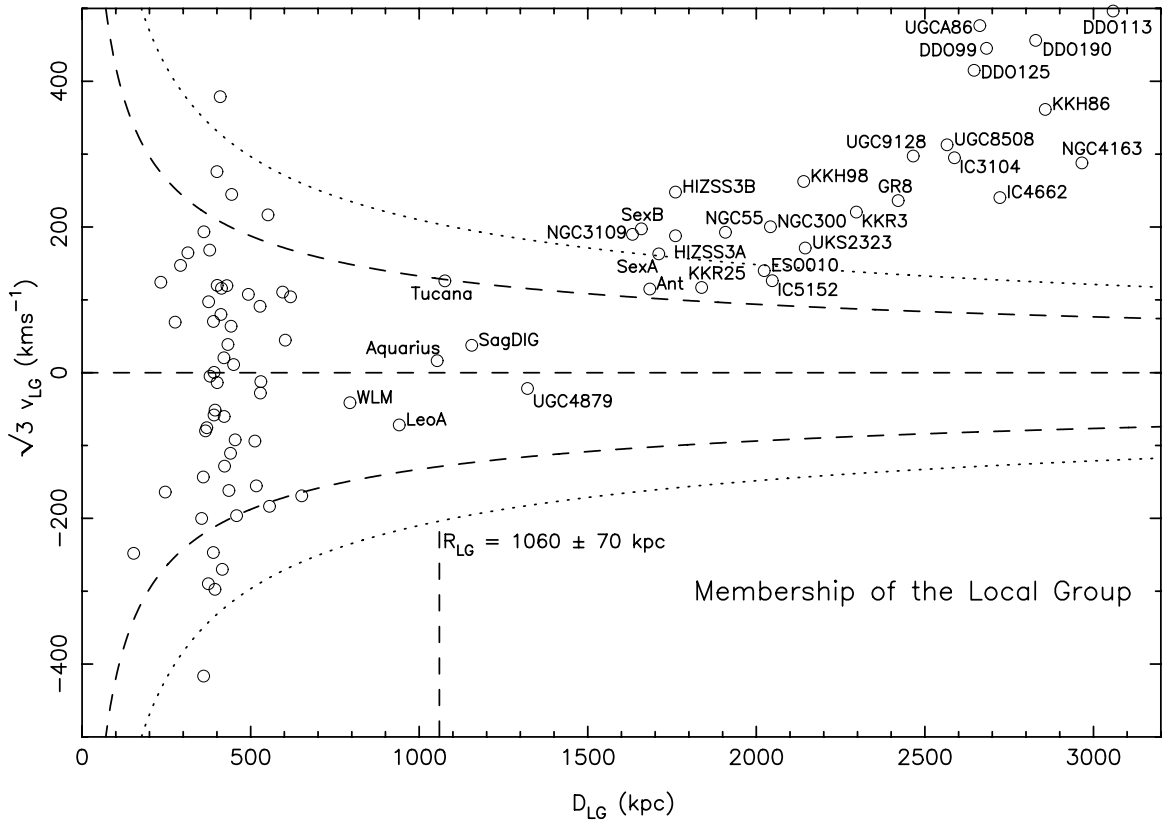

Figure 5. Local-Group-centric velocity vs. distance for all galaxies in the proximity of the Local Group. The *y*-ordinate has been multiplied by a factor of $\sqrt{3}$ to account for the unknown tangential motions of the galaxies. Dashed curves show the escape velocity from a $2 \times 10^{12}\ M_{\odot}$ point mass. Dotted curves show the escape velocity from a $5 \times 10^{12}\ M_{\odot}$ point mass, as implied from the timing argument (Lynden-Bell 1981). The vertical dashed line indicates the zero-velocity surface of the Local Group ($R_{\rm LG} = 1060 \pm 70$ kpc), derived here from the mean distance of the six highlighted galaxies that cluster around zero velocity.

that are satellites of either the MW or M31. These systems are dynamically dominated by the gravitational potential of these massive hosts rather than the Local Group as a whole.

There is a clear separation in Figure 5 between outer, apparently bound, Local Group members (the outermost of which is UGC 4879) and the next nearest galaxies (the four members of the NGC 3109 grouping; see van den Bergh 1999). The rise in velocity with distance for all the nearby neighbors is due to the Hubble expansion, and the reader is referred to Karachentsev et al. (2009) for a beautiful analysis of the Hubble flow around the Local Group.

The six outermost Local Group members cluster around $v_{\rm LG} = 0$, and their mean velocity is consistent with zero ($\langle v \rangle = 4 \pm 16$ km s^{-1}, where the uncertainty is the random error in the mean). As such, their mean distance can be used as an estimate of the zero-velocity surface of the Local Group and is $R_{\rm LG} = 1060 \pm 70$ kpc (where the uncertainty is the random error in the mean; cf. Courteau & van den Bergh 1999; Karachentsev et al. 2002b, 2009; and others). It is also worth pointing out that the velocity dispersion of the Local Group can be estimated using those Local Group galaxies that are far from either the MW or M31 and that have published velocities. The six Local Group galaxies identified in Figure 5, with the addition of IC 1613 and Cetus, are all more than 500 kpc from either of the two large galaxies and yield $\sigma_{\rm LG} = 49 \pm 36$ km s^{-1} (where the uncertainty is the random error in the dispersion). Note that there is a systematic error component in all these estimates caused by our choice for the location of the barycenter of the Local Group, although it has a generally weak effect on any values given here. The fact that the measured velocity dispersion for the entire Local Group is so low that it is of order the velocity dispersion of the gas in the SMC is peculiar and well noted (e.g., Sandage 1986, and references therein). It may result from the necessity to measure the dispersion from galaxies that are mostly at or near turnaround.

Not including satellites of the MW and M31, it is highly likely that the census of Local Group galaxies remains severely incomplete. Unlike recently discovered MW satellites, isolated Local Group galaxies are not nearby. Unlike the M31 subgroup, isolated Local Group galaxies do not cluster in a specific area of sky amenable to dedicated surveys. The middle panel of Figure 1 shows that 8 of the 13 (quasi-)isolated Local Group galaxies are all in one quadrant of the sky (the same one that contains M31). However, it is also not clear what the expected spatial distribution of non-satellite Local Group galaxies should be, and it is likely naive to expect an isotropic distribution. Heroic searches for new Local Group galaxies and nearby neighbors have been made by groups led by I. Karachentsev, V. Karachentseva (e.g., Karachentseva & Karachentsev 1998; Karachentseva et al. 1999; Karachentsev et al. 2000 and many others), and A. Whiting (Whiting et al. 1997, 1999) through the visual inspection of literally every plate of the second Palomar Observatory Sky Survey and the ESO/Science Research Council survey, and these remain the most comprehensive all-sky searches to date. Whiting et al. (2007) attempt to quantify their visual search of these plates; they estimate that their search is ∼80% complete in the region away from interference from the MW disk (more than 70% of the sky) to a surface brightness level approaching 26 mag arcsec^{-2}. This translates to (at most) 1 or 2 currently uncataloged Local Group members down to this limit, away from the disk of the Galaxy. Current and future large-scale digital surveys of the sky—including blind H I surveys as well as optical studies—are potentially rich hunting grounds to try to improve the census of nearby galaxies, be they members of the Local Group or the nearby neighbors that help define its environment.

4. PHOTOMETRIC AND STRUCTURAL PARAMETERS

Table 3 presents global photometric and structural parameters for each galaxy in the sample.

Column 1. Galaxy name.
Column 2. Apparent magnitude in V (Vega magnitudes). In general, these have been corrected for foreground extinction (but not internal extinction), although in some cases the original papers are unclear as to whether extinction corrections were applied to the apparent magnitudes. For many of the fainter galaxies that have been resolved into stars, the magnitude may not be based on integrated light (often undetectable) and is instead estimated by measuring the luminosity of the brighter stars and by making assumptions regarding the luminosity function of stars below the detection limit.
Column 3. Radius (arcmin) containing half the light of the galaxy, measured on the semimajor axis. A vast array of different scale radii are used in the literature, and in cases where the original papers use other scale radii (e.g., core, exponential, half-brightness, R_{25}, etc.), I have derived half-light radii by integrating under the appropriate profile, normalized to the apparent magnitude (and with the appropriate ellipticity if measured, otherwise assumed to be circular). In cases where the original papers did not fit a profile, I have assumed an exponential profile. The latter estimates are particularly uncertain, and in these cases I have also given the original scale radius in Column 11.
Column 4. Central surface brightness (mag arcsec^{-2}). Where possible, I cite directly measured values, although in many cases (including in the original papers) this parameter is derived by normalizing the measured profile to the apparent magnitude.
Column 5. Position angle of major axis, measured in degrees east from north. For systems that show a change in this quantity as a function of radius, a mean value has been estimated.
Column 6. Ellipticity $\epsilon = 1 - b/a$, where b is the semiminor axis and a is the semimajor axis. For systems that show a change in this quantity as a function of radius, a mean value has been estimated.
Column 7. Absolute visual magnitude, derived from Column 2 by subtraction of the distance modulus given in Table 2.
Column 8. Half-light radius in parsecs, derived from Column 3 assuming the distance modulus given in Table 2.
Column 9. The mean surface brightness within the isophote defined by the half-light radius, derived using values from Columns 2, 3, and 6. In cases where no ellipticity is measured, I have assumed circular isophotes.
Column 10. References.
Column 11. Comments.

For each galaxy I have tried to minimize the number of different papers that I cite to provide complete information, with the result that Table 3 references 45 papers from the last 21 years. Concern must be given to the systematic uncertainties that exist between measurements: they are necessarily complex, they are essentially unquantifiable, and they probably present the primary limitation for examination of the global properties of this population.

Despite the usefulness of parameters such as total luminosity and half-light radius, it should be strongly stressed that these

Table 3
Luminosity and Structural Parameters

(1) Galaxy	(2) V		(3) r_h (′)		(4) μ_V ($M/\square''$)		(5) θ (°)		(6) ϵ		(7) M_V		(8) r_h (pc)		(9) $\mu_{\rm eff}$ ($M/\square''$)	(10) References[a]	(11) Comments
The Galaxy																	
Canis Major	−0.1	0.8	...	...	24.0[b]	0.6	123:[c]		0.8:		−14.4[d]	0.8	...	...	...	(1) (2)	
Sagittarius dSph	3.6	0.3	342.00	12.00	25.2	0.3	102	2	0.64	0.02	−13.5	0.3	2587	219	26.0	(3) (4)	
Segue	15.3	0.8	4.40	$^{+1.2}_{-0.6}$	27.6	1.0	85	8	0.48	0.13	−1.5	0.8	29	$^{+8}_{-5}$	28.7	(5)	
Ursa Major II	13.3	0.5	16.00	1.00	27.9	0.6	98	4	0.63	0.05	−4.2	0.6	149	21	29.1	(5)	
Bootes II	15.4	0.9	4.20	1.40	28.1	1.6	145	55	0.21	0.21	−2.7	0.9	51	17	29.1	(5)	
Segue II	15.2	0.3	3.40	0.20	27.4	0.4	182	17	0.15	0.10	−2.5	0.3	35	3	28.6	(6)	
Willman 1	15.2	0.7	2.30	0.40	26.1	0.9	77	5	0.47	0.08	−2.7	0.8	25	6	27.2	(5)	
Coma Berenices	14.1	0.5	6.00	0.60	27.3	0.7	115	10	0.38	0.14	−4.1	0.5	77	10	28.4	(5)	
Bootes III	12.6	0.5	...	...	31.3[e]	0.3	90:		0.50:		−5.8[d]	0.5	...	...	...	(7)	
LMC	0.4	0.1									−18.1	0.1				(8)	
SMC	2.2	0.2									−16.8	0.2				(8)	
Bootes	12.8	0.2	12.60	1.00	27.5	0.3	14	6	0.39	0.06	−6.3	0.2	242	21	28.7	(5)	
Draco	10.6	0.2	10.00	0.30	25.0	0.2	89	2	0.31	0.02	−8.8	0.3	221	19	26.1	(5)	
Ursa Minor	10.6	0.5	8.20	1.20	26.0	0.5	53	5	0.56	0.05	−8.8	0.5	181	27	25.2	(9)	
Sculptor	8.6	0.5	11.30	1.60	23.5	0.5	99	1	0.32	0.03	−11.1	0.5	283	45	24.3	(9)	
Sextans	10.4	0.5	27.80	1.20	27.1	0.5	56	5	0.35	0.05	−9.3	0.5	695	44	28.0	(9)	
Ursa Major	14.4	0.3	11.30	1.70	27.7	0.5	71	3	0.80	0.04	−5.5	0.3	319	50	28.8	(5)	
Carina	11.0	0.5	8.20	1.20	25.5	0.5	65	5	0.33	0.05	−9.1	0.5	250	39	26.0	(9)	
Hercules	14.0	0.3	8.60	$^{+1.8}_{-1.1}$	27.2	0.6	102	4	0.68	0.08	−6.6	0.4	330	$^{+75}_{-52}$	28.3	(5)	
Fornax	7.4	0.3	16.60	1.20	23.3	0.3	41	1	0.30	0.01	−13.4	0.3	710	77	24.0	(9)	
Leo IV	15.1	0.4	4.60	0.80	27.5	0.7	121	9	0.49	0.11	−5.8	0.4	206	37	28.6	(10)	
Canes Venatici II	16.1	0.5	1.60	0.30	26.1	0.7	177	9	0.52	0.11	−4.9	0.5	74	14	27.2	(5)	
Leo V	16.0	0.4	2.60	0.60	27.1	0.8	96	13	0.50	0.15	−5.2	0.4	135	32	28.2	(10)	
Pisces II	16.3	0.5	1.10	0.10	25.7	0.6	77	12	0.40	0.10	−5.0:		58	99	26.8	(11)	
Canes Venatici	13.1	0.2	8.90	0.40	27.1	0.2	70	4	0.39	0.03	−8.6	0.2	564	36	28.2	(5)	
Leo II	12.0	0.3	2.60	0.60	24.2	0.3	12	10	0.13	0.05	−9.8	0.3	176	42	24.8	(9)	
Leo I	10.0	0.3	3.40	0.30	22.6	0.3	79	3	0.21	0.03	−12.0	0.3	251	27	23.3	(9)	
Andromeda																	
M32	8.1	0.1	0.47	0.05	11.1:[f]		159	2	0.25	0.02	−16.4	0.2	110	16	17.0	(8) (12)	
Andromeda IX	16.3	1.1	2.50	0.10	28.0	1.2	...	...	...	...	−8.1	1.1	557	29	29.2	(13) (14)	
NGC 205	8.1	0.1	2.46	0.10	15.4:[g]		28	5	0.43	0.10	−16.5	0.1	590	31	20.3	(8) (12)	
Andromeda XVII	15.8	0.4	1.24	0.08	25.7	0.5	122	7	0.27	0.06	−8.7	0.4	286	23	26.8	(15)	
Andromeda I	12.7	0.1	3.10	0.30	24.7	0.2	22	15	0.22	0.04	−11.7	0.1	672	69	25.8	(16)	
Andromeda XXVII[h]	16.7	0.5	1.80	0.30	27.6	0.5	150	10	0.40	0.20	−7.9	0.5	434	76	28.3	(17)	
Andromeda III	14.4	0.3	2.20	0.20	24.8	0.2	136	3	0.52	0.02	−10.0	0.3	479	46	26.2	(16)	
Andromeda XXV	14.8	0.5	3.00	0.20	27.1	0.5	170	10	0.25	0.05	−9.7	0.5	709	61	27.8	(17)	
Andromeda XXVI	17.3	0.5	1.00	0.10	27.4	0.5	145	10	0.25	0.05	−7.1	0.5	222	25	27.9	(17)	
Andromeda XI	17.5	1.2	0.71	0.03	26.5	1.3	...	...	...	...	−6.9	1.3	157	$^{+16}_{-37}$	27.6	(13) (14)	
Andromeda V	15.3	0.2	1.40	0.20	25.3	0.2	32	10	0.18	0.05	−9.1	0.2	315	46	26.7	(16)	
Andromeda X	16.6	1.0	1.30	0.10	26.3	1.1	46	5	0.44	0.06	−7.6	1.0	265	33	27.4	(15)	
Andromeda XXIII	14.2	0.5	4.60	0.20	28.0	0.5	138	5	0.40	0.05	−10.2	0.5	1029	76	27.8	(17)	
Andromeda XX	18.2	0.8	0.53	$^{+0.14}_{-0.04}$	26.2	0.8	80	20	0.30	0.15	−6.3	$^{+1.1}_{-0.8}$	124	$^{+53}_{-17}$	27.3	(18)	
Andromeda XII	18.3	1.2	1.20	0.20	28.5	1.3	...	...	...	...	−6.4	1.2	304	66	29.6	(13) (14)	

Table 3
(Continued)

(1) Galaxy	(2) V		(3) r_h (′)		(4) μ_V ($M/\square''$)		(5) θ (°)		(6) ϵ		(7) M_V		(8) r_h (pc)		(9) $\mu_{\rm eff}$ ($M/\square''$)	(10) References[a]	(11) Comments
NGC 147	9.5	0.1	3.17:		21.2:		25	3	0.41	0.02	−14.6	0.1	623:		22.3	(8)	$r_{25} = 6.6 \pm 0.3$ arcmins
Andromeda XXI	14.8	0.6	3.50	0.30	27.0	0.4	110	15	0.20	0.07	−9.9	0.6	875	91	28.2	(19)	
Andromeda XIV	15.9	0.5	1.70	0.80	27.2	0.6	...	...	0.31	0.09	−8.4	0.6	363	180	27.5	(20)	
Andromeda XV	14.6	0.3	1.21	0.05	24.8	0.4	0:		0.00:		−9.4	0.4	222	22	25.9	(21)	
Andromeda XIII	18.1	1.2	0.78	0.08	27.3	1.3	...	...	...	...	−6.7	1.3	207	$^{+23}_{-44}$	28.4	(13) (14)	
Andromeda II	11.7	0.2	6.20	0.20	24.5	0.2	34	6	0.20	0.08	−12.4	0.2	1176	50	26.3	(16)	
NGC 185	9.2	0.1	2.55:		20.8:		35	3	0.15	0.01	−14.8	0.1	458:		21.9	(8)	$r_{25} = 5.8 \pm 0.3$ arcmins
Andromeda XXIX	16.0	0.3	1.70	0.20	27.6	0.4	51	8	0.35	0.06	−8.3	0.4	361	56	27.6	(22)	
Andromeda XIX	15.6	0.6	6.20	0.10	29.3	0.7	37	8	0.17	0.02	−9.2	0.6	1683	105	30.2	(18)	
Triangulum	5.7	0.1					23		0.41		−18.8	0.1				(8)	
Andromeda XXIV	16.3	0.5	2.10	0.10	27.8	0.5	5	10	0.25	0.05	−7.6	0.5	367	27	28.5	(17)	
Andromeda VII	11.8	0.3	3.50	0.10	23.2	0.2	94	8	0.13	0.04	−12.6	0.3	776	42	25.3	(16)	
Andromeda XXII	18.0	0.8	0.94	0.10	26.7	0.6	114	15	0.56	0.11	−6.5	9.9	217	99	27.9	(19)	
IC 10	9.5	0.2	2.65:		24.6	0.2	...	...	0.19	0.02	−15.0	0.2	612:		22.3	(8) (23)	$r_{25} = 3.2 \pm 0.1$ arcmins
LGS 3	14.3	0.1	2.10	0.20	24.8	0.1	0:		0.20:		−10.1	0.1	470	47	26.6	(24)	
Andromeda VI	13.2	0.2	2.30	0.20	24.1	0.2	163	3	0.41	0.03	−11.3	0.2	524	49	25.3	(16)	
Andromeda XVI	14.4	0.3	0.89	0.05	23.9	0.4	0:		0.00:		−9.2	0.4	136	15	25.0	(21)	
Andromeda XXVIII	15.6	$^{+0.4}_{-0.9}$	1.11	0.21	26.3	$^{+0.4}_{-0.9}$	39	16	0.34	0.13	−8.5	$^{+0.4}_{-1.0}$	213	$^{+64}_{-45}$	26.3	(25)	
IC 1613	9.2	0.1	6.81:		22.8:		50	2	0.11	0.03	−15.2	0.2	1496:		24.1	(8)	$r_{25} = 8.1 \pm 0.2$ arcmins
Phoenix	13.2	0.4	3.76:		25.8:		5[i]	1	0.40[j]	0.10	−9.9	0.4	454:		26.4	(26) (27)	$r_t = 15.8^{+4.3}_{-2.8}$ arcmins; assumed $c = 0.7$
NGC 6822	8.1	0.2	2.65:		19.7:		330	10	0.24	0.05	−15.2	0.2	354:		20.8	(8) (28)	$r_{25} = 7.7 \pm 0.2$ arcmins
Cetus	13.2	0.2	3.20	0.10	25.0	0.2	63	3	0.33	0.06	−11.2	0.2	703	31	26.2	(16)	
Pegasus dIrr	12.6	0.2	2.10:		22.8:		120	2	0.46	0.02	−12.2	0.2	562:		24.4	(8)	
Leo T	15.1[k]	0.5	0.99	0.06	24.8	0.6	0:		0.00:		−8.0	0.5	120	9	26.0	(29)	
WLM	10.6	0.1	7.78:		23.7:		4	2	0.65	0.01	−14.2	0.1	2111:		24.8	(8)	
Leo A	12.4	0.2	2.15:		22.8:		114	5	0.40	0.03	−12.1	0.2	499:		24.4	(8) (30)	$r_{25} = 2.6 \pm 0.1$ arcmins
Andromeda XVIII	16.0	9.9	0.92	0.06	25.6:		...	...	...	...	−9.7:		363	32	26.7	(18)	Lower limits on V and μ_V
Aquarius	14.5	0.1	1.47	0.04	23.6	0.2	99	1	0.50	0.10	−10.6	0.1	458	21	25.5	(31)	
Tucana	15.2	0.2	1.10	0.20	25.0	0.1	97	2	0.48	0.03	−9.5	0.2	284	54	25.6	(32)	
Sagittarius dIrr	13.6	0.2	0.91	0.05	23.9	0.2	90:		0.50:		−11.5	0.3	282	28	23.5	(33)	r_h from integral under central King profile
UGC 4879	13.2	0.2	0.41	0.04	21.2	0.2	84	11	0.44	0.04	−12.5	0.2	162	16	21.5	(34)	
NGC 3109	10.7	0.1	4.30	0.10	22.6	0.1	92	1	0.82	0.01	−14.9	0.1	1626	71	22.9	(35)	
Sextans B	11.3	0.2	1.06	0.10	21.9	0.3	110	2	0.31	0.03	−14.5	0.2	440	42	21.9	(8) (36)	
Antlia	15.2	0.2	1.20	0.12	23.9	0.2	135	5	0.40	0.04	−10.4	0.2	471	52	25.9	(37) (36)	
Sextans A	11.5	0.1	2.47:		22.8:		0	1	0.17	0.02	−14.3	0.1	1029:		24.1	(8) (38)	$r_{25} = 2.9 \pm 0.1$ arcmins
HIZSS 3(A)	...	...	...	...	...	...	...	...	...	...	...	...	...	...	...		
HIZSS 3B	...	...	...	...	...	...	...	...	...	...	...	...	...	...	...		
KKR 25	15.9	0.2	0.40:		24.0	0.2	...	...	0.41	0.02	−10.5	0.2	222:		24.2	(39)	$r_{26.5} = 0.55$ arcmins
ESO 410- G 005	14.9	0.3	0.50	0.05	22.2	0.2	57:		0.37:		−11.5	0.3	280:		23.8	(40) (36)	
NGC 55	7.9	0.1	5.16:		19.3:		108	2	0.83	0.01	−18.5	0.2	2900:		20.4	(8)	$r_{25} = 16.2 \pm 0.4$ arcmins
ESO 294- G 010	15.3	0.3	0.42	0.04	22.3	0.2	8:		0.51:		−11.2	0.3	248	24	23.5	(40) (36)	
NGC 300	8.1	0.1	5.00:		21.0:		111	2	0.29	0.01	−18.5	0.1	3025:		22.1	(8)	$r_{25} = 10.1 \pm 0.3$ arcmins
IC 5152	10.9:[l]		0.97:		20.1:		100	2	0.38	0.02	−15.6:		550:		21.2	(8)	$r_{25} = 2.6 \pm 0.1$ arcmins
KKH 98	15.2	0.3	0.64	0.06	22.8	0.2	−5	1	0.41	0.01	−11.8	0.3	470	48	24.5	(36) (38)	
UKS 2323-326	13.5	0.2	0.90	0.10	22.9	0.2	−60	4	0.10	0.01	−13.2	0.2	578	69	24.0	(41) (38)	
KKR 3	17.2	0.3	0.36	0.04	23.8	0.2	0	1	0.05	0.01	−9.5	0.3	229	28	25.8	(36) (38)	

Table 3
(Continued)

(1) Galaxy	(2) V		(3) r_h (′)		(4) μ_V ($M/\square''$)		(5) θ (°)		(6) ϵ		(7) M_V		(8) r_h (pc)		(9) $\mu_{\rm eff}$ ($M/\square''$)	(10) References[a]	(11) Comments
GR 8	14.5	0.2	0.32	0.04	22.6	0.2	61	2	0.20	0.05	−12.2	0.2	203	28	22.7	(42) (43)	
UGC 9128	14.4	0.3	0.64	0.07	22.6	0.2	46	2	0.40	0.05	−12.4	0.3	427	47	23.8	(43) (36)	
UGC 8508	13.7	0.1	0.42	0.04	21.5	0.2	−60	2	0.45	0.05	−13.4	0.1	315	30	22.1	(43) (36)	
IC 3104	12.8:[l]		2.01:		23.3:		45	2	0.52	0.02	−14.0:		1327:		24.4	(8)	$r_{25} = 1.9 \pm 0.1$ arcmins
DDO 125	12.7	0.3	1.04	0.10	22.1	0.2	−68	4	0.41	0.01	−14.4	0.3	781	77	23.1	(36) (38)	
UGCA 86	14.2:[l]		0.94:		22.8:		25	1	0.32	0.03	−13.2:		811:		24.5	(44) (38)	$r_{25} = 2.3 \pm 0.2$ arcmins
DDO 99	13.9	0.1	0.90	0.09	22.9	0.2	70	4	0.29	0.01	−13.2	0.2	679	81	24.2	(42) (38)	
IC 4662	11.1	0.3	0.48	0.05	18.7	0.2	−69	4	0.27	0.01	−15.8	0.3	341	44	20.1	(36) (38)	
DDO 190	12.8	0.1	0.64	0.06	21.4	0.2	82	5	0.10	0.02	−14.4	0.1	520	49	22.6	(45) (36)	
KKH 86	17.1	0.3	0.28	0.03	23.2	0.2	−3	1	0.39	0.01	−10.0	0.3	210	27	24.7	(36) (38)	
NGC 4163	13.2	0.3	0.45	0.05	21.1	0.2	11	2	0.30	0.05	−14.1	0.3	374	42	22.0	(43) (36)	
DDO 113	16.4	0.3	0.70	0.07	24.0	0.2	0:		0.00	0.09	−11.0	0.3	601	62	26.5	(8) (36)	

[a] **References:** (1) Bellazzini et al. 2006; (2) Butler et al. 2007; (3) Mateo et al. 1998; (4) Majewski et al. 2003; (5) Martin et al. 2008b; (6) Belokurov et al. 2009; (7) Correnti et al. 2009; (8) de Vaucouleurs et al. 1991; (9) Irwin & Hatzidimitriou 1995; (10) de Jong et al. 2010; (11) Belokurov et al. 2010; (12) Choi et al. 2002; (13) Collins et al. 2010; (14) Collins 2011; (15) Brasseur et al. 2011b; (16) McConnachie & Irwin 2006; (17) Richardson et al. 2011; (18) McConnachie et al. 2008; (19) Martin et al. 2009; (20) Majewski et al. 2007; (21) Ibata et al. 2007; (22) Bell et al. 2011; (23) Sanna et al. 2010; (24) Lee 1995; (25) Slater et al. 2011; (26) van de Rydt et al. 1991; (27) Martínez-Delgado et al. 1999; (28) Dale et al. 2007; (29) de Jong et al. 2008; (30) Vansevičius et al. 2004; (31) McConnachie et al. 2006; (32) Saviane et al. 1996; (33) Lee & Kim 2000; (34) Bellazzini et al. 2011; (35) Hidalgo et al. 2008; (36) Sharina et al. 2008; (37) Aparicio et al. 1997; (38) Fingerhut et al. 2010; (39) Karachentsev et al. 2001b; (40) Loveday 1996; (41) Lee & Byun 1999; (42) Makarova 1999; (43) Vaduvescu et al. 2005; (44) Karachentsev et al. 1997; (45) Aparicio & Tikhonov 2000.

[b] Measured within central 2×2 deg.

[c] Broadly aligned with the Galactic Plane.

[d] Distance-independent absolute magnitude estimate.

[e] Measured within projected radius of 0.8 deg.

[f] B magnitude, corresponding to "standard fit" in Table 1 of Choi et al. (2002).

[g] B magnitude; see Table 1 of Geha et al. (2006b).

[h] Measurement of structural parameters complicated by presence of surrounding stream.

[i] Corresponds to "outer component"; $\theta_{\rm inner} = 95°$.

[j] Corresponds to "outer component"; $\epsilon_{\rm inner} = 0.4$.

[k] Converted from g, r.

[l] B magnitude.

numbers are wholly inadequate in reflecting the known complexity of galaxy structures. It is standard practice to decompose bright galaxies into components such as nucleus and envelope, or a bulge, a disk (several disks?), and a halo. More recently, however, a vast number of independent studies of galaxies included in Table 3 have shown that a full description of their structure requires decomposition of their surface brightness profile into multiple components (e.g., Irwin & Hatzidimitriou 1995; Martínez-Delgado et al. 1999; Lee et al. 1999; Lee & Byun 1999; Lee & Kim 2000; Vansevičius et al. 2004; McConnachie et al. 2007; Hidalgo et al. 2008, among many others). The addition of spectroscopic data (see Section 5) adds new complexity to the discussion as well, since dynamically distinct (e.g., Kleyna et al. 2003, 2004) and chemo-dynamically distinct (e.g., Tolstoy et al. 2004; Battaglia et al. 2006, 2008, 2011) populations of stars have been shown to reside within individual dwarf galaxies that do not necessarily always reveal themselves as features in the global surface brightness profiles. Thus, not only are integrated photometric properties such as r_h and M_V inadequate to describe the complex structures exhibited by many galaxies, but so too are single velocity dispersion or rotation measurements (Section 5; true for H I as well as stars; e.g., Lo et al. 1993; Young & Lo 1996, 1997a, 1997b; Young et al. 2003).

Figures 6 and 7 show basic scaling relations using the galaxy parameters given in Table 3, first studied in detail in Kormendy (1985). In Figure 6, I plot absolute magnitude against half-light radius. Here, I have converted the half-light radius given in Table 3 to the geometric mean half-light radius of the major and minor axes ($r = \sqrt{r_a r_b}$, where r_a and r_b are radii measured on the major and minor axes, respectively) to account for the presence of highly elliptical systems. The top panel includes as small dots the location of the Galactic globular clusters, from the data compiled by Harris (1996), and the dashed line shows the direction defined by points of constant surface brightness (averaged within the half-light radius). I have labeled obvious outlying points, and I have also labeled some of the least luminous (candidate) dwarf galaxies. The lower panel shows an expansion of the region $-17 \leqslant M_V \leqslant -7$.

The observed relationship between absolute magnitude and half-light radius shown in the top panel of Figure 6 spans a factor of one million in luminosity. The galaxies seem well separated from the (Galactic) globular clusters in this two-dimensional projection, although the limited number of low-luminosity galaxies (and the fact that all of them are MW satellites) complicates interpretation of this region of the diagram. When M_V and r_h are considered separately, the one-dimensional distributions do overlap, such that the smallest, least luminous (candidate) dwarf galaxies are as faint as any known globular clusters and smaller than the most extended clusters. The distinction between these stellar systems in this parameter space becomes less clear when other types of compact stellar systems, such as ultracompact dwarfs and the nuclei of early-type galaxies, are included (e.g., see Figures 5 and 8 of Brodie et al. 2011).

Three galaxies are clear outliers in the top panel of Figure 6: Andromeda XIX is extremely extended for its luminosity (see also Figure 7), whereas the compact elliptical M32 is a known outlier in this projection due to its extreme concentration (see also Kormendy & Bender 2012, and references therein). Interestingly, the recently identified Local Group galaxy UGC 4879 (Kopylov et al. 2008) tends to the same side of the relation as M32, although not as extreme. Bellazzini et al. (2011) note that UGC 4879 has an unusual structure, insofar as there appear

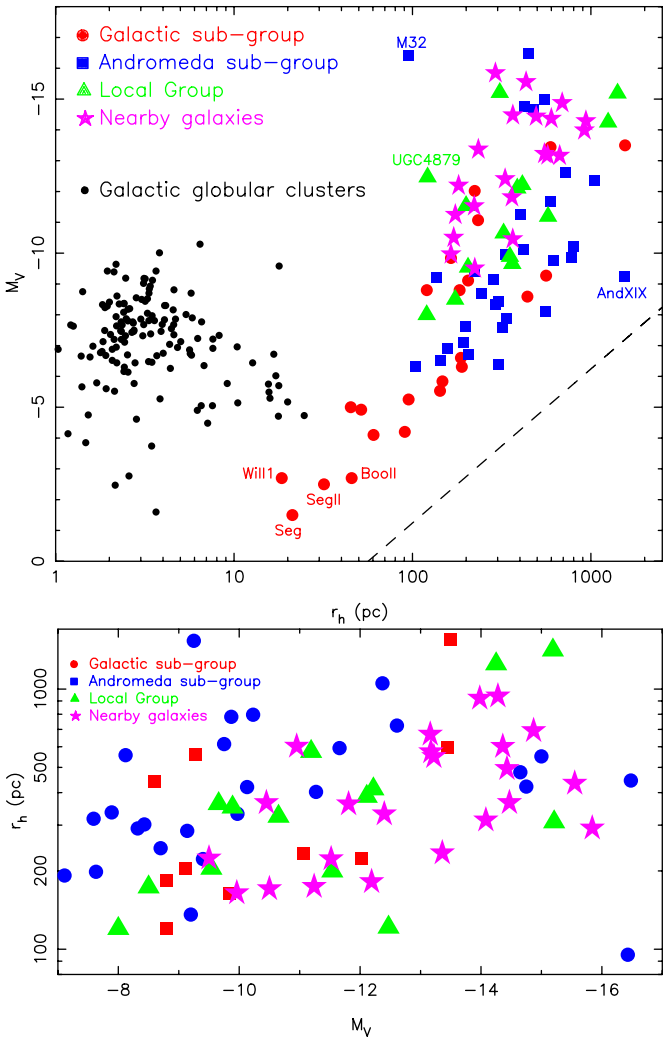

Figure 6. Top panel: the absolute visual magnitude vs. half-light radius (geometric mean of the major and minor axes) for the galaxy sample (where the symbols and color-coding identify Galactic, M31, Local Group, and nearby galaxies, as explained in the key). Also indicated as small black dots are the location of the Galactic globular clusters, using the data compiled by Harris (1996). Obvious outliers to the overall trend displayed by the galaxies are highlighted by name, as are some of the least luminous (candidate) dwarf galaxies. The dashed line indicates the direction defined by points of constant surface brightness (averaged within the half-light radius). Bottom panel: same parameters as top panel showing an enlargement around $-17 \leqslant M_V \leqslant -7$.
(A color version of this figure is available in the online journal.)

to be two flattened wings emanating from the central spheroid of stars, perhaps indicating the presence of a disk. More work is needed to determine the significance of the structure of UGC 4879 and its position in this diagram.

The lower panel of Figure 6 enlarges the region $-17 \leqslant M_V \leqslant -7$ to demonstrate the very large scatter that exists in this regime (see below for discussion of the fainter systems). McConnachie & Irwin (2006) originally pointed out that, at a given luminosity, the M31 dwarf satellites were generally larger than the MW population. With a large number of new discoveries since this time, Brasseur et al. (2011a) demonstrate that the mean relations of the M31 and MW populations are statistically consistent with each other[3]. The limited number of points contributing to the relations for these different sub-groups

[3] Note added in Proof: See also the recent study by Tollerud et al. (2012).

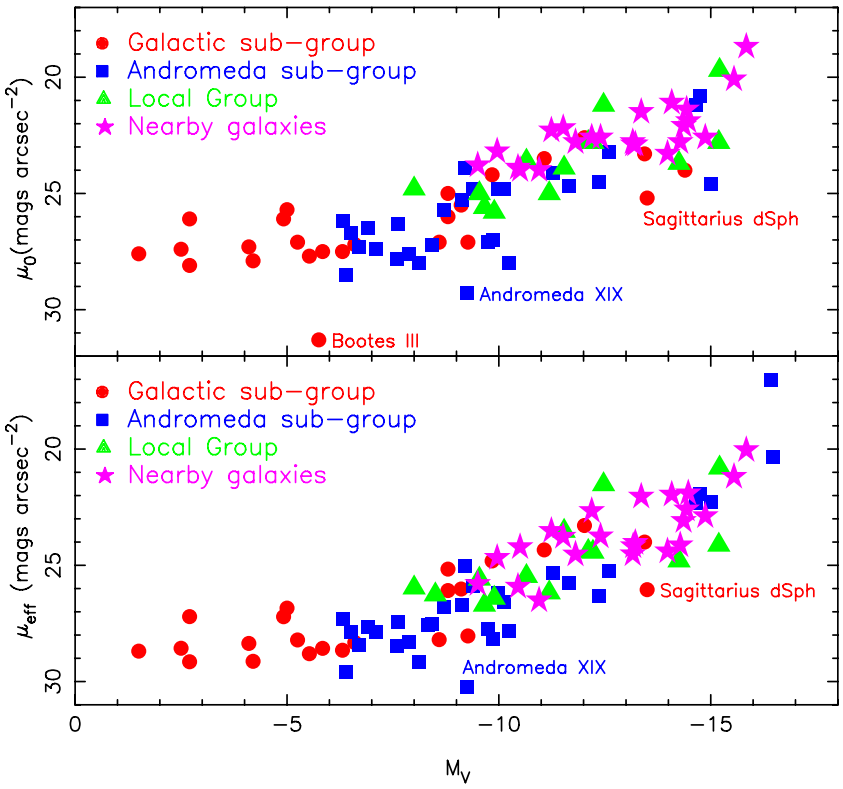

Figure 7. Surface brightness vs. absolute visual magnitude for the galaxy sample, where symbols have the same meaning as in Figure 6. The top panel uses central surface brightness, whereas the bottom panel uses the surface brightness averaged over the half-light radius. Obvious outliers to the overall trends are highlighted by name. Note that Bootes III is not present in the lower panel due to the lack of a measured value for r_h.

(A color version of this figure is available in the online journal.)

makes interpretation difficult; for example, 4 out of 10 MW satellites have $r_h > 250$ pc, whereas 20 out of 26 M31 satellites are this large. It may be that local environment contributes to determining the sizes of dwarf galaxies, but perhaps the most important conclusion that can be drawn from the lower panel of Figure 6 is the *lack* of a strong relation between M_V–r_h in this regime; at any given luminosity, galaxy sizes vary by nearly an order of magnitude, and there is only a weak dependence on luminosity.

At even fainter magnitudes, the line of constant surface brightness (averaged within the half-light radius) included in the top panel of Figure 6 runs approximately parallel to the relation defined by the galaxy locus for $M_V \gtrsim -8$ (and this also has a different slope than the weak relation at brighter magnitudes). This indicates that the smallest galaxies so far discovered all have similar surface brightnesses and further suggests that selection effects may be driving the form of the $M_V - r_h$ relation at faint magnitudes. To explore this further, I plot surface brightness against absolute magnitude in Figure 7. The top panel shows the central surface brightness, whereas the bottom panel uses the average surface brightness within the half-light radius. The former is in principle more susceptible to localized features (e.g., nuclei, individual bright stars, etc.) than the latter. I have labeled points that are obvious outliers in *both* panels (note that Bootes III is not present in the lower panel of Figure 7 due to the lack of a measured value for r_h). These galaxies are all known or suspected to be undergoing tidal disruption.

There is a clear correlation between absolute magnitude and surface brightness in both panels of Figure 7 for galaxies more luminous than $M_V \sim -9$. Of considerable interest, however, is the change in the observed relationship between surface brightness and absolute magnitude *within* the dwarf regime. In particular, dwarf galaxies fainter than $M_V \simeq -8.5$ do not continue to decrease in surface brightness with decreasing luminosity. Instead, the surface brightness levels off at faint magnitudes, as implied in Figure 6. The central surface brightness distribution for the 26 galaxies fainter than $M_V = -8.5$ in Figure 7 can be characterized by a median surface brightness of 27.35 mag arcsec^{-2} and an inter-quartile range of 1.2 mag. Thus, the central surface brightness for galaxies fainter than $M_V = -8.5$ appears remarkably constant given that the luminosity changes by a factor of ∼600 within the sample.

Surface brightness selection effects must be seriously considered in examining the correlations in Figure 7 (see, for example, earlier discussion by Impey & Bothun 1997, and references therein). Here, the work of Koposov et al. (2008) provides the most relevant reference. The selection functions are complex and depend on distance, magnitude, and surface brightness. However, Table 3 of Koposov et al. (2008) indicates that galaxies as faint as $M_V \sim -4.4$, at distances of ∼180 kpc, could be recovered even if their central surface brightness is as faint as 29.9 mag arcsec^{-2}, more than 2 mag fainter than the median observed surface brightness at faint luminosities. There is also tentative evidence that the M31 satellites appear to behave in a similar way to the MW satellites (although they do not extend to the same low-luminosity limits). Searches for M31 satellites are subject to different (and as yet unquantified) selection effects compared to the MW satellites. Taken together, it appears possible that the "break" in the scaling relations at

around $M_V \sim -9$ may be real. If so, it may imply that—as a result of either formation (e.g., inflow of gas into dark matter haloes) or subsequent feedback/evolution (e.g., star formation)—there is a low-density limit to the central stellar densities of dwarf galaxies. If the effect is instead due to selection, then we are only observing those low-luminosity galaxies with the highest surface brightness, indicating that there may be very significant scatter in this property at faint magnitudes. Regardless of this speculation, the behavior of surface brightness with luminosity shown in Figure 7 certainly requires further consideration and explanation.

5. MASSES AND KINEMATICS

Table 4 lists various information regarding the masses and kinematics of the galaxy sample.

Column 1. Galaxy name.
Column 2. Mass of the galaxy in stellar masses, assuming a stellar mass-to-light ratio of 1. This has been adopted for simplicity and to allow easy scaling to whatever mass-to-light ratio is preferred (in particular, by adopting values estimated through near-infrared observations).
Column 3. The observed velocity dispersion of the stellar component and its uncertainty, generally based on multiple velocity measurements of individual (giant) stars, otherwise commented on in Column 10. Note that a single value for the velocity dispersion is often insufficient to describe the dynamics of the galaxy (e.g., multiple components and/or radial trends).
Column 4. The observed rotational velocity of the stellar component and its uncertainty. Where available, I quote the peak (observed) rotational velocity, otherwise the maximum observed rotational velocity.[4] In general, I try to give the rotational velocity uncorrected for inclination or asymmetric drift, although it is sometimes unclear in the original papers whether these corrections have been applied. "N/A" indicates that a rotational signature has been looked for and none has been observed. Where only weak gradients in velocity are detected and/or the rotational signature is ambiguous, I comment on this in Column 10. In most cases, it is probably safest to interpret the absence of a rotational signature as the absence of any rotation with a magnitude equal to or greater than the magnitude of the velocity dispersion.
Column 5. Mass of H I in each galaxy. Here, I have scaled the values cited in the relevant papers to the distance given in Column 6 of Table 2. Where only an upper limit from a non-detection is available and that upper limit is small in comparison to the stellar mass, I give the H I mass as zero.
Column 6. The observed velocity dispersion of the H I component and its uncertainty. Note that the H I velocity dispersion is affected by local processes, such as heating due to star formation, and so caution is urged in interpreting these numbers. Note also that many galaxies are observed to contain multiple H I components (e.g., Lo et al. 1993; Young & Lo 1996, 1997a, 1997b; Young et al. 2003).
Column 7. The observed rotational velocity of the H I component and its uncertainty. Where available, I quote the peak (observed) rotational velocity, otherwise the maximum rotational velocity (see footnote 4). In general, I try to give the rotational velocity uncorrected for inclination or asymmetric drift, although it is sometimes unclear in the original papers whether these corrections have been applied. "N/A" indicates that a rotational signature has been looked for and none has been observed. In most cases, it is probably safest to interpret the absence of a rotational signature as the absence of any rotation with a magnitude equal to or greater than the magnitude of the velocity dispersion.
Column 8. Dynamical mass within the observed half-light radius. I have derived this quantity following the relation of Walker et al. (2009c), where $M_{\rm dyn}(\leqslant r_h) = 580\, r_h\, \sigma_\star^2$ (see also Wolf et al. 2010) and so values are only given when both a *stellar* velocity dispersion and a half-light radius are available. Here, I adopt the value of the half-light radius measured on the semimajor axis. Dynamical masses can, of course, be estimated for all systems with measured structures and kinematics, but it is beyond the scope of this article to do so. While limited, the dynamical mass estimates in Column 8 are at least relatively homogeneous and hence comparable.
Column 9. References.
Column 10. Comments.

Figure 8 shows the mass of H I relative to visual luminosity for galaxies in the Local Group and its immediate vicinity, expressed in solar units, as a function of distance to either the MW or M31 (whichever is closer). Blue diamonds indicate galaxies with confirmed H I content. Orange arrows indicate the separations of gas-deficient galaxies, where the symbols for Sculptor and Fornax indicate that the presence of H I in these galaxies is ambiguous. Symbol size is proportional to absolute visual magnitude. The vertical dashed line indicates the approximate virial radius of the two host galaxies. Also indicated on the top axis is the "free-fall time," which is the time required for the galaxy to fall from rest at its current position and reach the host galaxy, acted upon only by the gravity of the giant galaxy,

$$t_{ff} \simeq 14.4\,{\rm Gyr} \left(\frac{r}{1\,{\rm Mpc}}\right)^{\frac{3}{2}} \left(\frac{M}{10^{12}\,M_\odot}\right)^{-\frac{1}{2}}. \qquad (1)$$

Dwarf galaxies with short free-fall timescales have likely had many chances to interact with the MW or M31, whereas galaxies with longer free-fall timescales likely have not had the time to complete many orbits. For systems where the free-fall time is of order or longer than a Hubble time (indicated with a dot-dashed line in Figure 8), it is reasonable to assume that interactions with giant galaxies have had a negligible effect on their evolution.

Figure 8 shows the well-noted Local Group position–morphology relation, first highlighted by Einasto et al. (1974), in which the gas-deficient dSph galaxies are preferentially found in close proximity to either the MW or M31. Gas-rich dwarfs are preferentially located far from either of these two galaxies. Similar behavior has been noted in other galaxy groupings (e.g., Skillman et al. 2003b; Geha et al. 2006a; Bouchard et al. 2009, and references therein), and this has long been interpreted as evidence of the importance of external effects, such as tidal or ram-pressure stripping, on the evolution of dwarf galaxies. Indeed, many simulations show that the combined effects of these processes are in principle sufficient to remove the gas from dIrr-type galaxies (e.g., Mayer et al. 2006). However, Grebel et al. (2003) argue that dSph galaxies are too metal-rich for their luminosity in comparison to the (old) stellar populations in dIrr galaxies; if so, then this requires that the early

[4] For observations that do not extend to sufficiently large Galactocentric radius, the maximum observed rotational velocity will not necessarily equal the peak rotational velocity of the galaxy.

Table 4
Masses and Kinematics

(1) Galaxy	(2) $M_\star$ ($10^6\ M_\odot$)	(3) σ^* (km s^{-1})		(4) v_r^* (km s^{-1})		(5) $M_{\rm H\,I}$ ($10^6\ M_\odot$)	(6) $\sigma^{\rm H\,I}$ (km s^{-1})		(7) $v_r^{\rm H\,I}$ (km s^{-1})		(8) $M_{\rm dyn}(\leqslant r_h)$ ($10^6\ M_\odot$)	(9) References[a]	(10) Comments
The Galaxy													
Canis Major	49	20.0	3.0	...	...	...	...	...	...	...	...	(1)	H I measurements complex due to location!
Sagittarius dSph	21	11.4	0.7	N/A	N/A	N/A[b]	N/A	N/A	N/A	N/A	190	(2) (3) (4) (5)	
Segue (I)	0.00034	3.9[c]	0.8	N/A	N/A	N/A	N/A	N/A	N/A	N/A	0.26	(6) (5)	Stellar velocity gradient constrained to <5 km s^{-1} at 90% confidence
Ursa Major II	0.0041	6.7	1.4	N/A	N/A	N/A	N/A	N/A	N/A	N/A	3.9	(7) (5)	Velocity difference of 8.4 ± 1.4 km s^{-1} between stars in the east and west
Bootes II	0.0010	10.5	7.4	...	...	N/A	N/A	N/A	N/A	N/A	3.3	(8) (5)	
Segue II	0.00086	3.4	$^{+2.5}_{-1.2}$	...	...	...	...	...	...	...	0.23	(9)	
Willman 1	0.0010	4.3	$^{+2.3}_{-1.3}$	...	...	N/A	N/A	N/A	N/A	N/A	0.27	(10) (5)	
Coma Berenices	0.0037	4.6	0.8	N/A	N/A	N/A	N/A	N/A	N/A	N/A	0.94	(7) (5)	Stellar velocity gradient of 5.5 ± 1.2 km s^{-1} deg^{-1}
Bootes III	0.017	14.0	3.2	...	...	...	...	...	...	...	...	(11)	
LMC	1500	20.2	0.5	49.8	15.9	460	15.8	0.2	63.0	3.0		(12) (13) (14)	Stellar velocities based on carbon stars; H I boundaries between LMC, SMC, bridge, and interface regions not clearly defined
SMC	460	27.6	0.5	N/A	N/A	460	22.0[d]	2.0	60.0	5.0		(15) (16) (14)	Stellar velocities based on red giant branch stars; stellar velocity gradient of 8.3 km s^{-1} deg^{-1}; H I boundaries between LMC, SMC, bridge, and interface regions not clearly defined
Bootes (I)	0.029	2.4	$^{+0.9}_{-0.5}$	...	...	N/A	N/A	N/A	N/A	N/A	0.81	(17) (5)	Stellar velocity dispersion corresponds to dominant component, and there is evidence for a hotter component with $\sigma^* \sim 9$ km s^{-1}
Draco	0.29	9.1	1.2	N/A	N/A	N/A	N/A	N/A	N/A	N/A	11	(18) (19) (5)	
Ursa Minor	0.29	9.5	1.2	N/A	N/A	N/A	N/A	N/A	N/A	N/A	9.5	(20) (19) (5)	
Sculptor	2.3	9.2	1.4	N/A	N/A	*0.22*[e]	N/A	N/A	N/A	N/A	14	(21) (22) (23) (5)	Stellar velocity gradient of 5.5 ± 0.5 km s^{-1} deg^{-1}
Sextans (I)	0.44	7.9	1.3	N/A	N/A	N/A	N/A	N/A	N/A	N/A	25	(21) (22) (5)	
Ursa Major (I)	0.014	7.6	1.0	...	...	N/A	N/A	N/A	N/A	N/A	11	(7) (5)	
Carina	0.38	6.6	1.2	N/A	N/A	N/A	N/A	N/A	N/A	N/A	6.3	(21) (22) (5)	Stellar velocity gradient of 2.5 ± 0.8 km s^{-1} deg^{-1}
Hercules	0.037	3.7	0.9	...	...	N/A	N/A	N/A	N/A	N/A	2.6	(24) (5)	
Fornax	20	11.7	0.9	N/A	N/A	*0.17*[f]	N/A	N/A	N/A	N/A	56	(21) (22) (25) (5)	Stellar velocity gradient of 6.3 ± 0.2 km s^{-1} deg^{-1}
Leo IV	0.019	3.3	1.7	...	...	N/A	N/A	N/A	N/A	N/A	1.3	(7) (5)	
Canes Venatici II	0.0079	4.6	1.0	...	...	N/A	N/A	N/A	N/A	N/A	0.91	(7) (5)	
Leo V	0.011	3.7	$^{+2.3}_{-1.4}$	...	...	N/A	N/A	N/A	N/A	N/A	1.1	(26) (27) (5)	
Pisces II	0.0086	...	...	...	...	...	...	...	...	...	...		
Canes Venatici (I)	0.23	7.6	0.4	...	...	N/A	N/A	N/A	N/A	N/A	19	(7) (5)	
Leo II	0.74	6.6	0.7	...	...	N/A	N/A	N/A	N/A	N/A	4.6	(18) (5)	
Leo I	5.5	9.2	1.4	N/A	N/A	N/A	N/A	N/A	N/A	N/A	12	(28) (5)	
Andromeda													
M32	320	92.0	5.0	55.0	3.0	N/A	N/A	N/A	N/A	N/A	540	(29) (5)	Stellar velocity dispersion rises rapidly toward center and presents strong evidence for a supermassive black hole (e.g., see also van der Marel et al. 1997)
Andromeda IX	0.15	4.5	3.6	...	...	N/A	N/A	N/A	N/A	N/A	6.5	(30) (5)	
NGC 205	330	35.0	5.0	11.0	5.0	0.40	16.1[g]		N/A	N/A	420	(31) (32)	H I velocity gradient of ~42 km s^{-1} measured over ~3 arcmin
Andromeda XVII	0.26	...	...	...	...	N/A	N/A	N/A	N/A	N/A	...	(5)	

Table 4
(Continued)

(1) Galaxy	(2) $M_\star$ ($10^6\ M_\odot$)	(3) σ^* (km s^{-1})		(4) v_r^* (km s^{-1})		(5) $M_{\rm H\,I}$ ($10^6\ M_\odot$)	(6) $\sigma^{\rm H\,I}$ (km s^{-1})		(7) $v_r^{\rm H\,I}$ (km s^{-1})		(8) $M_{\rm dyn}(\leqslant r_h)$ ($10^6\ M_\odot$)	(9) References[a]	(10) Comments
Andromeda I	3.9	10.6	1.1	...	...	N/A	N/A	N/A	N/A	N/A	44	(33) (5)	
Andromeda XXVII	0.12	...	...	...	...	...	...	...	...	...	...		
Andromeda III	0.83	4.7	1.8	...	...	N/A	N/A	N/A	N/A	N/A	6.1	(33) (34)[h]; (5)	
Andromeda XXV	0.68	...	...	...	...	...	...	...	...	...	...		
Andromeda XXVI	0.060	...	...	...	...	...	...	...	...	...	...		
Andromeda XI	0.049	$\leqslant$4.6		...	...	N/A	N/A	N/A	N/A	N/A	1.9	(30) (5)	
Andromeda V	0.39	11.5	$^{+5.3}_{-4.4}$	...	...	N/A	N/A	N/A	N/A	N/A	...	(35) (34) (5)	Not associated with H I detection in Blitz & Robishaw (2000)
Andromeda X	0.096	3.9	1.2	...	...	N/A	N/A	N/A	N/A	N/A	2.3	(33) (5)	
Andromeda XXIII	1.1	...	...	...	...	...	...	...	...	...	...		
Andromeda XX	0.029	...	...	...	...	...	...	...	...	...	...		
Andromeda XII	0.031	2.6	$^{+5.1}_{-2.6}$	...	...	N/A	N/A	N/A	N/A	N/A	1.2	(30) (5)	
NGC 147	62	16.0	1.0	17.0	2.0	N/A	N/A	N/A	N/A	N/A	93	(36) (5)	
Andromeda XXI	0.76	...	...	...	...	...	...	...	...	...	...		
Andromeda XIV	0.20	5.4	1.3	...	...	N/A	N/A	N/A	N/A	N/A	6.1	(33) (5)	
Andromeda XV	0.49	11.0	$^{+7.0}_{-5.0}$	...	...	N/A	N/A	N/A	N/A	N/A	16	(37) (5)	
Andromeda XIII	0.041	9.7	$^{+8.9}_{-4.5}$	...	...	N/A	N/A	N/A	N/A	N/A	11	(30) (5)	Stellar velocity dispersion based on three stars
Andromeda II	7.6	7.3	0.8	...	...	N/A	N/A	N/A	N/A	N/A	36	(33) (5)	
NGC 185	68	24.0	1.0	15.0	5.0	0.11	15.3	0.8	N/A[i]	N/A	150	(36) (32)	
Andromeda XXIX	0.18	...	...	...	...	...	...	...	...	...	...		
Andromeda XIX	0.43	...	...	...	...	...	...	...	...	...	...		
Triangulum	2900												
Andromeda XXIV	0.093	...	...	...	...	...	...	...	...	...	...		
Andromeda VII	9.5	9.7	1.6	...	...	N/A	N/A	N/A	N/A	N/A	42	(33) (5)	
Andromeda XXII	0.034	...	...	...	...	...	...	...	...	...	...		
IC 10	86	...	...	...	...	50	8.0	1.0	34.0	5.0	...	(38) (39)	Gaseous disk embedded in complex, extended H I distribution, (with a dispersion of around 30–40 km s^{-1})
LGS 3	0.96	7.9	$^{+5.3}_{-2.9}$	...	...	0.38	9.1	0.3	$\leqslant$ 5.0		17	(40) (41)	Stellar velocity dispersion based on four stars
Andromeda VI	2.8	9.4	$^{+3.2}_{-2.4}$	...	...	N/A	N/A	N/A	N/A	N/A	...	(35) (5)	
Andromeda XVI	0.41	$\leqslant$ 10.0		...	...	N/A	N/A	N/A	N/A	N/A	7.9	(37) (5)	
Andromeda XXVIII	0.21	...	...	...	...	...	...	...	...	...	...		
IC 1613	100	...	...	...	...	65	25.0	3.0	5.9	1.0	...	(42) (43)	
Phoenix	0.77	...	...	...	...	0.12	10.0	4.0	N/A	N/A	...	(44)	H I cloud offset from optical center of Phoenix, proposed as supernova-driven outflow; H I velocity gradient of $\sim$10 km s^{-1} observed over $\sim$8 arcmin
NGC 6822	100	...	...	...	...	130	5.8	1.9	47.0	2.0	...	(45) (46)	Demers et al. (2006) obtain velocities for >100 AGB stars.
Cetus	2.6	17.0[j]	2.0	7.7	1.2	N/A	N/A	N/A	N/A	N/A	120	(47) (5)	Tentative stellar velocity gradient across minor axis of 7.7 $\pm$ 1.2 km s^{-1}; unassociated with nearby H I cloud
Pegasus dIrr	6.61	...	...	...	...	5.9	<9.0		21.0:		...	(48) (49)	
Leo T	0.14	7.5	1.6	...	...	0.28	6.9	1.0	N/A	N/A	3.9	(7) (50)	
WLM	43	17.5	2.0	20.8	2.0	61	4.5	1.0	30.0	3.0	380	(51) (52)	
Leo A	6.0	9.3	1.3	N/A	N/A	11	9.3	1.4	N/A	N/A	25	(53) (54)	Stellar kinematics derived using 10 young B supergiants + H II regions; H I gradient of $\sim$1.3 km s^{-1} arcmin^{-1}

Table 4
(Continued)

(1) Galaxy	(2) $M_\star$ ($10^6\ M_\odot$)	(3) σ^* (km s^{-1})		(4) v_r^* (km s^{-1})		(5) $M_{\rm H\,I}$ ($10^6\ M_\odot$)	(6) $\sigma^{\rm H\,I}$ (km s^{-1})		(7) $v_r^{\rm H\,I}$ (km s^{-1})		(8) $M_{\rm dyn}(\leqslant r_h)$ ($10^6\ M_\odot$)	(9) References[a]	(10) Comments
Andromeda XVIII	0.63	...	...	...	...	...	...	...	...	...	...		
Aquarius	1.6	...	...	...	...	4.1	5.8	0.1	N/A	N/A	...	(48)	H I velocity gradient of 6 km s^{-1} arcmin^{-1}.
Tucana	0.56	15.8	$^{+4.1}_{-3.1}$	N/A	N/A	N/A	N/A	N/A	N/A	N/A	41	(55) (5)	Stellar velocity gradient of $\sim$16 km s^{-1} over $\sim 2 \times r_h$; unlikely associated with nearby H I cloud
Sagittarius dIrr	3.5	...	...	...	...	8.8	10.0	1.0	N/A	N/A	...	(41)	
UGC 4879	8.3	...	...	...	...	0.95	11.0	1.1	N/A	N/A	...	(56)	
NGC 3109	76	...	...	...	...	450	10.0:		72.4	0.5	...	(57) (58) (59)	
Sextans B	52	...	...	...	...	51	<18.0		71:			(60) (49)	
Antlia	1.3	...	...	...	...	0.73	6.4	0.7	N/A	N/A	...	(58)	
Sextans A	44	...	...	...	...	77	8.0	1.0	20.0	2.0	...	(61)	
HIZSS 3(A)	...	...	...	...	...	14	...	...	42.0	4.0	...	(62)	
HIZSS 3B	...	...	...	...	...	2.6	...	...	N/A	N/A	...	(62)	H I velocity gradient of $\sim$2.5 km s^{-1} arcmin^{-1}
KKR 25	1.4	...	...	...	...	...	...	...	...	...	...		See Huchtmeier et al. (2000) for attempted H I observations
ESO 410- G 005	3.5	...	...	...	...	0.73	14.2	0.6	...	...	...	(63)	
NGC 55	2200	...	...	...	...	1300	...	...	86.0	6.0	...	(64)	Castro et al. (2008) obtain stellar velocities for $\sim$200 massive blue stars and find that their kinematics closely trace the H I rotation curve
ESO 294- G 010	2.7	...	...	...	...	0.34	9.7	0.9	...	...	...	(63)	
NGC 300	2100	...	...	...	...	1800	13.0	5.0	98.8	3.1	...	(65) (66)	H I velocity dispersion shows significant spatial variation
IC 5152	270	...	...	...	...	87	...	...	...	...	...	(45)	H I line widths available in Koribalski et al. (2004)
KKH 98	4.5	...	...	...	...	6.6	...	...	...	...	...	(67)	H I line widths available in Begum et al. (2008b) and Huchtmeier et al. (2003)
UKS 2323-326	17	...	...	...	...	17:	...	...	...	...	...	(68)	See also Huchtmeier & Richter (1986); H I line widths available in Longmore et al. (1982) and Huchtmeier & Richter (1986)
KKR 3	0.54	...	...	...	...	2.5	7.5	0.5	N/A	N/A	...	(69)	H I velocity gradient of $\sim$3.3 km s^{-1} arcmin^{-1}
GR 8	6.4	...	...	...	...	11	7.0	0.2	N/A	N/A	...	(48)	Lumpy H I velocity distribution, with some evidence of an overall velocity gradient
UGC 9128	7.8	...	...	...	...	18	<15.0		56.0:		...	(49)	See also Begum et al. (2008b)
UGC 8508	19	...	...	...	...	29	...	...	31.2	2.3	...	(67) (70)	
IC 3104	62	...	...	...	...	13	...	...	...	...	...	(45)	H I line widths available in Koribalski et al. (2004)
DDO 125	47	...	...	...	...	35	7.3	1.5	11.2	2.7	...	(71) (72)	H I rotational velocity measured at $r = 2$ arcmin; see also Huchtmeier et al. (2003), Begum et al. (2008b), and Swaters et al. (2009)
UGCA 86	16	...	...	...	...	860	8.8	1.0	122.0	5.0	...	(73)	H I structure consists of a rotating disk and a kinematically distinct, elongated "spur"
DDO 99	16	...	...	...	...	52	...	...	...	...	...	(67)	H I line widths available in Begum et al. (2008b)
IC 4662	190	...	...	...	...	180	...	...	...	...	...	(45)	H I line widths available in Koribalski et al. (2004)
DDO 190	51	...	...	...	...	43	10.0	2.4	24.7	2.5	...	(71) (72)	H I rotational velocity measured at $r = 1.5$ arcmin
KKH 86	0.82	...	...	...	...	0.88	...	...	...	...	...	(74)	H I line widths available in Karachentsev et al. (2001a)
NGC 4163	37	...	...	...	...	7.9	<7.4		8.7:		...	(75)	
DDO 113	2.1	...	...	...	...	48[k]	...	...	...	...	...	(76)	H I line widths available in Huchtmeier & Richter (1986)

Table 4
(Continued)

[a] **References:** (1) Martin et al. 2005; (2) Ibata et al. 1994; (3) Ibata et al. 1997; (4) Peñarrubia et al. 2011; (5) Grcevich & Putman 2009; (6) Simon et al. 2011; (7) Simon & Geha 2007; (8) Koch et al. 2009; (9) Belokurov et al. 2009; (10) Martin et al. 2007; (11) Carlin et al. 2009; (12) Kim et al. 1998; (13) van der Marel et al. 2002; (14) Brüns et al. 2005; (15) Harris & Zaritsky 2006; (16) Stanimirović et al. 2004; (17) Koposov et al. 2011; (18) Walker et al. 2007; (19) Wilkinson et al. 2004; (20) Walker et al. 2009c; (21) Walker et al. 2009b; (22) Walker et al. 2008; (23) Carignan et al. 1998; (24) Adén et al. 2009a; (25) Bouchard et al. 2006; (26) Belokurov et al. 2008; (27) Walker et al. 2009a; (28) Mateo et al. 2008; (29) Bender et al. 1996; (30) Collins et al. 2010; (31) Geha et al. 2006b; (32) Young & Lo 1997a; (33) Kalirai et al. 2010; (34) Blitz & Robishaw 2000; (35) Collins et al. 2011; (36) Geha et al. 2010; (37) Letarte et al. 2009; (38) Shostak & Skillman 1989; (39) Wilcots & Miller 1998; (40) Cook et al. 1999; (41) Young & Lo 1997b; (42) Lake & Skillman 1989; (43) Silich et al. 2006; (44) Young et al. 2007; (45) Koribalski et al. 2004; (46) Weldrake et al. 2003; (47) Lewis et al. 2007; (48) Young et al. 2003; (49) Hoffman et al. 1996; (50) Ryan-Weber et al. 2008; (51) Kepley et al. 2007; (52) Leaman et al. 2009; (53) Brown et al. 2007; (54) Young & Lo 1996; (55) Fraternali et al. 2009; (56) Bellazzini et al. 2011; (57) Jobin & Carignan 1990; (58) Barnes & de Blok 2001; (59) Blais-Ouellette et al. 2001; (60) Epinat et al. 2008; (61) Skillman et al. 1988; (62) Begum et al. 2005; (63) Bouchard et al. 2005; (64) Puche et al. 1991; (65) Westmeier et al. 2011; (66) Hlavacek-Larrondo et al. 2011; (67) Begum et al. 2008b; (68) Longmore et al. 1982; (69) Begum et al. 2006; (70) Begum et al. 2008a; (71) Stil & Israel 2002a; (72) Stil & Israel 2002b; (73) Stil et al. 2005; (74) Karachentsev et al. 2001a; (75) Simpson & Gottesman 2000; (76) Huchtmeier & Richter 1986.

[b] See Putman et al. (2004) for possible detection of gas in the Sagittarius stream.

[c] Upper limit (uncorrected for binaries) and with a possible member star removed that otherwise boosts the dispersion to $\sim$5.5 km s^{-1}.

[d] Varies from 5 to 40 km s^{-1} across face of SMC.

[e] Ambiguous detection of two H I clouds offset from optical center that could belong to the Magellanic Stream or Sculptor Group.

[f] Ambiguous H I detection of cloud offset from optical center that could be Galactic H I emission.

[g] Estimated from mean velocities of seven prominent H I clumps.

[h] See their *Note added in proof*.

[i] Apparent north–south gradient of 20km s^{-1} due to two distinct H I clumps.

[j] Uncorrected for possible rotational signature.

[k] Calculated following Huchtmeier & Richter (1988).

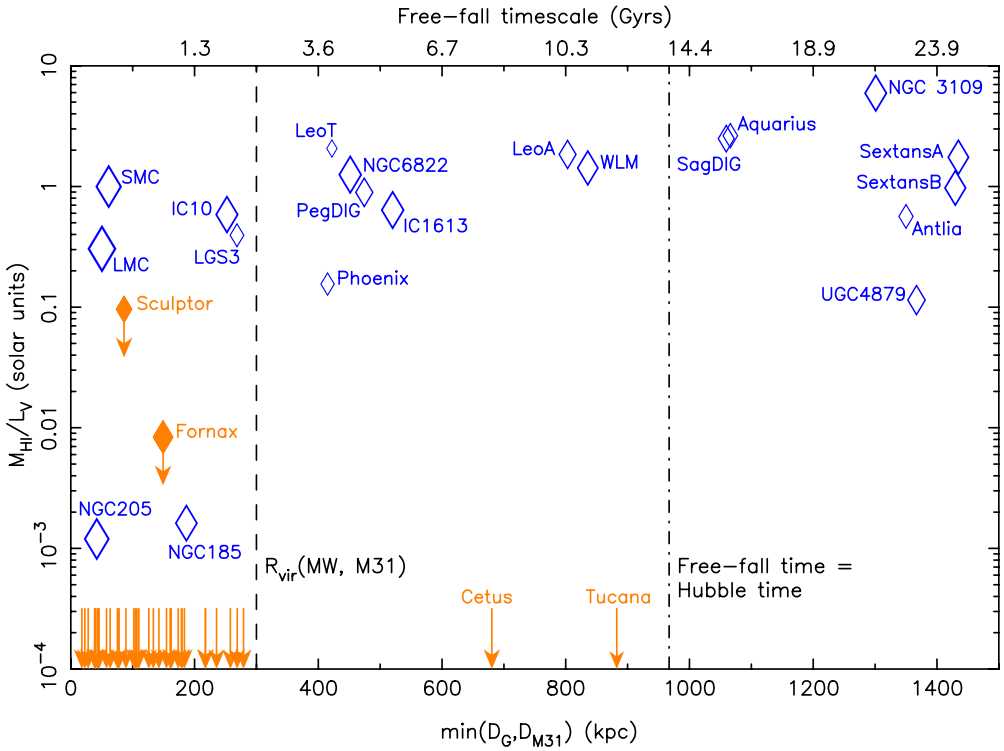

Figure 8. H I fraction, expressed as $M_{\rm H\,I}/L_V$ in solar units, as a function of proximity to a giant galaxy. Blue diamonds indicate galaxies with confirmed H I content. Orange arrows indicate the separation of gas-deficient galaxies from either the MW or M31. The symbols for Sculptor and Fornax indicate that the presence of H I in these galaxies is ambiguous. Symbol size is proportional to absolute visual magnitude. The vertical dashed line indicates the approximate virial radius of the MW/M31. Also indicated on the top axis is the time required for the galaxy to accelerate from rest and reach the MW/M31. The dot-dashed line indicates the separation at which this time equals a Hubble time.

(A color version of this figure is available in the online journal.)

metallicity evolution of the two morphological types (and not just their environments) were also different.

The visual appearance of dIrr galaxies is usually very different from that of dSph systems and reflects the presence of very young stellar populations and ongoing star formation in the former. Some dwarf galaxies are additionally classified as "dIrr/dSph": these so-called transition systems, such as DDO 210, distinguish themselves from dIrrs primarily through the absence of *current* star formation (formally, detectable H I but no detectable H II regions), despite having very young stellar populations. While star formation in some of these galaxies may have ceased permanently, in others it may be possible that low-level star formation is continuing without the production of H II regions (Fumigalli et al. 2011). Alternatively, ongoing, low-level star formation may be interrupted by periods of inactivity ("gasping"; see Tosi et al. (1991) for an example), in which case the distinction between a dIrr and a transition system merely reflects the moment we happen to be observing it.

The HST/ANGST survey (Dalcanton et al. 2009) has recently derived star formation histories (SFHs) for many nearby dwarf galaxies, including a large number of the more distant galaxies in this compilation. They show a tremendous diversity in the SFHs, and highlight that in a statistical sense there is essentially no difference between the SFHs of dIrr galaxies and the transition systems (Weisz et al. 2011). They suggest that many of the transition dwarfs are perhaps best treated as low mass dIrr galaxies, and if any of the transition dwarfs are deserving of the moniker it is likely the less isolated, low gas fraction systems. Weisz et al. (2011) also demonstrate that the "average" SFHs of dIrrs and dSphs in their sample are actually similar over most of cosmic time. It is only within the past few Gyr, and particularly within the past 1 Gyr, that the SFHs differ. However, the HST/ANGST survey generally samples only bright dSphs (comparable in luminosity to Fornax, for example), and low-luminosity systems comparable to Ursa Minor, Draco, and their ilk are either absent or underrepresented (due to the difficulty of finding such galaxies outside of the Local Group). The reader is referred to the HST/LCID survey (Monelli et al. 2010a, 2010b; Hidalgo et al. 2011, and references therein) that is presently investigating the possible connections between dIrr, transition, and dSph using isolated dwarfs within the Local Group.

A final distinction between dIrr and dSph galaxies is traditionally made based on their kinematics, although this is not necessarily well motivated from an observational perspective, particularly at faint magnitudes. It is generally argued that dIrr galaxies are rotationally supported systems, whereas dSph galaxies are pressure-supported systems. However, as is visible in Table 4, the majority of dynamical studies of dSph galaxies are based on resolved spectroscopy of individual (giant) stars. Until recently, essentially all dynamical studies of Local Group dIrr galaxies were based on H I, which generally shows significant rotation. However, recent work by Leaman et al. (2009) has shown that the evolved RGB population in WLM has $(v_r/\sigma)_\star \simeq 1.2$, whereas $(v_r/\sigma)_{\rm H\,I} \simeq 6.7$. Thus, while it may be true that the stellar component of dIrrs shows significant rotation compared to dSphs, caution should be exercised in comparing H I kinematics to those of evolved stellar populations.

Figure 9 plots the stellar velocity dispersion given in Table 4 against the half-light radius for all galaxies for which this

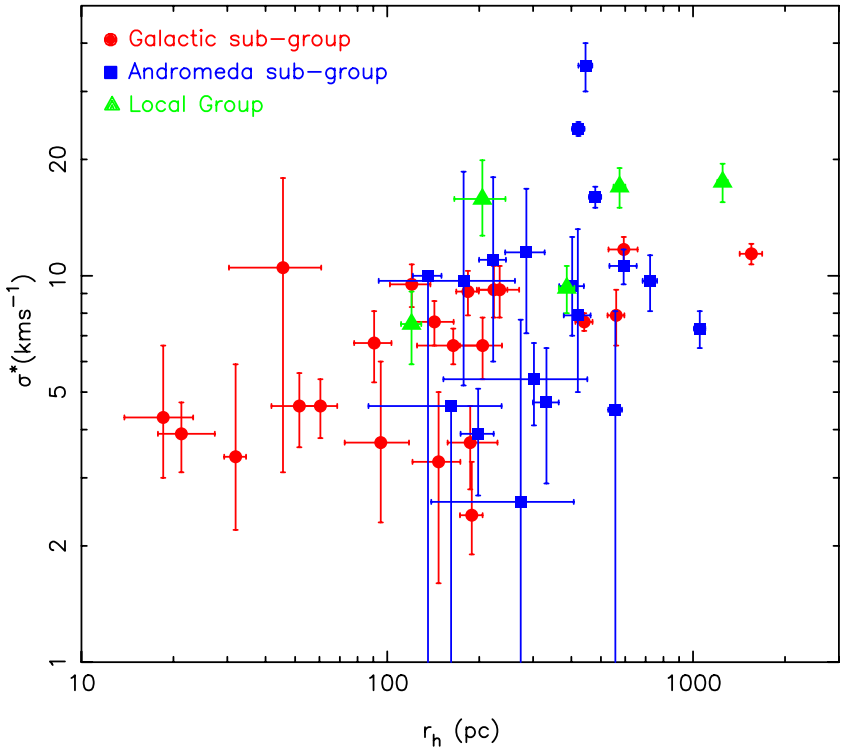

Figure 9. Stellar velocity dispersion vs. the (geometric-mean) half-light radius measured for all galaxies for which this information is available.
(A color version of this figure is available in the online journal.)

information exists. A broad correlation exists, such that colder systems have smaller scale sizes, although the scatter in this relationship is roughly an order of magnitude at a given scale radius. Measuring some of these values is challenging: Martin et al. (2008b) and Muñoz et al. (2012) both discuss the problems of determining structural parameters for galaxies in which few bright stars can be identified (generally the case for galaxies much fainter than $M_V \simeq -8$). For velocity dispersions, too, the lack of a large number of bright spectroscopic targets and the low expected dispersions make these measurements particularly challenging. Typically, the velocity errors on individual stellar measurements that are used as a basis for deriving the overall dispersion are a few km s^{-1}, which is of order the measured dispersion for some of the galaxies in Figure 9. One should also consider that the expected velocity dispersion of a faint system like Segue, due only to its baryonic mass, is exceptionally small, at around $\sigma_\star \simeq 0.1$ km s^{-1} (McConnachie & Côté 2010).

There are a couple of primary sources of contamination when measuring velocity dispersions, all of which have been shown to bias the measured "intrinsic" dispersion of faint galaxies to higher values. Foreground contamination can have a significant effect. The first measurement of the velocity dispersion of the Hercules dwarf gave $\sigma_\star = 5.1 \pm 0.9$ km s^{-1} (Simon & Geha 2007). However, Adén et al. (2009a) obtained Stromgren photometry for stars in the direction of Hercules and were able to separate member stars from interloping dwarf stars in the halo of the Galaxy. Without doing this separation, Adén et al. (2009a) measure a value of $\sigma_\star = 7.3 \pm 1.1$ km s^{-1} (in broad agreement with Simon & Geha 2007). By additionally being able to reject foreground dwarfs, they find a considerably lower value of $\sigma_\star = 3.7 \pm 0.9$ km s^{-1} (see also Adén et al. 2009b).

Binary stars are a further source of known contamination when measuring the velocity dispersions of dwarf galaxies, where the reflex motion of an unresolved binary star is mistaken as a component of the intrinsic dispersion of the galaxy. This potential source of contamination was originally investigated prior to the identification of extremely faint dwarf galaxies to determine if it could inflate the measured velocity dispersion sufficiently to incorrectly infer the need for non-baryonic mass-to-light ratios. Numerous studies (e.g., Aaronson & Olszewski 1987; Mateo et al. 1993; Olszewski et al. 1996; Hargreaves et al. 1996) all concluded that, barring a pathological or extremely high binary population, binary stars were insufficient to boost a stellar system with $\sigma_\star \lesssim 1$ km s^{-1} to $\sigma_\star \simeq 8$–10 km s^{-1}, although some inflation of the dispersion is to be expected. Minor et al. (2010) have developed a methodology to statistically correct the velocity dispersions of dwarf galaxies for this binary inflation; their own study indicates that systems with intrinsic dispersions of 4–10 km s^{-1} are unlikely to have their dispersion inflated by more than 20% as a result of binaries. For systems with lower intrinsic dispersions than this, McConnachie & Côté (2010) argue that the inflation effect due to binaries could be significant, although this depends on the as-yet-unmeasured stellar binary fraction(s) in dwarf galaxies.

Recently, Koposov et al. (2011) developed a procedure for obtaining accurate radial velocities with demonstrably reliable uncertainties at faint magnitudes and conducted a multi-epoch spectroscopic study of the Bootes dwarf galaxy. Approximately 10% of the stars in their sample show evidence for velocity variability. Their data favor a two-component model for Bootes (see discussion in Section 4), where the central, dominant component has a velocity dispersion of $\sigma_\star = 2.4^{+0.9}_{-0.5}$ km s^{-1}. Their preferred value is notably lower than earlier values of order $\sigma_\star \simeq 6$ km s^{-1} reported by Muñoz et al. (2006) and Martin et al. (2007) (although they are in statistical agreement). These results all emphasize the difficulties in obtaining reliable estimates of the intrinsic velocity dispersions of very faint dwarf galaxies:

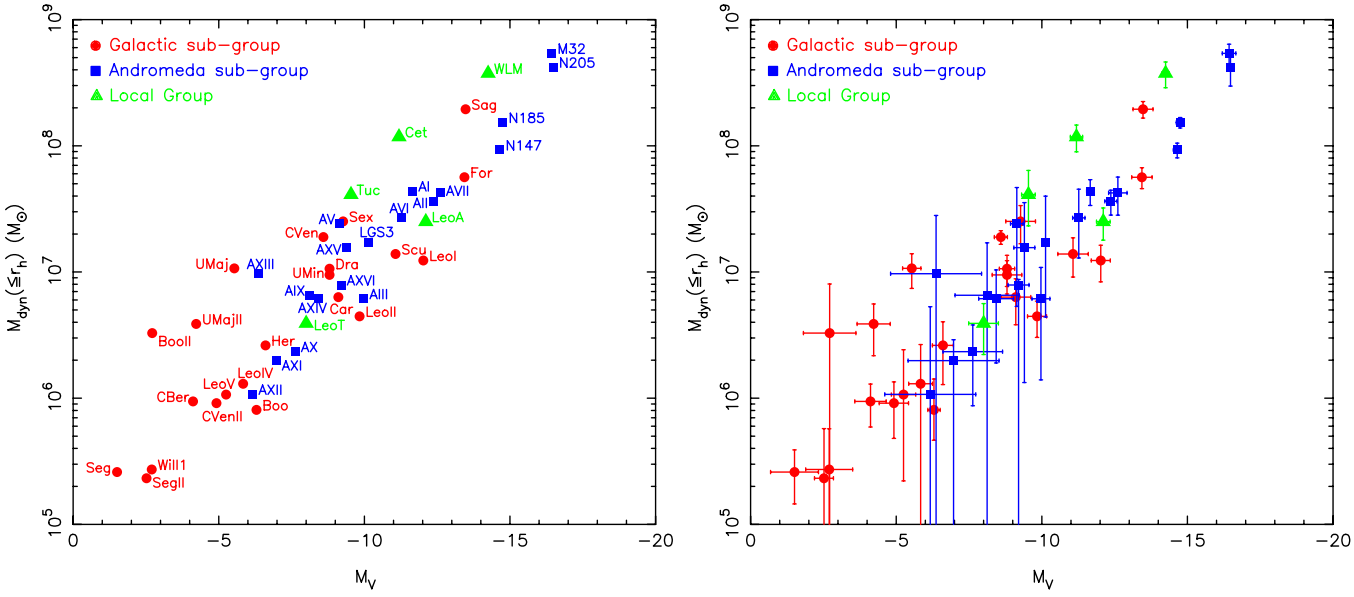

Figure 10. Dynamical mass estimates within the half-light radius vs. absolute visual magnitude, for all galaxies for which stellar velocity dispersion and half-light radius information is available. These have been calculated using the relation from Walker et al. (2009c). Individual galaxies are identified in the left panel, and error bars are indicated in the right panel. Note that the errors were calculated by propagating the uncertainties on the stellar velocity dispersion and half-light radius in the usual way and do not account for any systematic uncertainties in either these quantities or the dynamical state of the galaxy.

(A color version of this figure is available in the online journal.)

reliable (and small!) velocity uncertainties, multi-epoch data, and dwarf-giant separation are all essential components to any successful measurement.

With the above caveats on the basic dynamical data, Figure 10 shows the dynamical mass estimates for each dwarf galaxy within its half-light radius, as a function of absolute visual magnitude. Here, I have used the formalism by Walker et al. (2009c); Wolf et al. (2010) justify in detail why the mass within the half-light radius is in general able to be reliably measured for dispersion-supported spheroids. The left panel highlights by name each galaxy for which the necessary data exist, whereas the right panel shows the formal uncertainties on propagating the quoted uncertainties on $\sigma_\star$ and r_h. Note that these estimates do not take into consideration errors introduced as a result of the dynamical state of the galaxy. For example, a few galaxies in Figure 10 show some rotation in addition to dispersion support (M32, NGC 205, NGC 147, NGC 185, Cetus, WLM), and other galaxies may or may not be in dynamical equilibrium. Further, the Walker et al. formalism assumes that the velocity dispersion profile is flat with radius (the Wolf et al. formalism adopts a luminosity-weighted mean velocity dispersion); however, for many galaxies shown in Figure 10 the form of the radial velocity dispersion profile is unknown. A full study of the dynamics of these galaxies is clearly outside the scope of this article, and the current estimates are provided solely to demonstrate the status of the observational data in terms of its basic implications regarding the mass content of the galaxies. Figure 11 shows the same data as Figure 10, except I have now normalized $M_{\rm dyn}$ by $0.5\,L_\star$ to estimate the implied mass-to-light ratio of each system within its half-light radius.

Figures 10 and 11 demonstrate that there appears to be a well-defined relation consistent with a power law between $M_{\rm dyn}(\leqslant r_h)$ and M_V that holds across a factor of nearly 1 million in luminosity, in agreement with the finding reported by Walker et al. (2009c). As discussed above, systematic errors in the measurements of the relevant quantities, as well as the necessary assumptions that must be made in converting these quantities to a mass estimate, mean that the precise position of any single point in these plots is open to considerable debate. Further, it should be stressed that observational selection effects such as that discussed for Figure 6 (which may be responsible for the precise form of the M_V–r_h relationship at low luminosities) will also affect these figures due to the dependence of $M_{\rm dyn}$ on r_h.

Measurements such as those on which Figures 10 and 11 are based have also been used to argue for a common mass scale for the (MW) dwarfs (Strigari et al. 2007). However, this is usually made with reference to the mass enclosed with an absolute radial scale (typically $r = 300$ pc), a quantity that is used because of its usefulness in dark-matter-only simulations, where there is no information regarding the size of the baryonic components of galaxies. However, given that the half-light radii of the dwarfs in and around the Local Group have $20 \lesssim r_h \lesssim 2000$ pc, from an observational perspective this is a far less well-defined quantity than $M_{\rm dyn}(\leqslant r_h)$.

6. MEAN STELLAR METALLICITIES

Table 5 lists the available data for the mean stellar metallicities, $\langle$[Fe/H]$\rangle$, of the galaxies.

Column 1. Galaxy name.
Column 2. Mean stellar metallicity and error, generally derived from observations of mostly evolved giants, otherwise commented on in Column 5. Note that I quote the *mean* metallicity of all stars (as opposed to the median, mode, etc.) in the observed metallicity distribution function, and so this will be susceptible to any uncorrected biases in the observed sample. The mean stellar metallicity refers to the mean iron-peak metallicity expressed in logarithmic notation relative to the solar value.
Column 3. Technique used to estimate stellar metallicity. A discussion is given below.

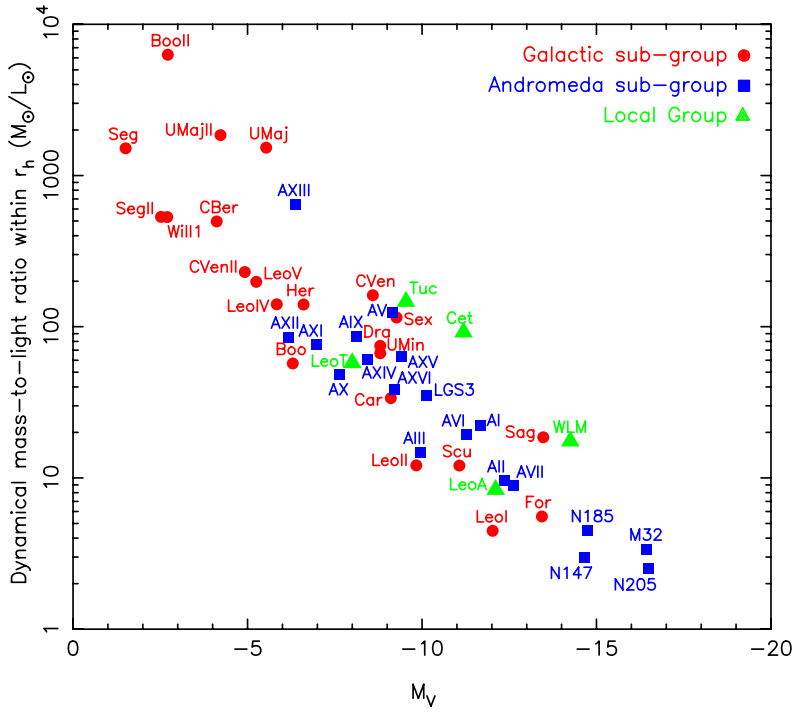

Figure 11. Mass-to-light ratio, in solar units, calculated within the half-light radius for all dwarf galaxies for which the necessary data exist, as a function of absolute visual magnitude.

(A color version of this figure is available in the online journal.)

Column 4. References.
Column 5. Comments.

Figure 12 shows mean stellar metallicity as a function of absolute visual magnitude, where by definition both axes are logarithmic quantities. In the left panel, all tabulated data from Table 5 are given, whereas in the right panel only data that use spectroscopically determined quantities are shown.

Generally the most well-accepted method of determining [Fe/H] for a given star is from direct high-resolution spectroscopy (HRS) from which the strengths of iron lines can be measured directly. However, Table 5 lists estimates for ⟨[Fe/H]⟩ that stem from a variety of additional techniques.

1. *RGB color*. Da Costa & Armandroff (1990) derive a relation between the mean color of RGB stars in globular clusters measured at $M_V = -3$ and the mean stellar metallicity of the cluster. A refined calibration (derived at $M_V = -3.5$) using the same data was presented by Lee et al. (1993), and this has been used throughout the literature as a convenient means of estimating the mean stellar metallicity of a system when only photometry of bright stars is available. An obvious disadvantage, of course, is that it is calibrated on ancient stellar populations. Since RGB stars are subject to age and metallicity degeneracies, this technique may not be reliable if significantly younger stars are present. I note that in Table 5 and Figure 12 most of the non-Local-Group galaxies have their mean stellar metallicity determined in this way. There is a suggestion in Figure 12 that these estimates are low in comparison to Local Group galaxies with similar absolute visual magnitudes, but its cause or significance is difficult to determine.
2. *Isochrones*. The comparison of theoretical isochrones, evolutionary tracks, or globular cluster fiducials, to the CMDs of galaxies is usually heavily or entirely weighted toward the color of the RGB and so is, in principle, subject to the same systematic uncertainties regarding ages as discussed above. In addition, isochrones produced by different groups may have some systematic differences between the predicted RGB colors at any age. However, one potential advantage of isochrones over empirical RGB color relations is that, if additional information is available regarding ages (e.g., from the red clump or main-sequence turnoff), isochrones with appropriate ages can be used.
3. *CMD fitting*. The reader is referred to the many excellent papers on SFH analysis using resolved stellar populations for more details (e.g., Gallart et al. 2005; Tolstoy et al. 2009, and references therein). Here, age degeneracies will likely be much reduced since age information is available from elsewhere in the CMD (in particular the main-sequence turnoff region).
4. *Calcium II triplet equivalent widths (low, moderate resolution spectroscopy)*. The strengths of the three CaT absorption lines at $\lambda = 8498, 8542$, and 8662 Å in RGB stars have been shown to correlate with [Fe/H] if the temperature and surface gravity of the star are able to be estimated through measurement of its absolute magnitude. The CaT is a relatively strong feature, and consequently it can be relatively easily measured using low- to moderate-resolution spectroscopy (L/MRS). Many authors (e.g., Rutledge et al. 1997) have developed calibrations between CaT equivalent width and [Fe/H], most recently Starkenburg et al. (2010). These authors also examine the form of the correlation at [Fe/H] $\lesssim -2.5$. Using the new calibration, Starkenburg et al. (2010) demonstrate that the resulting estimates of [Fe/H] match those derived from HRS down to a limiting stellar metallicity of [Fe/H] $\simeq -4$. Many of the values listed in Table 5 use the earlier calibrations, which can potentially deviate from the new calibration for stellar metallicities lower than [Fe/H] $\simeq -2$, depending on the absolute magnitudes of the observed stars.

Table 5
Mean Stellar Metallicities

(1) Galaxy	(2) ⟨[Fe/H]⟩		(3) Technique	(4) References	(5) Comments
The Galaxy					
Canis Major	−0.5	0.2	CMD fitting	Bellazzini et al. (2004c)	Based primarily on MS stars
Sagittarius dSph	−0.4	0.2	HRS	Chou et al. (2007)[a]	
Segue (I)	−2.72	0.40	MRS	Norris et al. (2010)	See also Simon et al. (2011)
Ursa Major II	−2.47	0.06	MRS	Kirby et al. (2008b, 2011)	
Bootes II	−1.79	0.05	MRS (CaT)	Koch et al. (2009)	
Segue II	−2.00	0.25	HRS	Belokurov et al. (2009)	
Willman 1	−2.1:		MRS	Willman et al. (2011)	Based on three stars
Coma Berenices	−2.60	0.05	MRS	Kirby et al. (2008b, 2011)	
Bootes III	−2.1	0.2	MRS	Carlin et al. (2009)	
LMC	−0.5		MRS (CaT)	Carrera et al. (2008)	See also Cole et al. (2005)
SMC	−1.00	0.02	MRS (CaT)	Parisi et al. (2010)	
Bootes (I)	−2.55	0.11	MRS	Norris et al. (2010)	See also Lai et al. (2011)
Draco	−1.93	0.01	MRS	Kirby et al. (2011)	See also Winnick (2003)
Ursa Minor	−2.13	0.01	MRS	Kirby et al. (2011)	See also Winnick (2003)
Sculptor	−1.68	0.01	MRS	Kirby et al. (2009, 2011)	See also Battaglia et al. (2008)
Sextans (I)	−1.93	0.01	MRS	Kirby et al. (2011)	See also Battaglia et al. (2011)
Ursa Major (I)	−2.18	0.04	MRS	Kirby et al. (2008b, 2011)	
Carina	−1.72	0.01	MRS (CaT)	Koch et al. (2006)	
Hercules	−2.41	0.04	MRS	Kirby et al. (2008b, 2011)	
Fornax	−0.99	0.01	MRS	Kirby et al. (2011)	See also Battaglia et al. (2006)
Leo IV	−2.54	0.07	MRS	Kirby et al. (2008b, 2011)	HRS of a single star in Simon et al. (2010)
Canes Venatici II	−2.21	0.05	MRS	Kirby et al. (2008b, 2011)	
Leo V	−2.00	0.2	Isochrones	de Jong et al. (2010)	
Pisces II	−1.9:		Isochrones	Belokurov et al. (2010)	
Canes Venatici (I)	−1.98	0.01	MRS	Kirby et al. (2008b, 2011)	
Leo II	−1.62	0.01	MRS	Kirby et al. (2011)	See also Koch et al. (2007a)
Leo I	−1.43	0.01	MRS	Kirby et al. (2011)	See also Koch et al. (2007b)
Andromeda					
M32	−0.25		Isochrones	Grillmair et al. (1996)	Likely significant age spread and gradients?
Andromeda IX	−2.2	0.2	Co-added MRS (CaT)	Collins et al. (2010)	
NGC 205	−0.8	0.2	Isochrones	McConnachie et al. (2005)	
Andromeda XVII	−1.9	0.2	Isochrones	Brasseur et al. (2011b)	
Andromeda I	−1.45	0.04	Isochrones	Kalirai et al. (2010)	
Andromeda XXVII	−1.7	0.2	Isochrones	Richardson et al. (2011)	
Andromeda III	−1.78	0.04	Isochrones	Kalirai et al. (2010)	
Andromeda XXV	−1.8	0.2	Isochrones	Richardson et al. (2011)	
Andromeda XXVI	−1.9	0.2	Isochrones	Richardson et al. (2011)	
Andromeda XI	−2.0	0.2	Co-added MRS (CaT)	Collins et al. (2010)	
Andromeda V	−1.6	0.3	Co-added LRS (CaT)	Collins et al. (2011)	
Andromeda X	−1.93	0.11	Isochrones	Kalirai et al. (2010)	
Andromeda XXIII	−1.8	0.2	Isochrones	Richardson et al. (2011)	
Andromeda XX	−1.5	0.1	Isochrones	McConnachie et al. (2008)	
Andromeda XII	−2.1	0.2	Co-added MRS (CaT)	Collins et al. (2010)	
NGC 147	−1.1	0.1	MRS (CaT)	Geha et al. (2010)	
Andromeda XXI	−1.8	0.2	Isochrones	Martin et al. (2009)	
Andromeda XIV	−2.26	0.05	Isochrones	Kalirai et al. (2010)	
Andromeda XV	−1.8	0.2	Co-added MRS (CaT)	Letarte et al. (2009)	
Andromeda XIII	−1.9	0.2	Co-added MRS (CaT)	Collins et al. (2010)	
Andromeda II	−1.64	0.04	Isochrones	Kalirai et al. (2010)	
NGC 185	−1.3	0.1	MRS (CaT)	Geha et al. (2010)	
Andromeda XXIX	−1.8:		Isochrones	Bell et al. (2011)	
Andromeda XIX	−1.9	0.1	Isochrones	McConnachie et al. (2008)	
Triangulum					
Andromeda XXIV	−1.8	0.2	Isochrones	Richardson et al. (2011)	
Andromeda VII	−1.40	0.30	Isochrones	Kalirai et al. (2010)	
Andromeda XXII	−1.8:		Isochrones	Martin et al. (2009)	
IC 10	−1.28:		Isochrones/RGB color	Tikhonov & Galazutdinova (2009)	
LGS 3	−2.10	0.22	RGB color	Lee (1995)	
Andromeda VI	−1.3	0.14	Co-added MRS (CaT)	Collins et al. (2011)	

Table 5
(Continued)

(1) Galaxy	(2) ⟨[Fe/H]⟩		(3) Technique	(4) References	(5) Comments
Andromeda XVI	−2.1	0.2	Co-added MRS (CaT)	Letarte et al. (2009)	
Andromeda XXVIII	...	...			
IC 1613	−1.6	0.2	CMD modeling	Bernard et al. (2010)	Derived in E. Skillman et al., (2012 in preparation)
Phoenix	−1.37	0.2	RGB color	Martínez-Delgado et al. (1999)	
NGC 6822	−1.0	0.5	LRS (CaT)	Tolstoy et al. (2001)	
Cetus	−1.9	0.10	MRS (CaT)	Lewis et al. (2007)	
Pegasus dIrr	−1.4	0.2	Isochrones	McConnachie et al. (2005)	
Leo T	−1.99	0.05	MRS	Kirby et al. (2008b, 2011)	
WLM	−1.27	0.04	MRS (CaT)	Leaman et al. (2009)	
Leo A	−1.4	0.2	CMD modeling	Cole et al. (2007)	
Andromeda XVIII	−1.8	0.1	Isochrones	McConnachie et al. (2008)	
Aquarius	−1.3	0.2	Isochrones	McConnachie et al. (2006)	Assumes an age of 4 Gyr; for an ancient population, find [Fe/H] $\simeq -1.9$
Tucana	−1.95	0.15	MRS (CaT)	Fraternali et al. (2009)	
Sagittarius dIrr	−2.1	0.2	Isochrones	Momany et al. (2002)	
UGC 4879	−1.5	0.2	Isochrones	Bellazzini et al. (2011)	
NGC 3109	−1.84	0.2	RGB color	Hidalgo et al. (2008)	
Sextans B	...	...			
Antlia	−1.6	0.1	RGB color	Aparicio et al. (1997)	
Sextans A	−1.85:		RGB color	Sakai et al. (1996)	Adopted $(V-I)_{-3.5} = 1.3$
HIZSS 3(A)	...	...			
HIZSS 3B	...	...			
KKR 25	−2.1	0.3	RGB color	Karachentsev et al. (2001b)	
ESO 410- G 005	−1.93	0.2	RGB color	Sharina et al. (2008)	
NGC 55					
ESO 294- G 010	−1.48	0.17	RGB color	Sharina et al. (2008)	
NGC 300					
IC 5152	...	...			
KKH 98	−1.94	0.25	RGB color	Sharina et al. (2008)	
UKS 2323-326	−1.68	0.19	RGB color	Sharina et al. (2008)	
KKR 3	−2.02	0.25	RGB color	Sharina et al. (2008)	
GR 8	...	...			
UGC 9128	−2.33	0.24	RGB color	Sharina et al. (2008)	
UGC 8508	−1.91	0.19	RGB color	Sharina et al. (2008)	
IC 3104	...	...			
DDO 125	−1.73	0.17	RGB color	Sharina et al. (2008)	
UGCA 86	...	...			
DDO 99	−2.13	0.22	RGB color	Sharina et al. (2008)	
IC 4662	−1.34	0.13	RGB color	Sharina et al. (2008)	
DDO 190	−2.00	0.08	RGB color	Aparicio & Tikhonov (2000)	
KKH 86	−2.33	0.29	RGB color	Sharina et al. (2008)	
NGC 4163	−1.65	0.15	RGB color	Sharina et al. (2008)	
DDO 113	−1.99	0.21	RGB color	Sharina et al. (2008)	

Note. [a] And references therein.

5. *Spectral synthesis (moderate-resolution spectroscopy).* Here, synthetic spectra spanning a range of key parameters (e.g., [Fe/H], [α/Fe], $T_{\rm eff}$, $\log g$) are compared to the measured stellar spectrum to determine the most likely [Fe/H]. Kirby et al. (2008a) have developed this technique for specific use on the dwarf galaxies of the MW with considerable success. Here, the main advantages are that one uses more spectral information than relying only on specific indices. Since one uses moderate resolutions, fainter targets can be studied than is possible with HRS.

Clearly, the range of techniques from which ⟨[Fe/H]⟩ has been derived in Table 5 may produce numerous systematic differences between results. Recent discussions of some of these issues can be found in Kirby et al. (2008a) (spectral synthesis), Starkenburg et al. (2010) (CaT), and Lianou et al. (2011) (isochrones, CaT), and the reader is referred to these papers for more details. I note that several of the ⟨[Fe/H]⟩ values listed in Table 5 only quote the uncertainty from the random error in the mean (i.e., $\sigma_{\rm [Fe/H]}/\sqrt{N}$) and do not include the additional systematic uncertainties (which cannot be treated in the same way). For galaxies for which this is the case, an additional systematic error component must be included, typically a tenth of a dex or more.

In addition to the systematic uncertainties introduced by the measurement technique, an additional systematic effect enters the calculation of the mean stellar metallicities in Table 5 through the spatial extent of the stars contributing to the measurement. Dwarf galaxies are known to exhibit radial gradients in stellar populations, ages, and/or metallicity distributions (e.g., Harbeck et al. 2001; Tolstoy et al. 2004; Battaglia

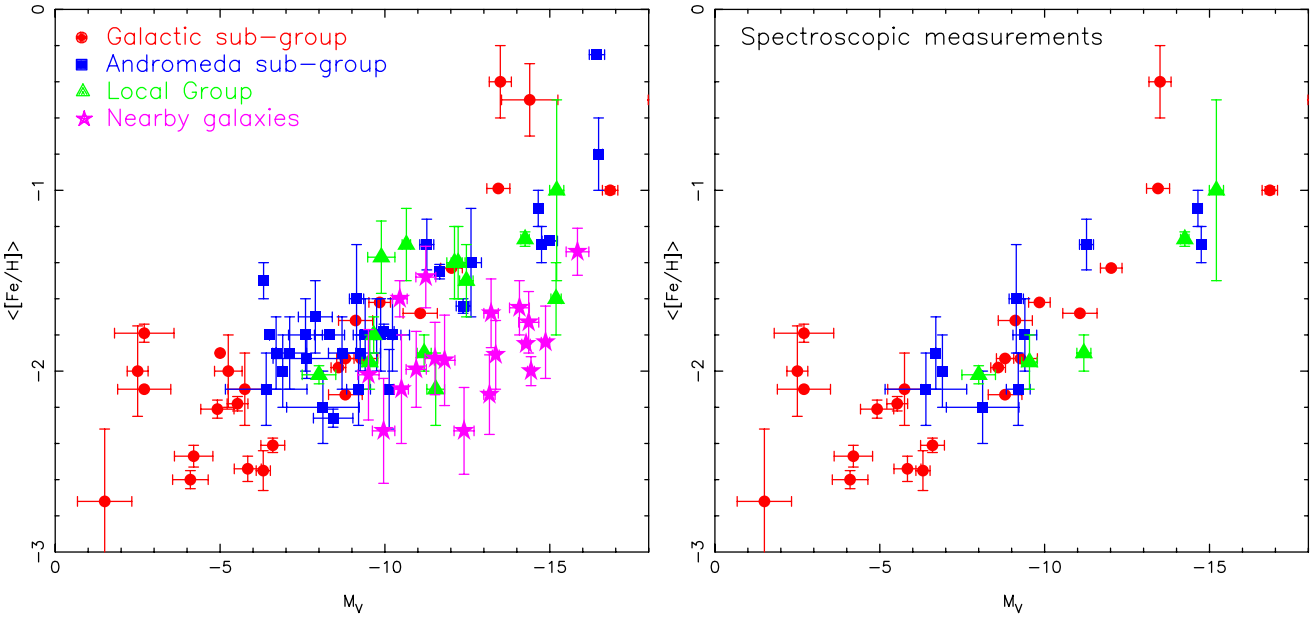

Figure 12. Absolute visual magnitude vs. stellar metallicity measurement (as listed in Table 5), for all galaxies in the sample for which this information is available. Color-coding is the same as in previous figures. The left panel shows all measurements regardless of the techniques used to estimate metallicity, whereas the right panel only shows those measurements derived from spectroscopic observations of resolved stars (typically giants).

(A color version of this figure is available in the online journal.)

et al. 2006; Bernard et al. 2008, and references therein). Thus far, all observed metallicity gradients are such that a higher "mean" stellar metallicity is observed in the central regions of the dwarf than in the outer regions. Two galaxies with identical metallicity distribution functions and radial gradients will therefore be measured to have different "mean" stellar metallicities if there is any difference in the radial distribution of stars that contribute to the measurement. Given the range in radial scale associated with the galaxies in Table 5 and the unknown spatial structure of the stellar populations/ages/metallicities within many of these systems, this effect may be significant.

With the above caveats, both panels of Figure 12 show the well-known luminosity–mean stellar metallicity relation, whereby more luminous galaxies are generally more metal-rich in the mean than faint galaxies (see also Tremonti et al. 2004; Lee et al. 2006; Kirby et al. 2008b, and references therein). The relation is better defined in the right panel, which uses only spectroscopic measurements of $\langle$[Fe/H]$\rangle$; the degree to which the scatter in the left panel is a result of systematic errors (age effects, measurement techniques, etc.) is unknown. As pointed out by Kirby et al. (2008b), the luminosity–mean stellar metallicity relation at faint magnitudes ($M_V > -8$) is entirely consistent with a continuation of the trend displayed for bright galaxies. However, it is also worth highlighting the dearth of data at faint magnitudes: if only galaxies fainter than $M_V = -8$ are considered, then the data are equally consistent with a scatter around a floor in mean stellar metallicity at $\langle$[Fe/H]$\rangle \simeq -2.1$. While more data are certainly needed, it is interesting to note that the magnitude at which one can start arguing for a floor in mean stellar metallicity is broadly the same point at which there is a break in the absolute magnitude–surface-brightness relation shown in Figure 7 (discussed in Section 4). While certainly speculative, this may suggest a direct link between the surface brightness of a galaxy (specifically, the *density* of baryons, rather than the total amount of baryons) and its mean stellar metallicity (see theoretical work by Dekel & Woo 2003; Revaz & Jablonka 2012, and references therein; see also Skillman et al. 2003a).

Many more parameters are required in order to fully define the metallicity distribution function of stars in any of the dwarf galaxies, and the reader is referred to Tolstoy et al. (2009) for a more complete discussion of ongoing observational efforts in this regard. As discussed in Tolstoy et al. (2009), detailed chemistry, such as abundance ratios of key elements, is now available for the nearest galaxies, with much more to come. In the near future, the combination of dynamical data with detailed information on the chemical evolution of galaxies is likely to continue to be a significant area of discovery and advance.

7. SUMMARY

Tables 1–5 provide observational parameters for approximately 100 nearby dwarf galaxies, including positional data; radial velocities; photometric and structural parameters; stellar, H I, and dynamical masses; internal kinematics (dispersions and rotation); and mean stellar metallicities. In addition to discussing the provenance of the values and possible sources of uncertainties affecting their usage, I also consider the membership and (limited?) spatial extent of the MW and M31 sub-groups; the morphological diversity of the M31 sub-group in comparison to the MW; the location of the zero-velocity surface of the Local Group; the timescales that can be associated with the orbital/interaction histories of the Local Group members; the scaling relations defined by the sample, including their behavior at the faintest magnitudes/surface brightnesses; and the luminosity–mean stellar metallicity relation, including its possible connection to the central surface brightness of the galaxies.

The dwarf galaxies discussed herein constitute all known satellite systems in the surroundings of the MW and M31, all quasi-isolated systems in the more distant reaches of the Local Group, and all other, generally very isolated, dwarf galaxies that surround the Local Group out to 3 Mpc, beyond which most of the known galaxies are members of Maffei, Sculptor, Canes Venatici, IC 342, M81, and the many other groups in the Local Volume found out to the Virgo Cluster and beyond. In some respects, these systems are stepping stones into the

Local Volume, and we are fortunate that they present us with a large and diverse range of properties to explore. This article has purposefully focused entirely on observable, quantifiable properties of these galaxies, and it is right that the published tables likely already contain obsolete numbers or do not include the most recent discoveries.[5,6] Our knowledge of many of these systems far exceeds that of other galaxies, and we will continue to be able to obtain ever more detailed observations of aspects of their structure, dynamics, stellar populations, and chemical signatures that are beyond the reach of observational programs of more distant galaxies. In the future as now, these are the galaxies for which we will know the most and so are perhaps destined to understand the least.

Updated versions of the core data available in Tables 1–5 for all dwarf galaxies within 3 Mpc are available at https://www.astrosci.ca/users/alan/Nearby_Dwarfs_Database.html. I thank Peter Stetson, Matthew Walker, Daniel Weisz, Sidney van den Bergh, and Else Starkenburg for careful readings of the manuscript and valuable comments; Ryan Leaman for his feedback, and for stressing the importance of radial metallicity gradients when considering mean stellar metallicities, which led to the addition of the relevant paragraph; and Josh Simon for highlighting relevant references. In addition, I am grateful to Vasily Belokurov, Michelle Collins, Patrick Côté, Stephanie Côté, Julianne Dalcanton, Tim Davidge, Marla Geha, Karoline Gilbert, Carl Grillmair, Mike Irwin, Bradley Jacobs, Ryan Leaman, Nicolas Martin, Emma Ryan-Weber, Evan Skillman, Peter Stetson, Brent Tully, Sidney van den Bergh, Matthew Walker, Daniel Weisz, and Lisa Young for their help in answering questions that came up during the preparation of this manuscript; to Wolfgang Steinicke and Harold Corwin Jr. for their invaluable assistance in tracing some of the early references relating to the original discoveries of these objects; and to the referees for their supportive comments and very helpful feedback that led to significant improvements in the text. Finally, thanks go to the organizers of the KITP program "First Galaxies and Faint Dwarfs: Clues to the Small Scale Structure of Cold Dark Matter," at which this article was completed. As such, this research was supported in part by the National Science Foundation under Grant No. NSF PHY11-25915.

REFERENCES

Aaronson, M., & Olszewski, E. 1987, in IAU Symp. 117, Dark Matter in the Universe, ed. J. Kormendy & G. R. Knapp (Cambridge: Cambridge Univ. Press), 153
Adén, D., Feltzing, S., Koch, A., et al. 2009a, A&A, 506, 1147
Adén, D., Wilkinson, M. I., Read, J. I., et al. 2009b, ApJ, 706, L150
Aparicio, A., Dalcanton, J. J., Gallart, C., & Martinez-Delgado, D. 1997, AJ, 114, 1447
Aparicio, A., & Tikhonov, N. 2000, AJ, 119, 2183
Armandroff, T. E., Davies, J. E., & Jacoby, G. H. 1998, AJ, 116, 2287
Armandroff, T. E., Jacoby, G. H., & Davies, J. E. 1999, AJ, 118, 1220
Arp, H. C., & Madore, B. F. (ed.) 1987, A Catalogue of Southern Peculiar Galaxies and Associations, 2 volume set (Cambridge: Cambridge University Press)
Barnard, E. E. 1884, Astron. Nachr., 110, 125
Barnes, D. G., & de Blok, W. J. G. 2001, AJ, 122, 825
Battaglia, G., Helmi, A., Tolstoy, E., et al. 2008, ApJ, 681, L13
Battaglia, G., Tolstoy, E., Helmi, A., et al. 2006, A&A, 459, 423
Battaglia, G., Tolstoy, E., Helmi, A., et al. 2011, MNRAS, 411, 1013
Begum, A., Chengalur, J. N., Karachentsev, I. D., Kaisin, S. S., & Sharina, M. E. 2006, MNRAS, 365, 1220
Begum, A., Chengalur, J. N., Karachentsev, I. D., & Sharina, M. E. 2005, MNRAS, 359, L53
Begum, A., Chengalur, J. N., Karachentsev, I. D., & Sharina, M. E. 2008a, MNRAS, 386, 138
Begum, A., Chengalur, J. N., Karachentsev, I. D., Sharina, M. E., & Kaisin, S. S. 2008b, MNRAS, 386, 1667
Bell, E. F., Slater, C. T., & Martin, N. F. 2011, ApJ, 742, L15
Bellazzini, M., Beccari, G., Oosterloo, T. A., et al. 2011, A&A, 527, A58
Bellazzini, M., Ferraro, F. R., Origlia, L., et al. 2002, AJ, 124, 3222
Bellazzini, M., Ferraro, F. R., & Pancino, E. 2001, ApJ, 556, 635
Bellazzini, M., Ferraro, F. R., Sollima, A., Pancino, E., & Origlia, L. 2004a, A&A, 424, 199
Bellazzini, M., Gennari, N., & Ferraro, F. R. 2005, MNRAS, 360, 185
Bellazzini, M., Gennari, N., Ferraro, F. R., & Sollima, A. 2004b, MNRAS, 354, 708
Bellazzini, M., Ibata, R., Martin, N., et al. 2006, MNRAS, 366, 865
Bellazzini, M., Ibata, R., Monaco, L., et al. 2004c, MNRAS, 354, 1263
Belokurov, V., Walker, M. G., Evans, N. W., et al. 2008, ApJ, 686, L83
Belokurov, V., Walker, M. G., Evans, N. W., et al. 2009, MNRAS, 397, 1748
Belokurov, V., Walker, M. G., Evans, N. W., et al. 2010, ApJ, 712, L103
Belokurov, V., Zucker, D. B., Evans, N. W., et al. 2006, ApJ, 647, L111
Belokurov, V., Zucker, D. B., Evans, N. W., et al. 2007, ApJ, 654, 897
Bender, R., Kormendy, J., & Dehnen, W. 1996, ApJ, 464, L123
Bernard, E. J., Gallart, C., Monelli, M., et al. 2008, ApJ, 678, L21
Bernard, E. J., Monelli, M., Gallart, C., et al. 2009, ApJ, 699, 1742
Bernard, E. J., Monelli, M., Gallart, C., et al. 2010, ApJ, 712, 1259
Blais-Ouellette, S., Amram, P., & Carignan, C. 2001, AJ, 121, 1952
Blitz, L., & Robishaw, T. 2000, ApJ, 541, 675
Bonanos, A. Z., Stanek, K. Z., Szentgyorgyi, A. H., Sasselov, D. D., & Bakos, G. Á. 2004, AJ, 127, 861
Bouchard, A., Carignan, C., & Staveley-Smith, L. 2006, AJ, 131, 2913
Bouchard, A., Da Costa, G. S., & Jerjen, H. 2009, AJ, 137, 3038
Bouchard, A., Jerjen, H., Da Costa, G. S., & Ott, J. 2005, AJ, 130, 2058
Brasseur, C. M., Martin, N. F., Macciò, A. V., Rix, H.-W., & Kang, X. 2011a, ApJ, 743, 179
Brasseur, C. M., Martin, N. F., Rix, H.-W., et al. 2011b, ApJ, 729, 23
Brodie, J. P., Romanowsky, A. J., Strader, J., & Forbes, D. A. 2011, AJ, 142, 199
Brown, T. M., Smith, E., Ferguson, H. C., et al. 2007, ApJ, 658, L95
Brüns, C., Kerp, J., Staveley-Smith, L., et al. 2005, A&A, 432, 45
Butler, D. J., Martínez-Delgado, D., Rix, H.-W., Peñarrubia, J., & de Jong, J. T. A. 2007, AJ, 133, 2274
Cannon, R. D., Hawarden, T. G., & Tritton, S. B. 1977, MNRAS, 180, 81P
Canterna, R., & Flower, P. J. 1977, ApJ, 212, L57
Carignan, C., Beaulieu, S., Côté, S., Demers, S., & Mateo, M. 1998, AJ, 116, 1690
Carlin, J. L., Grillmair, C. J., Muñoz, R. R., Nidever, D. L., & Majewski, S. R. 2009, ApJ, 702, L9
Carrera, R., Aparicio, A., Martínez-Delgado, D., & Alonso-García, J. 2002, AJ, 123, 3199
Carrera, R., Gallart, C., Hardy, E., Aparicio, A., & Zinn, R. 2008, AJ, 135, 836
Castro, N., Herrero, A., Garcia, M., et al. 2008, A&A, 485, 41
Cesarsky, D. A., Lequeux, J., Laustsen, S., Schuster, H., & West, R. M. 1977, A&A, 61, L31
Chapman, S. C., Peñarrubia, J., Ibata, R., et al. 2007, ApJ, 662, L79
Choi, P. I., Guhathakurta, P., & Johnston, K. V. 2002, AJ, 124, 310
Chou, M.-Y., Majewski, S. R., Cunha, K., et al. 2007, ApJ, 670, 346
Clementini, G., Gratton, R., Bragaglia, A., et al. 2003, AJ, 125, 1309
Cole, A. A., Skillman, E. D., Tolstoy, E., et al. 2007, ApJ, 659, L17
Cole, A. A., Tolstoy, E., Gallagher, J. S., III, & Smecker-Hane, T. A. 2005, AJ, 129, 1465
Coleman, M. G., de Jong, J. T. A., Martin, N. F., et al. 2007, ApJ, 668, L43
Collins, M. L. M. 2011, PhD thesis, University of Cambridge, Institute of Astronomy
Collins, M. L. M., Chapman, S. C., Irwin, M. J., et al. 2010, MNRAS, 407, 2411
Collins, M. L. M., Chapman, S. C., Rich, R. M., et al. 2011, MNRAS, 417, 1170
Cook, K. H., Mateo, M., Olszewski, E. W., et al. 1999, PASP, 111, 306
Corbelli, E., & Schneider, S. E. 1997, ApJ, 479, 244
Correnti, M., Bellazzini, M., & Ferraro, F. R. 2009, MNRAS, 397, L26
Corwin, H. G., de Vaucouleurs, A., & de Vaucouleurs, G. (ed.) 1985, Southern Galaxy Catalogue, A Catalogue of 5481 Galaxies South of Declination-17 Grad, Found on 1.2 m UK Schmidt IIIa J Plates (Austin: University of Texas)
Courteau, S., & van den Bergh, S. 1999, AJ, 118, 337
Courteau, S., Widrow, L. M., McDonald, M., et al. 2011, ApJ, 739, 20

[5] Updated versions of the core data available in Tables 1–5 for all dwarf galaxies within 3 Mpc are available at https://www.astrosci.ca/users/alan/Nearby_Dwarfs_Database.html.

[6] Note added in Proof: For example, see Papers by Tollerud et al. (2012) and Kirby et al. (2012).

Da Costa, G. S., & Armandroff, T. E. 1990, AJ, 100, 162
da Costa, L. N., Willmer, C. N. A., Pellegrini, P. S., et al. 1998, AJ, 116, 1
Dalcanton, J. J., Williams, B. F., Seth, A. C., et al. 2009, ApJS, 183, 67
Dale, D. A., Cohen, S. A., Johnson, L. C., et al. 2009, ApJ, 703, 517
Dale, D. A., Gil de Paz, A., Gordon, K. D., et al. 2007, ApJ, 655, 863
Dall'Ora, M., Clementini, G., Kinemuchi, K., et al. 2006, ApJ, 653, L109
de Jong, J. T. A., Harris, J., Coleman, M. G., et al. 2008, ApJ, 680, 1112
de Jong, J. T. A., Martin, N. F., Rix, H.-W., et al. 2010, ApJ, 710, 1664
de Vaucouleurs, G., de Vaucouleurs, A., Corwin, H. G., Jr., et al. 1991, Third Reference Catalogue of Bright Galaxies, Vol. 1–3 (Berlin: Springer), 2069 pp, chap. XII
Dekel, A., & Woo, J. 2003, MNRAS, 344, 1131
Demers, S., Battinelli, P., & Kunkel, W. E. 2006, ApJ, 636, L85
Dolphin, A. E. 2002, MNRAS, 332, 91
Dolphin, A. E., Saha, A., Claver, J., et al. 2002, AJ, 123, 3154
Dunlop, J. 1828, Phil. Trans. R. Soc. I, 118, 113
Eggen, O. J., Lynden-Bell, D., & Sandage, A. R. 1962, ApJ, 136, 748
Einasto, J., Saar, E., Kaasik, A., & Chernin, A. D. 1974, Nature, 252, 111
Epinat, B., Amram, P., Marcelin, M., et al. 2008, MNRAS, 388, 500
Evans, N. W., & Wilkinson, M. I. 2000, MNRAS, 316, 929
Evans, N. W., Wilkinson, M. I., Guhathakurta, P., Grebel, E. K., & Vogt, S. S. 2000, ApJ, 540, L9
Feitzinger, J. V., & Galinski, T. 1985, A&AS, 61, 503
Fingerhut, R. L., Lee, H., McCall, M. L., & Richer, M. G. 2007, ApJ, 655, 814
Fingerhut, R. L., McCall, M. L., Argote, M., et al. 2010, ApJ, 716, 792
Fiorentino, G., Monachesi, A., Trager, S. C., et al. 2010, ApJ, 708, 817
Fraternali, F., Tolstoy, E., Irwin, M. J., & Cole, A. A. 2009, A&A, 499, 121
Freeman, K., & Bland-Hawthorn, J. 2002, ARA&A, 40, 487
Fumigalli, M., da Silva, R. L., & Krumholz, M. R. 2011, ApJ, 741, L26
Gallagher, J. S., III, & Wyse, R. F. G. 1994, PASP, 106, 1225
Gallart, C., Martínez-Delgado, D., Gómez-Flechoso, M. A., & Mateo, M. 2001, AJ, 121, 2572
Gallart, C., Zoccali, M., & Aparicio, A. 2005, ARA&A, 43, 387
Geehan, J. J., Fardal, M. A., Babul, A., & Guhathakurta, P. 2006, MNRAS, 366, 996
Geha, M., Blanton, M. R., Masjedi, M., & West, A. A. 2006a, ApJ, 653, 240
Geha, M., Guhathakurta, P., Rich, R. M., & Cooper, M. C. 2006b, AJ, 131, 332
Geha, M., van der Marel, R. P., Guhathakurta, P., et al. 2010, ApJ, 711, 361
Geisler, D., Wallerstein, G., Smith, V. V., & Casetti-Dinescu, D. I. 2007, PASP, 119, 939
Gieren, W., Pietrzyński, G., Nalewajko, K., et al. 2006, ApJ, 647, 1056
Gieren, W., Pietrzyński, G., Soszyński, I., et al. 2008, ApJ, 672, 266
Graham, A. W., & Guzmán, R. 2003, AJ, 125, 2936
Grcevich, J., & Putman, M. E. 2009, ApJ, 696, 385
Grebel, E. K. 1997, Rev. Mod. Astron., 10, 29
Grebel, E. K., Gallagher, J. S., & Harbeck, D. 2003, AJ, 125, 1926
Greco, C., Dall'Ora, M., Clementini, G., et al. 2008, ApJ, 675, L73
Grillmair, C. J. 2009, ApJ, 693, 1118
Grillmair, C. J., Lauer, T. R., Worthey, G., et al. 1996, AJ, 112, 1975
Hammer, F., Puech, M., Chemin, L., Flores, H., & Lehnert, M. D. 2007, ApJ, 662, 322
Harbeck, D., Grebel, E. K., Holtzman, J., et al. 2001, AJ, 122, 3092
Hargreaves, J. C., Gilmore, G., & Annan, J. D. 1996, MNRAS, 279, 108
Harrington, R. G., & Wilson, A. G. 1950, PASP, 62, 118
Harris, J., & Zaritsky, D. 2006, AJ, 131, 2514
Harris, W. E. 1996, AJ, 112, 1487
Haynes, M. P., van Zee, L., Hogg, D. E., Roberts, M. S., & Maddalena, R. J. 1998, AJ, 115, 62
Henning, P. A., Staveley-Smith, L., Ekers, R. D., et al. 2000, AJ, 119, 2686
Herschel, J. F. W. 1833, Phil. Trans. R. Soc. I, 123, 359
Herschel, J. F. W. Sir (ed.) 1847, Results of Astronomical Observations Made during the Years 1834, 5, 6, 7, 8, at the Cape of Good Hope; Being the Completion of a Telescopic Survey of the Whole Surface of the Visible Heavens, Commenced in 1825 (London: Smith, Elder and Co.)
Herschel, W. 1789, Phil. Trans. R. Soc. I, 79, 212
Hidalgo, S. L., Aparicio, A., & Gallart, C. 2008, AJ, 136, 2332
Hidalgo, S. L., Aparicio, A., Martínez-Delgado, D., & Gallart, C. 2009, ApJ, 705, 704
Hidalgo, S. L., Aparicio, A., Skillman, E., et al. 2011, ApJ, 730, 14
Hlavacek-Larrondo, J., Marcelin, M., Epinat, B., et al. 2011, MNRAS, 416, 509
Hoffman, G. L., Salpeter, E. E., Farhat, B., et al. 1996, ApJS, 105, 269
Holmberg, E. 1958, Medd. Lunds Astron. Obs. Ser., II, 128
Huchra, J. P., Geller, M. J., & Corwin, H. G., Jr. 1995, ApJS, 99, 391
Huchra, J. P., Vogeley, M. S., & Geller, M. J. 1999, ApJS, 121, 287
Huchtmeier, W. K., Karachentsev, I. D., & Karachentseva, V. E. 2000, A&AS, 147, 187
Huchtmeier, W. K., Karachentsev, I. D., & Karachentseva, V. E. 2003, A&A, 401, 483
Huchtmeier, W. K., & Richter, O. G. 1986, A&AS, 63, 323
Huchtmeier, W. K., & Richter, O.-G. 1988, A&A, 203, 237
Huxor, A. P., Ferguson, A. M. N., Tanvir, N. R., et al. 2011, MNRAS, 414, 770
Ibata, R., Chapman, S., Ferguson, A. M. N., et al. 2004, MNRAS, 351, 117
Ibata, R., Martin, N. F., Irwin, M., et al. 2007, ApJ, 671, 1591
Ibata, R. A., Gilmore, G., & Irwin, M. J. 1994, Nature, 370, 194
Ibata, R. A., Wyse, R. F. G., Gilmore, G., Irwin, M. J., & Suntzeff, N. B. 1997, AJ, 113, 634
Impey, C., & Bothun, G. 1997, ARA&A, 35, 267
Irwin, M., & Hatzidimitriou, D. 1995, MNRAS, 277, 1354
Irwin, M., & Tolstoy, E. 2002, MNRAS, 336, 643
Irwin, M. J. 1994, in ESO/OHP Workshop No. 49 on Dwarf Galaxies, ed. G. Meylan & P. Prugniel (Garching: European Southern Observatory), 27
Irwin, M. J., Belokurov, V., Evans, N. W., et al. 2007, ApJ, 656, L13
Irwin, M. J., Bunclark, P. S., Bridgeland, M. T., & McMahon, R. G. 1990, MNRAS, 244, 16P
Irwin, M. J., Ferguson, A. M. N., Huxor, A. P., et al. 2008, ApJ, 676, L17
Jacobs, B. A., Tully, R. B., Rizzi, L., et al. 2011, AJ, 141, 106
Jerjen, H., Freeman, K. C., & Binggeli, B. 1998, AJ, 116, 2873
Jobin, M., & Carignan, C. 1990, AJ, 100, 648
Kaiser, N., Aussel, H., Burke, B. E., et al. 2002, Proc. SPIE, 4836, 154
Kalirai, J. S., Beaton, R. L., Geha, M. C., et al. 2010, ApJ, 711, 671
Kalirai, J. S., Gilbert, K. M., Guhathakurta, P., et al. 2006, ApJ, 648, 389
Karachentsev, I., Drozdovsky, I., Kajsin, S., et al. 1997, A&AS, 124, 559
Karachentsev, I. D. 2005, AJ, 129, 178
Karachentsev, I. D., Dolphin, A., Tully, R. B., et al. 2006, AJ, 131, 1361
Karachentsev, I. D., Grebel, E. K., Sharina, M. E., et al. 2003a, A&A, 404, 93
Karachentsev, I. D., & Karachentseva, V. E. 1999, A&A, 341, 355
Karachentsev, I. D., Karachentseva, V. E., & Huchtmeier, W. K. 2001a, A&A, 366, 428
Karachentsev, I. D., Karachentseva, V. E., Huchtmeier, W. K., & Makarov, D. I. 2004, AJ, 127, 2031
Karachentsev, I. D., Karachentseva, V. E., Suchkov, A. A., & Grebel, E. K. 2000, A&AS, 145, 415
Karachentsev, I. D., Kashibadze, O. G., Makarov, D. I., & Tully, R. B. 2009, MNRAS, 393, 1265
Karachentsev, I. D., & Makarov, D. A. 1996, AJ, 111, 794
Karachentsev, I. D., Sharina, M. E., Dolphin, A. E., & Grebel, E. K. 2003b, A&A, 408, 111
Karachentsev, I. D., Sharina, M. E., Dolphin, A. E., et al. 2001b, A&A, 379, 407
Karachentsev, I. D., Sharina, M. E., Dolphin, A. E., et al. 2002a, A&A, 385, 21
Karachentsev, I. D., Sharina, M. E., Makarov, D. I., et al. 2002b, A&A, 389, 812
Karachentsev, I. D., & Tikhonov, N. A. 1994, A&A, 286, 718
Karachentseva, V. E. 1976, Comm. Special Obs., 18, 42
Karachentseva, V. E., & Karachentsev, I. D. 1998, A&AS, 127, 409
Karachentseva, V. E., Karachentsev, I. D., & Richter, G. M. 1999, A&AS, 135, 221
Keller, S. C., Schmidt, B. P., Bessell, M. S., et al. 2007, PASA, 24, 1
Kennicutt, R. C., Jr., Armus, L., Bendo, G., et al. 2003, PASP, 115, 928
Kennicutt, R. C., Jr., Lee, J. C., Funes, S. J., et al. 2008, ApJS, 178, 247
Kepley, A. A., Wilcots, E. M., Hunter, D. A., & Nordgren, T. 2007, AJ, 133, 2242
Kim, S., Staveley-Smith, L., Dopita, M. A., et al. 1998, ApJ, 503, 674
Kirby, E., Cohen, J., & Bellazzini, M. 2012, ApJ, in press (arXiv:1203.4561)
Kirby, E. N., Guhathakurta, P., Bolte, M., Sneden, C., & Geha, M. C. 2009, ApJ, 705, 328
Kirby, E. N., Guhathakurta, P., & Sneden, C. 2008a, ApJ, 682, 1217
Kirby, E. N., Lanfranchi, G. A., Simon, J. D., Cohen, J. G., & Guhathakurta, P. 2011, ApJ, 727, 78
Kirby, E. N., Simon, J. D., Geha, M., Guhathakurta, P., & Frebel, A. 2008b, ApJ, 685, L43
Kleyna, J. T., Wilkinson, M. I., Evans, N. W., & Gilmore, G. 2004, MNRAS, 354, 543
Kleyna, J. T., Wilkinson, M. I., Gilmore, G., & Evans, N. W. 2003, ApJ, 588, L21
Klypin, A., Zhao, H., & Somerville, R. S. 2002, ApJ, 573, 597
Koch, A., Grebel, E. K., Kleyna, J. T., et al. 2007a, AJ, 133, 270
Koch, A., Grebel, E. K., Wyse, R. F. G., et al. 2006, AJ, 131, 895
Koch, A., Rich, R. M., Reitzel, D. B., et al. 2008, ApJ, 689, 958
Koch, A., Wilkinson, M. I., Kleyna, J. T., et al. 2007b, ApJ, 657, 241
Koch, A., Wilkinson, M. I., Kleyna, J. T., et al. 2009, ApJ, 690, 453
Kochanek, C. S. 1996, ApJ, 457, 228
Koposov, S., Belokurov, V., Evans, N. W., et al. 2008, ApJ, 686, 279

Koposov, S. E., Gilmore, G., Walker, M. G., et al. 2011, ApJ, 736, 146
Kopylov, A. I., Tikhonov, N. A., Fabrika, S., Drozdovsky, I., & Valeev, A. F. 2008, MNRAS, 387, L45
Koribalski, B. S., Staveley-Smith, L., Kilborn, V. A., et al. 2004, AJ, 128, 16
Kormendy, J. 1985, ApJ, 295, 73
Kormendy, J., & Bender, R. 2012, ApJS, 198, 2
Kowal, C. T., Lo, K. Y., & Sargent, W. L. W. 1978, IAU Circ., 3305, 2
Lai, D. K., Lee, Y. S., Bolte, M., et al. 2011, ApJ, 738, 51
Lake, G., & Skillman, E. D. 1989, AJ, 98, 1274
Lauberts, A. (ed.) 1982, ESO/Uppsala Survey of the ESO(B) Atlas (Garching: European Southern Observatory)
Lavery, R. J. 1990, IAU Circ., 5139, 2
Leaman, R., Cole, A. A., Venn, K. A., et al. 2009, ApJ, 699, 1
Lee, H., Skillman, E. D., Cannon, J. M., et al. 2006, ApJ, 647, 970
Lee, J. C., Gil de Paz, A., Kennicutt, R. C., Jr., et al. 2011, ApJS, 192, 6
Lee, M. G. 1995, AJ, 110, 1129
Lee, M. G., Aparicio, A., Tikonov, N., Byun, Y., & Kim, E. 1999, AJ, 118, 853
Lee, M. G., & Byun, Y.-I. 1999, AJ, 118, 817
Lee, M. G., Freedman, W. L., & Madore, B. F. 1993, ApJ, 417, 553
Lee, M. G., & Kim, S. C. 2000, AJ, 119, 777
Lee, M. G., Yuk, I., Park, H. S., Harris, J., & Zaritsky, D. 2009, ApJ, 703, 692
Legentil, G. 1755, in Sav. étrangers, Vol. II (Paris: Académie Royale des Sciences), 137
Letarte, B., Chapman, S. C., Collins, M., et al. 2009, MNRAS, 400, 1472
Lewis, G. F., Ibata, R. A., Chapman, S. C., et al. 2007, MNRAS, 375, 1364
Lianou, S., Grebel, E. K., & Koch, A. 2011, A&A, 531, A152
Little, B., & Tremaine, S. 1987, ApJ, 320, 493
Lo, K. Y., Sargent, W. L. W., & Young, K. 1993, AJ, 106, 507
Longmore, A. J., Hawarden, T. G., Goss, W. M., Mebold, U., & Webster, B. L. 1982, MNRAS, 200, 325
Longmore, A. J., Hawarden, T. G., Webster, B. L., Goss, W. M., & Mebold, U. 1978, MNRAS, 183, 97P
López-Corredoira, M., Momany, Y., Zaggia, S., & Cabrera-Lavers, A. 2007, A&A, 472, L47
Loveday, J. 1996, MNRAS, 278, 1025
Lunt, J. 1902, MNRAS, 62, 468
Lynden-Bell, D. 1981, Observatory, 101, 111
Majewski, S. R., Beaton, R. L., Patterson, R. J., et al. 2007, ApJ, 670, L9
Majewski, S. R., Skrutskie, M. F., Weinberg, M. D., & Ostheimer, J. C. 2003, ApJ, 599, 1082
Makarova, L. 1999, A&AS, 139, 491
Martin, N. F., Coleman, M. G., De Jong, J. T. A., et al. 2008a, ApJ, 672, L13
Martin, N. F., de Jong, J. T. A., & Rix, H.-W. 2008b, ApJ, 684, 1075
Martin, N. F., Ibata, R. A., Bellazzini, M., et al. 2004a, MNRAS, 348, 12
Martin, N. F., Ibata, R. A., Chapman, S. C., Irwin, M., & Lewis, G. F. 2007, MNRAS, 380, 281
Martin, N. F., Ibata, R. A., Conn, B. C., et al. 2004b, MNRAS, 355, L33
Martin, N. F., Ibata, R. A., Conn, B. C., et al. 2005, MNRAS, 362, 906
Martin, N. F., Ibata, R. A., Irwin, M. J., et al. 2006, MNRAS, 371, 1983
Martin, N. F., McConnachie, A. W., Irwin, M., et al. 2009, ApJ, 705, 758
Martínez-Delgado, D., Butler, D. J., Rix, H.-W., et al. 2005, ApJ, 633, 205
Martínez-Delgado, D., Gallart, C., & Aparicio, A. 1999, AJ, 118, 862
Mateo, M., Olszewski, E. W., & Morrison, H. L. 1998, ApJ, 508, L55
Mateo, M., Olszewski, E. W., Pryor, C., Welch, D. L., & Fischer, P. 1993, AJ, 105, 510
Mateo, M., Olszewski, E. W., & Walker, M. G. 2008, ApJ, 675, 201
Mateo, M. L. 1998, ARA&A, 36, 435
Mayer, L., Mastropietro, C., Wadsley, J., Stadel, J., & Moore, B. 2006, MNRAS, 369, 1021
McConnachie, A. W., Arimoto, N., & Irwin, M. 2007, MNRAS, 379, 379
McConnachie, A. W., Arimoto, N., Irwin, M., & Tolstoy, E. 2006, MNRAS, 373, 715
McConnachie, A. W., & Côté, P. 2010, ApJ, 722, L209
McConnachie, A. W., Huxor, A., Martin, N. F., et al. 2008, ApJ, 688, 1009
McConnachie, A. W., & Irwin, M. J. 2006, MNRAS, 365, 1263
McConnachie, A. W., Irwin, M. J., Ferguson, A. M. N., et al. 2005, MNRAS, 356, 979
McConnachie, A. W., Irwin, M. J., Ibata, R. A., et al. 2009, Nature, 461, 66
McMillan, P. J. 2011, MNRAS, 414, 2446
Melotte, P. J. 1926, MNRAS, 86, 636
Messier, C. 1798, in Connaissance des Temps, 1801, 461
Minor, Q. E., Martinez, G., Bullock, J., Kaplinghat, M., & Trainor, R. 2010, ApJ, 721, 1142
Moitinho, A., Vázquez, R. A., Carraro, G., et al. 2006, MNRAS, 368, L77
Momany, Y., Held, E. V., Saviane, I., & Rizzi, L. 2002, A&A, 384, 393
Momany, Y., Zaggia, S. R., Bonifacio, P., et al. 2004, A&A, 421, L29
Monaco, L., Bellazzini, M., Ferraro, F. R., & Pancino, E. 2004, MNRAS, 353, 874
Monelli, M., Gallart, C., Hidalgo, S. L., et al. 2010a, ApJ, 722, 1864
Monelli, M., Hidalgo, S. L., Stetson, P. B., et al. 2010b, ApJ, 720, 1225
Moretti, M. I., Dall'Ora, M., Ripepi, V., et al. 2009, ApJ, 699, L125
Muñoz, R. R., Carlin, J. L., Frinchaboy, P. M., et al. 2006, ApJ, 650, L51
Muñoz, R. R., Padmanabhan, N., & Geha, M. 2012, ApJ, 745, 127
Nilson, P. 1974, Uppsala Astrono. Obs. Rep., 5, 0
Norris, J. E., Wyse, R. F. G., Gilmore, G., et al. 2010, ApJ, 723, 1632
Okamoto, S., Arimoto, N., Yamada, Y., & Onodera, M. 2008, A&A, 487, 103
Olszewski, E. W., Pryor, C., & Armandroff, T. E. 1996, AJ, 111, 750
Parisi, M. C., Geisler, D., Grocholski, A. J., Clariá, J. J., & Sarajedini, A. 2010, AJ, 139, 1168
Paturel, G., Petit, C., Prugniel, P., et al. 2003, A&A, 412, 45
Peñarrubia, J., Zucker, D. B., Irwin, M. J., et al. 2011, ApJ, 727, L2
Pickering, E. C. 1899, ApJ, 9, 173
Pickering, E. C. 1908, Ann. Harv. Coll. Obs., 60, 147
Pietrzyński, G., Gieren, W., Szewczyk, O., et al. 2008, AJ, 135, 1993
Pietrzyński, G., Górski, M., Gieren, W., et al. 2009, AJ, 138, 459
Puche, D., Carignan, C., & Wainscoat, R. J. 1991, AJ, 101, 447
Putman, M. E., Thom, C., Gibson, B. K., & Staveley-Smith, L. 2004, ApJ, 603, L77
Reaves, G. 1956, AJ, 61, 69
Revaz, Y., & Jablonka, P. 2012, A&A, 538, A82
Rice, W., Lonsdale, C. J., Soifer, B. T., et al. 1988, ApJS, 68, 91
Richardson, J. C., Irwin, M. J., McConnachie, A. W., et al. 2011, ApJ, 732, 76
Rizzi, L., Tully, R. B., Makarov, D., et al. 2007, ApJ, 661, 815
Rutledge, G. A., Hesser, J. E., Stetson, P. B., et al. 1997, PASP, 109, 883
Ryan-Weber, E. V., Begum, A., Oosterloo, T., et al. 2008, MNRAS, 384, 535
Sakai, S., Madore, B. F., & Freedman, W. L. 1996, ApJ, 461, 713
Sakamoto, T., & Hasegawa, T. 2006, ApJ, 653, L29
Sandage, A. 1986, ApJ, 307, 1
Sanna, N., Bono, G., Stetson, P. B., et al. 2010, ApJ, 722, L244
Saviane, I., Held, E. V., & Piotto, G. 1996, A&A, 315, 40
Schlegel, D. J., Finkbeiner, D. P., & Davis, M. 1998, ApJ, 500, 525
Schuster, H., & West, R. M. 1976, A&A, 49, 129
Searle, L., & Zinn, R. 1978, ApJ, 225, 357
Shane, C. D. 1947, PASP, 59, 182
Shapley, H. 1938a, Harv. Coll. Obs. Bull., 908, 1
Shapley, H. 1938b, Nature, 142, 715
Sharina, M. E., Karachentsev, I. D., Dolphin, A. E., et al. 2008, MNRAS, 384, 1544
Shostak, G. S., & Skillman, E. D. 1989, A&A, 214, 33
Silich, S., Lozinskaya, T., Moiseev, A., et al. 2006, A&A, 448, 123
Silva, D. R., Massey, P., DeGioia-Eastwood, K., & Henning, P. A. 2005, ApJ, 623, 148
Simon, J. D., Frebel, A., McWilliam, A., Kirby, E. N., & Thompson, I. B. 2010, ApJ, 716, 446
Simon, J. D., & Geha, M. 2007, ApJ, 670, 313
Simon, J. D., Geha, M., Minor, Q. E., et al. 2011, ApJ, 733, 46
Simpson, C. E., & Gottesman, S. T. 2000, AJ, 120, 2975
Skillman, E. D., Côté, S., & Miller, B. W. 2003a, AJ, 125, 610
Skillman, E. D., Côté, S., & Miller, B. W. 2003b, AJ, 125, 593
Skillman, E. D., Terlevich, R., Teuben, P. J., & van Woerden, H. 1988, A&A, 198, 33
Slater, C. T., Bell, E. F., & Martin, N. F. 2011, ApJ, 742, L14
Sohn, S. T., Majewski, S. R., Muñoz, R. R., et al. 2007, ApJ, 663, 960
Soszyński, I., Gieren, W., Pietrzyński, G., et al. 2006, ApJ, 648, 375
Stanimirović, S., Staveley-Smith, L., & Jones, P. A. 2004, ApJ, 604, 176
Starkenburg, E., Hill, V., Tolstoy, E., et al. 2010, A&A, 513, A34
Steinicke, W. (ed.) 2010, Observing and Cataloguing Nebulae and Star Clusters—from Herschel to Dreyer's New General Catalogue (Cambridge: Cambridge University Press)
Stil, J. M., Gray, A. D., & Harnett, J. I. 2005, ApJ, 625, 130
Stil, J. M., & Israel, F. P. 2002a, A&A, 389, 29
Stil, J. M., & Israel, F. P. 2002b, A&A, 389, 42
Strigari, L. E., Bullock, J. S., Kaplinghat, M., et al. 2007, ApJ, 669, 676
Sulentic, J. W., & Tifft, W. G. (ed.) 1973, The Revised New Catalogue of Nonstellar Astronomical Objects (Tucson: University of Arizona Press)
Swaters, R. A., Sancisi, R., van Albada, T. S., & van der Hulst, J. M. 2009, A&A, 493, 871
Swift, L. 1888, Astron. Nachr., 120, 33
Tammann, G. A., Sandage, A., & Reindl, B. 2008, ApJ, 679, 52
Tikhonov, N. A., & Galazutdinova, O. A. 2009, Astron. Lett., 35, 748
Tollerud, E., Seaton, R., Geha, M., et al. 2012, ApJ, in press (arXiv:1112.1067)
Tollerud, E. J., Bullock, J. S., Strigari, L. E., & Willman, B. 2008, ApJ, 688, 277

Tolstoy, E., Hill, V., & Tosi, M. 2009, ARA&A, 47, 371
Tolstoy, E., Irwin, M. J., Cole, A. A., et al. 2001, MNRAS, 327, 918
Tolstoy, E., Irwin, M. J., Helmi, A., et al. 2004, ApJ, 617, L119
Tosi, M., Greggio, L., Marconi, G., & Focardi, P. 1991, AJ, 102, 951
Tremonti, C. A., Heckman, T. M., Kauffmann, G., et al. 2004, ApJ, 613, 898
Tully, R. B. 1987, ApJ, 321, 280
Tully, R. B., Rizzi, L., Dolphin, A. E., et al. 2006, AJ, 132, 729
Tully, R. B., Rizzi, L., Shaya, E. J., et al. 2009, AJ, 138, 323
Udalski, A., Szymanski, M., Kubiak, M., et al. 1999, Acta Astron., 49, 201
Vaduvescu, O., McCall, M. L., Richer, M. G., & Fingerhut, R. L. 2005, AJ, 130, 1593
van de Rydt, F., Demers, S., & Kunkel, W. E. 1991, AJ, 102, 130
van den Bergh, S. 1959, Publ. David Dunlop Obs., 2, 147
van den Bergh, S. 1972, ApJ, 171, L31
van den Bergh, S. 1998, AJ, 116, 1688
van den Bergh, S. 1999, ApJ, 517, L97
van den Bergh, S. (ed.) 2000, The Galaxies of the Local Group (Cambridge: Cambridge University Press)
van der Marel, R. P., Alves, D. R., Hardy, E., & Suntzeff, N. B. 2002, AJ, 124, 2639
van der Marel, R. P., de Zeeuw, P. T., & Rix, H.-W. 1997, ApJ, 488, 119
van Loon, J. T., & Oliveira, J. M. (ed.) 2009, IAU Symp. 256, The Magellanic System: Stars, Gas, and Galaxies (Cambridge: Cambridge Univ. Press)
Vansevičius, V., Arimoto, N., Hasegawa, T., et al. 2004, ApJ, 611, L93
Vorontsov-Velyaminov, B. A. 1959, in Atlas and Catalog of Interacting Galaxies (Moscow: Sternberg Institute, Moscow State University)
Vorontsov-Vel'Yaminov, B. A., & Krasnogorskaya, A. A. 1962, Trudy Gosudarstvennogo Astronomicheskogo Instituta, 32, 207
Walker, M. G., Belokurov, V., Evans, N. W., et al. 2009a, ApJ, 694, L144
Walker, M. G., Mateo, M., & Olszewski, E. W. 2008, ApJ, 688, L75
Walker, M. G., Mateo, M., & Olszewski, E. W. 2009b, AJ, 137, 3100
Walker, M. G., Mateo, M., Olszewski, E. W., et al. 2007, ApJ, 667, L53
Walker, M. G., Mateo, M., Olszewski, E. W., et al. 2009c, ApJ, 704, 1274
Walsh, S. M., Jerjen, H., & Willman, B. 2007, ApJ, 662, L83
Walsh, S. M., Willman, B., Sand, D., et al. 2008, ApJ, 688, 245
Walter, F., Brinks, E., de Blok, W. J. G., et al. 2008, AJ, 136, 2563
Watkins, L. L., Evans, N. W., & An, J. H. 2010, MNRAS, 406, 264
Weisz, D. R., Dalcanton, J. J., Williams, B. F., et al. 2011, ApJ, 739, 5
Weldrake, D. T. F., de Blok, W. J. G., & Walter, F. 2003, MNRAS, 340, 12
Westerlund, B. E. (ed.) 1997, The Magellanic Clouds (Cambridge: Cambridge University Press)
Westmeier, T., Braun, R., & Koribalski, B. S. 2011, MNRAS, 410, 2217
Whiting, A. B., Hau, G. K. T., & Irwin, M. 1999, AJ, 118, 2767
Whiting, A. B., Hau, G. K. T., Irwin, M., & Verdugo, M. 2007, AJ, 133, 715
Whiting, A. B., Irwin, M. J., & Hau, G. K. T. 1997, AJ, 114, 996
Wilcots, E. M., & Miller, B. W. 1998, AJ, 116, 2363
Wilkinson, M. I., & Evans, N. W. 1999, MNRAS, 310, 645
Wilkinson, M. I., Kleyna, J. T., Evans, N. W., et al. 2004, ApJ, 611, L21
Willman, B., Blanton, M. R., West, A. A., et al. 2005a, AJ, 129, 2692
Willman, B., Dalcanton, J. J., Martinez-Delgado, D., et al. 2005b, ApJ, 626, L85
Willman, B., Geha, M., Strader, J., et al. 2011, AJ, 142, 128
Willman, B., Masjedi, M., Hogg, D. W., et al. 2006, arXiv:astro-ph/0603486
Wilson, A. G. 1955, PASP, 67, 27
Winnick, R. A. 2003, PhD thesis, Yale Univ.
Wolf, J., Martinez, G. D., Bullock, J. S., et al. 2010, MNRAS, 406, 1220
Wolf, M. 1906, MNRAS, 67, 91
Wolf, M. 1910, Astron. Nachr., 183, 187
Yin, J., Hou, J. L., Prantzos, N., et al. 2009, A&A, 505, 497
Young, L. M., & Lo, K. Y. 1996, ApJ, 462, 203
Young, L. M., & Lo, K. Y. 1997a, ApJ, 476, 127
Young, L. M., & Lo, K. Y. 1997b, ApJ, 490, 710
Young, L. M., Skillman, E. D., Weisz, D. R., & Dolphin, A. E. 2007, ApJ, 659, 331
Young, L. M., van Zee, L., Lo, K. Y., Dohm-Palmer, R. C., & Beierle, M. E. 2003, ApJ, 592, 111
Zaritsky, D., Olszewski, E. W., Schommer, R. A., Peterson, R. C., & Aaronson, M. 1989, ApJ, 345, 759
Zucker, D. B., Belokurov, V., Evans, N. W., et al. 2006a, ApJ, 650, L41
Zucker, D. B., Belokurov, V., Evans, N. W., et al. 2006b, ApJ, 643, L103
Zucker, D. B., Kniazev, A. Y., Bell, E. F., et al. 2004, ApJ, 612, L121
Zucker, D. B., Kniazev, A. Y., Martínez-Delgado, D., et al. 2007, ApJ, 659, L21
Zwicky, F. 1942, Phys. Rev., 61, 489